UNIVERSITAT DE BARCELONA

Production, purification and characterization of virus-like particles from chimeric HPV-HIV L1P18 protein expressed in *Pichia pastoris*: Lessons learned

Yoshiki Eto

University of Barcelona
Doctoral program in Biomedicine
Faculty of Medicine

Production, purification and characterization of virus-like particles from chimeric HPV-HIV L1P18 protein expressed in *Pichia pastoris*: Lessons learned.

Doctoral thesis

Yoshiki Eto

Director:
Joan Joseph Munné, MD, PhD.

Tutor:
Rosa Maria Aligué Alemany, PhD.

Co-director:
Pau Ferrer Alegre, PhD

Barcelona, 1 July 2021

Contents

1. Introduction

1.1 Structure, genome and life cycle of Human papillomavirus (HPV)

Human papillomavirus (HPV) are small, non-enveloped, icosahedral DNA viruses with a diameter of 52–55 nm. The HPV particles consist of a single double-stranded DNA molecule of approximately 8000 base-pairs (bp) bound to cellular histones and contained in a protein capsid of 72 pentameric capsomers [1] (Figure 1).

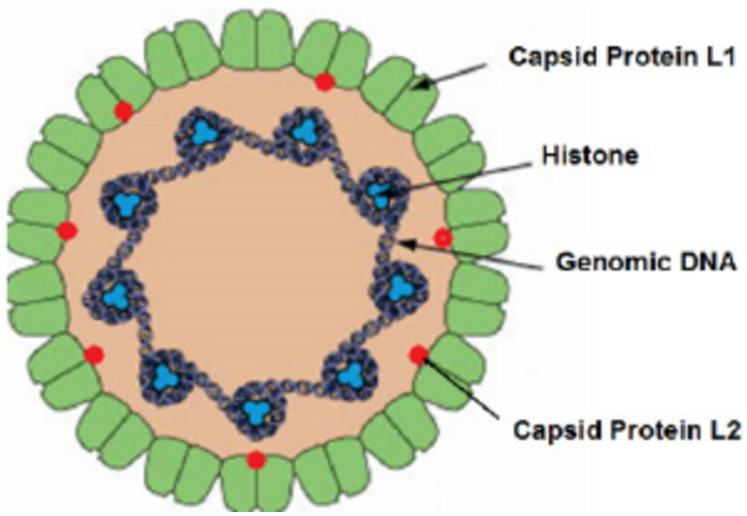

Figure 1. The structure of HPV [1].

All HPV genomes are circular and most of them encode eight major proteins. Specifically, 6 “early viral genes encode viral replication proteins and 2 “late” genes encode the viral capsid proteins [4] (Figure 2). The capsid is composed of two structural proteins — late 1 (L1) (55 kDa) and late 2 (L2) (70 kDa) [2,3].

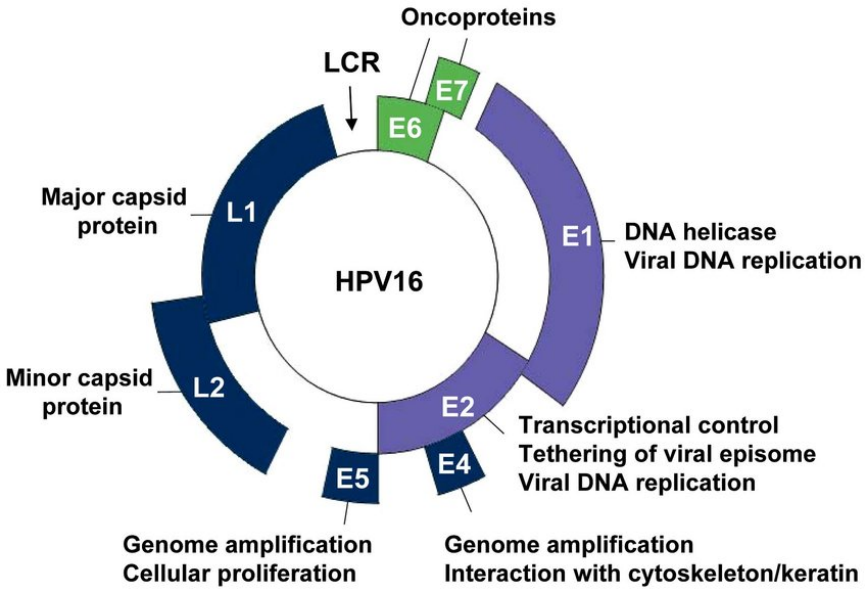

Figure 2. Genomic organization of the HPV genome [4]. Schematic representation of the HPV16 circular genome showing the location of the early (E) and late genes (L1 and L2), and of the long control region (LCR). The HPV genome encodes eight well-characterized proteins, whose functions are indicated. E4 and E5 regulates genome amplification and L1 and L2 are responsible for capsid protein. The viral replication proteins E1 and E2 (violet) and the viral oncogenes E6 and E7 (green) have been validated as essential for viral pathogenesis and represent genuine targets for small molecule-based approaches for the treatment of HPV-associated diseases.

The HPV infects basal keratinocytes through microabrasions in the skin or mucosa; with viral DNA replication, the copy number of the virus is amplified to approximately 50 to 100 copies per cell [5] (Figure 3). The initial genome amplification is followed by an episomal maintenance phase. Infected basal cells then enter the suprabasal compartment, where abundant expression of early and late genes and productive genome amplification to high copy numbers is triggered in the terminally differentiating compartments. Viral assembly occurs in the upper layer of the squamous epithelium, and virions are then released and may infect adjacent tissue (Figure 3). Because of the mechanism by which HPV infects and replicates in the host's epithelial cells, the virus is able to largely evade the host's immune system. Thus, the innate and adaptive immune responses to natural infection are limited, and although most infections are controlled eventually, antibody concentrations tend to be low or undetectable.

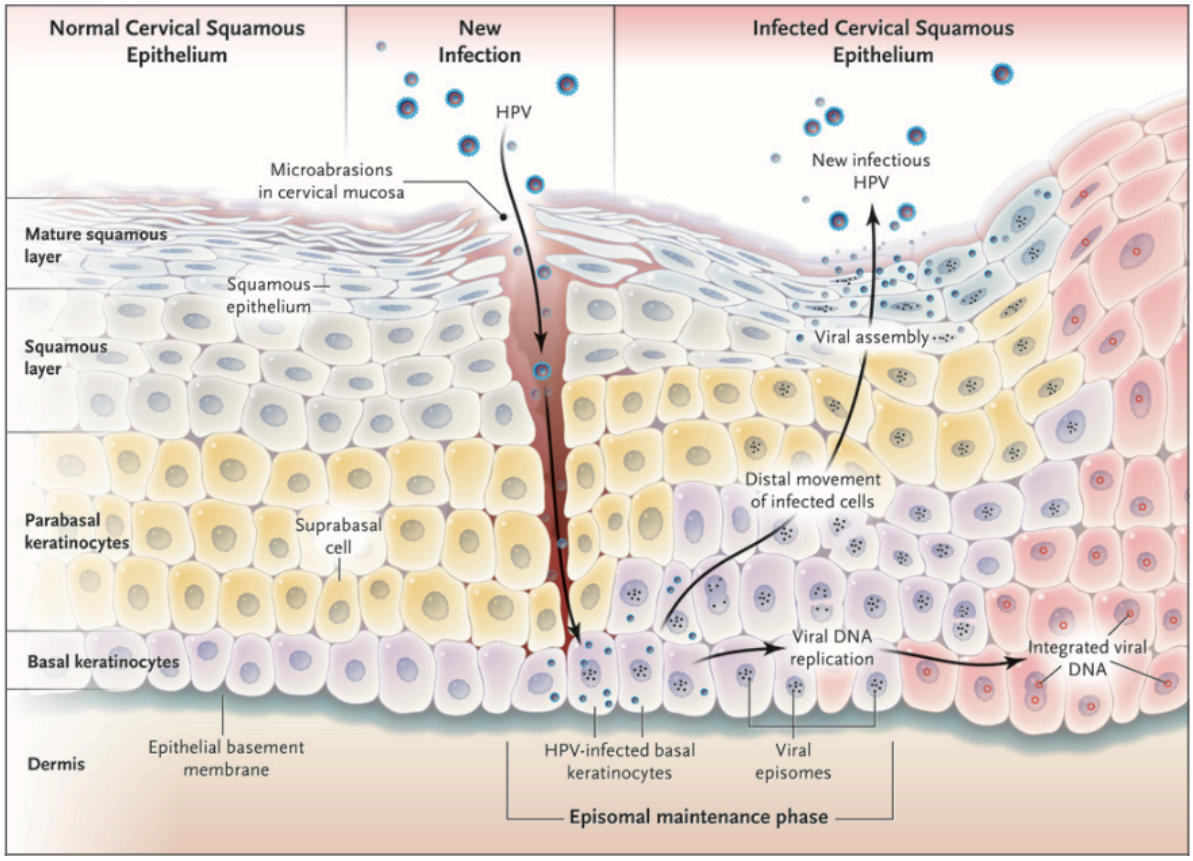

Figure 3. Human papillomavirus life cycle in the Normal Cervical Squamous Epithelium [5].

1.2 Epidemiology of HPV

De Martel et al. [6] showed in 2017 that cervical cancers represent 530,000 new cases per year and account for the vast majority of all HPV-attributable cancer cases worldwide. Nearly half of the cases are diagnosed in women <50 years old (Table 1), and more than two-thirds are diagnosed in less developed countries (Table 2). Most of cervical cancer cases occurs in South-Eastern Asia with an especially large burden in India, Latin America and sub-Saharan Africa (Table 2). Countries in which the age standardized incidence rate (ASR) is over 30 per 100,000 are mainly located in sub-Saharan Africa but a few are also found in Latin America and Oceania (Figure 4). HPV 16 and 18 together are responsible globally for 71% of cervical cancer. This percentage rises to 90% for HPV6/11/16/18/31/33/45/52/58 (Table 3).

Table 1. Number of cancer cases attributable to HPV and corresponding attributable fraction (AF) by cancer site, sex and age; World, 2012

HPV-related cancer site (ICD-10 code)	Number of incident cases[1,2]	Number attributable to HPV	AF (%)	Number attributable to HPV by gender		Number attributable to HPV by age group		
				Males	Females	<50 years	50–69 years	70+ years
Cervix uteri (C53)	530,000	530,000	100.0	0	530,000	250,000	220,000	58,000
Anus[3] (C21)	40,000	35,000	88.0	17,000	18,000	6,600	17,000	12,000
Vulva[3] (C51)	34,000	8,500	24.9	0	8,500	2,600	3,400	2,500
Vagina[3] (C52)	15,000	12,000	78.0	0	12,000	2,500	5,200	3,900
Penis[3] (C60)	26,000	13,000	50.0	13,000	0	2,700	5,800	4,400
Oropharynx[3] (C01, C09–10)	96,000	29,000	30.8	24,000	5,500	5,400	18,000	6,000
Oral cavity[3] (C02–06)	200,000	4,400	2.2	2,900	1,500	890	2,300	1,200
Larynx (C32)	160,000	3,800	2.4	3,300	460	420	2,200	1,200
Other pharynx[3] (C12–C14)	78,000	0	0	–	–	–	–	–
Total HPV-related sites	1,200,000	630,000	54.0	60,000	570,000	270,000	270,000	88,000

[1]Source: Globocan 2012.
[2]Numbers are rounded to two significant digits.
[3]These cancer sites were not directly available in GLOBOCAN 2012; therefore, data from the Cancer Incidence in Five Continents (CI5-X) database were used to estimate the corresponding number of cases.

Table 2. Number of all cancer cases attributable to HPV and corresponding attributable fraction (AF) for all cancers, by region, cancer site(s) and sex; World, 2012

Region	Cervix uteri[1]	Anus		Penis	Vulva/ vagina	Head and neck		All cancer Attributable to HPV	AF (%)		
	F	M	F	M	F	M	F	Both sexes	M	F	Both
Africa											
Sub-Saharan Africa	93,000	1,000	1,200	1,000	2,100	360	150	99,000	0.9	26.1	15.8
Northern Africa/ Western Asia	10,000	430	350	70	650	240	80	12,000	0.3	4.3	2.2
Asia											
India	120,000	2,600	1,900	3,200	2,800	5,600	1,000	140,000	2.4	23.9	13.8
Other Central Asia	29,000	490	410	30	460	760	300	31,000	0.5	11.4	6.3
China	62,000	5,900	3,600	1,300	1,600	950	270	75,000	0.5	5.4	2.5
Japan/Republic of Korea	13,000	600	560	250	460	1,500	350	16,000	0.5	3.5	1.8
Other Eastern Asia	54,000	550	530	1,100	1,000	1,000	280	59,000	0.6	11.7	6.2
America											
Latin America	69,000	1,000	1,900	2,000	2,500	980	280	78,000	0.8	13.0	7.1
Northern America	14,000	1,800	2,700	1,100	3,300	7,000	1,900	32,000	1.1	2.6	1.8
Europe											
Europe	58,000	2,700	4,200	2,700	5,100	11,000	2,800	87,000	0.9	4.4	2.5
Oceania											
Australia/New Zealand	940	150	190	50	150	290	80	1,900	0.6	2.2	1.3
Other Oceania	1,300	10	10	10	30	30	10	1,300	0.8	18.5	11.1
Less developed countries	370,000	10,000	7,600	6,800	8,300	8,600	2,100	410,000	0.8	13.2	6.7
More developed countries	160,000	6,800	10,000	6,100	12,000	22,000	5,500	220,000	0.8	5.0	2.8
World	530,000	17,000	18,000	13,000	20,000	30,000	7,500	630,000	0.8	8.6	4.5

[1]Numbers over 100 are rounded to two significant digits; numbers <100 are rounded to the closest ten.

Table 3. Relative contribution of HPV 16/18 or HPV6/11/16/18/31/33/45/52/58 to HPV-associated cancers by site and by sex; World, 2012

HPV-related cancer site (ICD-10 code)	Number attributable to HPV[1]	Relative contribution of HPV16/18[2]		Relative contribution of HPV6/11/16/18/31/33/45/52/58[2]	
		Percent	Number	Percent	Number
Cervix uteri (C53)	530,000	70.8	370,000	89.5	470,000
Anus (C21)	35,000	87.0	30,000	95.9	33,000
Vulva (C51)	8,500	72.6	6,200	87.1	7,400
Vagina (C52)	12,000	63.7	7,400	85.3	9,900
Penis (C60)	13,000	70.2	9,100	84.6	11,000
Head and neck (C01-06, C09-10, C32)	38,000	84.9	32,000	89.7	34,000
Total HPV-related sites in women	570,000	71.4	410,000	89.6	510,000
Total HPV-related sites in men	60,000	82.3	50,000	90.4	55,000
Total HPV-related sites	630,000	72.4	460,000	89.7	570,000

[1]Derived from Plummer, de Martel *et al.*[8]; numbers are rounded to two significant digits.
[2]Derived from Serrano *et al.*,[14] Alemany *et al.*[12] and Castellsague *et al.*[13]

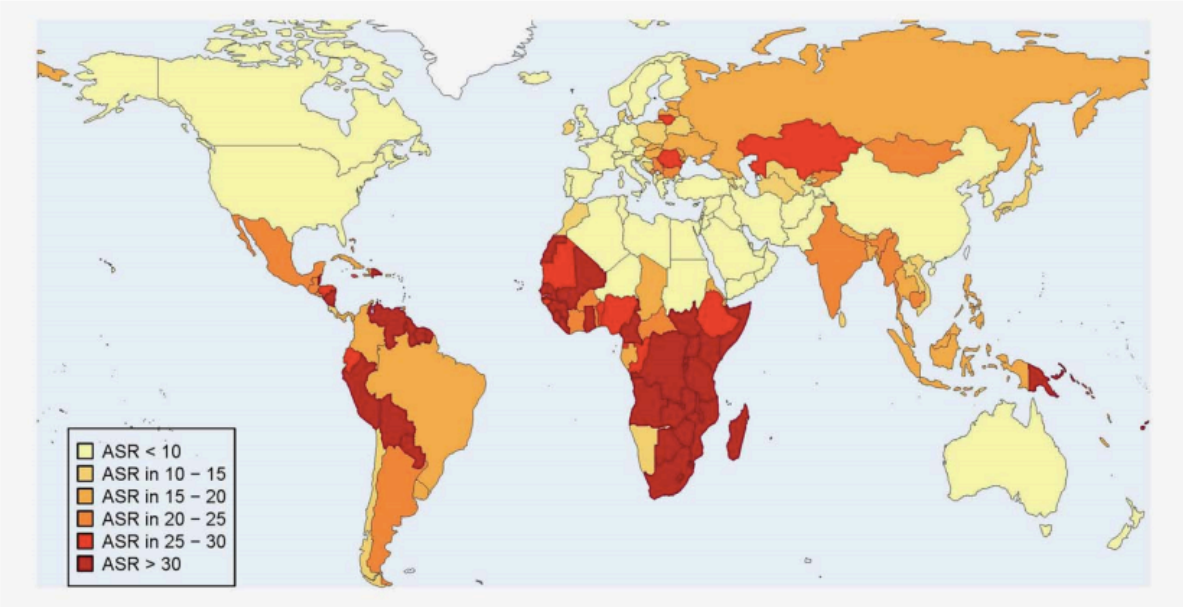

Figure 4. Age standardized (world) incidence rates (per 100,000) of cervical cancer cases attributable to HPV in 2012.

In Spain, about 1,942 new cervical cancer cases are diagnosed and 825 cervical cancer deaths occur annually (estimates for 2018) [17]. Cervical cancer ranks as the 16th leading cause of female cancer and cervical cancer is the 4th most common female cancer in women aged 15 to 44 years in Spain [17]. In addition, more new cases of cervical cancer are diagnosed among women aged 40 to 64 years compared to women under 40 or over 64 years old [17] (Figure 5). As of 2012, 58.0 % of cervical cancer is caused by HPV genotype 16 (HPV-16), 5.1 % by genotype 33, and 5.1 % by genotype 18 respectively [17] (Figure 6). In Catalonia, uterus cancer occurs in 7.2 out of every 100,000 women per year (2003-2007). This represents 2.8% of all female cancers. Between the ages of 35-64 this figure rises to 16.1 cases for every 100,000 women [18].

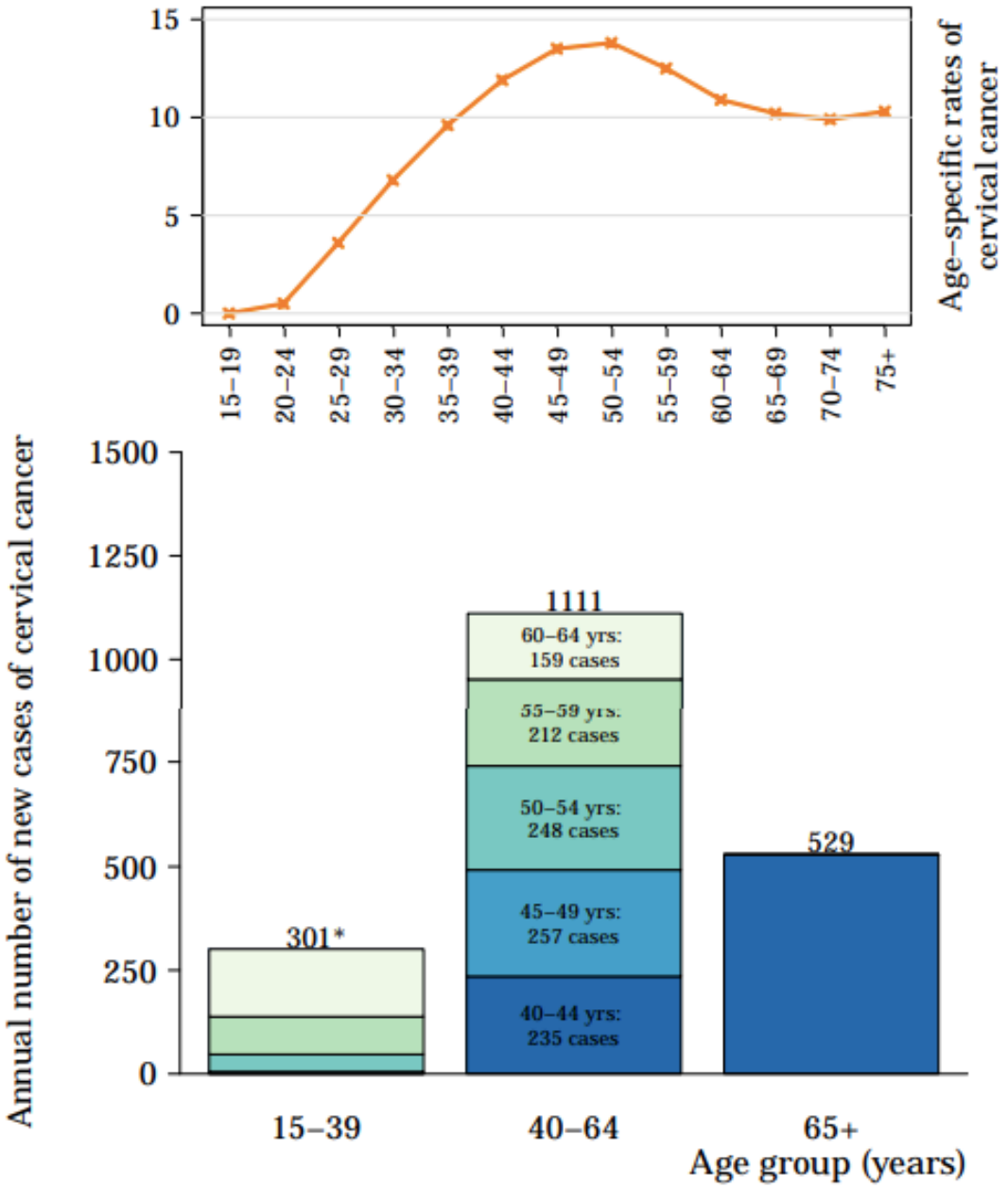

Figure 5. Annual number of new cases and age-specific incidence rates of cervical cancer in Spain (estimates for 2018) [17]. *15-19 yrs: 0 cases. 20-24 yrs: 5 cases. 25-29 yrs: 42 cases. 30-34 yrs: 91 cases. 35-39 yrs: 163 cases. Rates per 100,000 women per year.

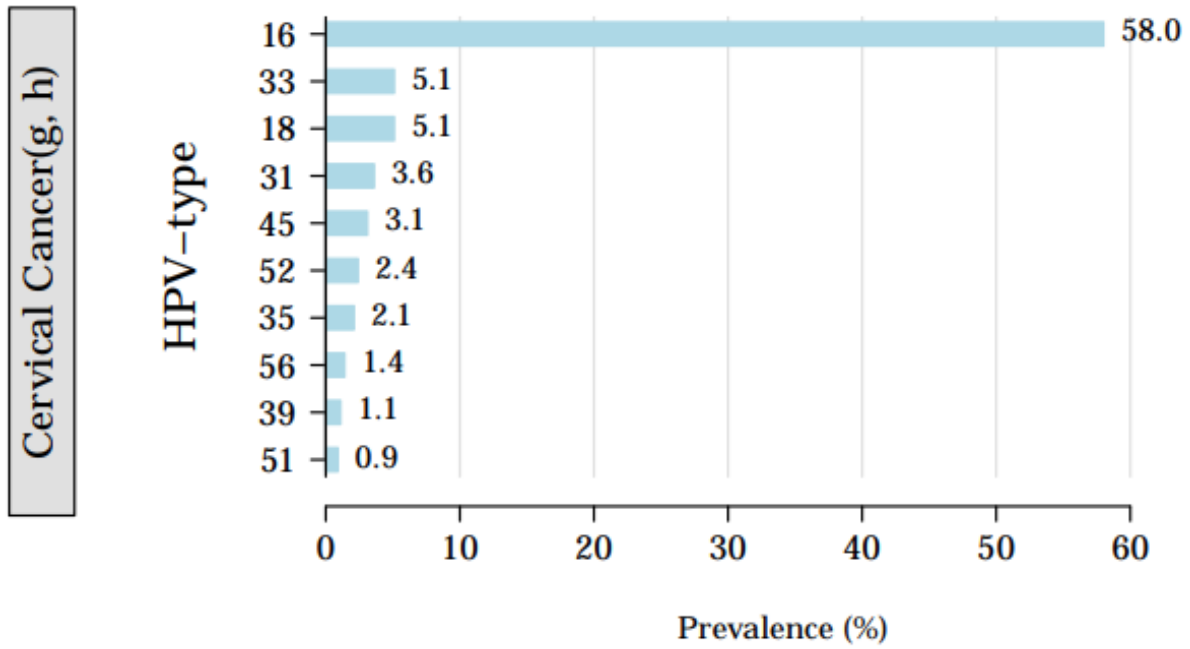

Figure 6. The frequency of the cause of cervical cancer by HPV-type in Spain [17].

1.3 HPV-specific immune responses

1.3.1 Innate Immunity against HPV

The innate immunity is the nonspecific part of the immune system. It is mediated by epithelial barrier, the complement system, and a variety of cells that phagocytose antigens and present them to other cells or destroy them [7].

The immunosurveillance of squamous epithelium of the cervix is managed by Langerhans cells (LCs), immature dendritic cells. LCs, which are abundant in the skin and mucosa, are considered to take up and process antigens in order to present them to the B and T-cells, eliciting both innate and adaptive immunity against the virus [67]. In transformation zone compared to the exocervix, significantly decreased numbers of LCs are observed. In squamous intraepithelial lesions (SILs), a small increase in the density of LCs is observed but their function appears deficient [68, 69]. Dendritic cells recognize special patterns on the pathogens utilizing their Toll-like receptors and use major histocompatibility complex (MHC) to present the antigens to the T-cells, sometimes assisted by inflammatory agents such as chemokines and cytokines. However, even in absence of lesions, Langerhans cells of the epidermis do not produce a sufficient T-cell response, compared to the dendritic cells of the dermis, due to the lack of appropriate costimulatory microenvironment. Consequently,

Langerhans cells may be unable to elicit a successful immune response and become a part of the virus tolerance tactics. Accordingly, potential vaccines should avoid using LC as presenting agent without using costimuli [70].

Toll-like receptors (TLRs) play a critical role in innate immunity. They can be found on a variety of cells of innate immunity and recognize both endogenous and exogenous threats, specifically pathogen-associated molecular patterns (PAMP) and damage-associated molecular patterns (DAMP) [7]. The activation of TLRs elicits a proinflammatory expression profile which promotes innate immunity. The double stranded HPV DNA is recognized mainly by TLR 9, and a cascade of interferons (IFN-α, IFN-β, and IFN-γ), and is initiated [71]. TLRs and interferons pathways are targeted by HPV oncoproteins resulting in an aberrant expression pattern which contributes to the virus tenacity and carcinogenic potential [72]. The tumorigenic E6 and E7 genes in HPV 16 are responsible for the downregulation of TLR9, which is known to respond to DNA threats and evoke an innate immune reply [73]. Moreover, an increasing trend in TLR 3 expression, which usually recognizes RNA viruses, is observed in dysplastic epithelium [72]. Additionally, IFN-κ and IL-10 production appears disrupted in premalignant or malignant epithelium. IFN-κ decreased expression is considered to be originated either from the methylation of IFN-κ promoter or the direct downregulation by the HPV oncogenes [74, 75]. Although TLRs and cytokines signaling is not yet completely clarified, the upregulation of certain TLRs is considered to be an attractive target for new treatments for cervical cancer [76, 77].

Macrophages are derived from monocytes and are located in tissues. They belong to the phagocyte family and have a crucial part in both innate and initiating adaptive immune responses, by digesting pathogens and additionally stimulating lymphocytes and other immune cells [7]. Certain proteins such as monocyte chemotactic protein-1 (MCP-1) and macrophage inflammatory protein (MIPa3) help the aggregation of macrophages. Both of these proteins appear downregulated directly or indirectly by HPV [78, 79]. Tumor environment observations have helped us see a different aspect of macrophage function. Accumulating evidence suggests that tumors are infiltrated by large amounts of macrophages which aggregate to the site due to the recognition of cancer cells as foreign cells [80]. Contrary to the predictable proinflammatory and antitumor functionality, macrophages inside the microenvironment of solid tumors can have a part in disease progression. Tumor associated

macrophages (TAMs) promote cancer cell proliferation and migration, angiogenesis and restriction of immune defenses [19]. This can be explained by the identification of two distinct macrophage phenotypes: M1 proinflammatory and M2 immunomodulatory. M2 profile elicits an increased vascular endothelial growth factor (VEGF) and metalloprotease-9 in order to help in tissue repair, but when it is activated by tumor, it results in basement membrane disruption, tumor growth, and metastasis [81, 82]. As cervical lesions progress, an increase in the number of macrophages is observed and M2 macrophages are the main population in HPV-associated tumors [83, 84]. M2 macrophages promote the differentiation of naïve T cells to T-regulatory cells through IL-10 and consequently tumor expansion [84, 85]. Depletion of TAM can be considered as a possible target of immunotherapy [7].

Another important part of innate immune response against viral attack is attributed to natural killer cells (NK cells) [7]. NK cells are lymphocytes which respond quickly to stressed cells, either under viral attack or cancerous ones, without the need of major histocompatibility system (MHC) [7]. It was recently observed that in high grade squamous intraepithelial lesions (HSILs) and cervical cancer by HPV16, the NK-activating receptors NKp30 and NKp45 (and NKG2D only in cancer) are considerably decreased, affecting the cytolytic functionality [86].

1.3.2 Adaptive Immunity against HPV

Adaptive immunity, the specific immune response against the pathogens, consists of B cells and T cells. B cells are responsible for the humoral immune response and T cells, which are divided in helper T cells, cytotoxic T cells (CTLs), and regulatory T cells (Tregs), are responsible for a variety of functions [7].

T-helper cells, distinguishable due to the CD4 protein on their surface, set the cytokine milieu, determining the direction of the immune response. The conditions under which the mature, but immunologically virgin, T-helper lymphocytes are activated determine their phenotype and result in two distinct populations, Th1 and Th2. This differentiation between Th1 and Th2 is determined by a variety of factors such as the type of the antigen presenting cell, the existence of costimulating signals, the amount, the structure, and the entry point of the antigen, the duration and the repetitiveness of the antigen exposure, the presence of adjuvants, and the local microenvironment of cytokines and hormones [87]. Both IFN-γ and IL-12 are required for the differentiation of Th0 (naïve lymphocyte) to Th1, which produces

IFN-γ, lymphotoxin, and IL-2 (and IL10, TNF-α) and leads to the activation of cell mediated immunity [87]. On the other hand for the Th2 phenotype, IL-4 and IL-2 are prerequisite, and the cytokine products consist of IL-4, IL-5, IL-13, IL-25, IL-10, and amphiregulin, contributing to the development of humoral immune response [20, 21]. In general, after studying the unique pattern of T-cell response among women with different grades of cervical neoplasia, T-helper cells are suggested as the dominant response needed for an HPV lesion to be cleared [22]. The equilibrium between Th1 and Th2 must be sustained invariably in order to front intracellular or extracellular attacks. Nowadays, it is supported by a variety of studies that in HPV lesion the delicate balance between the two phenotypes is distorted. The HPV, as an intracellular enemy, should evoke Th1 immune response. However, it appears that in patients with intraepithelial and invasive cervical HPV lesions Th2 cytokine profile is prevalent. It has been demonstrated that reduced Th1 response and increased Th2 response lead to suppression of cellular immunity and lesion progression [23, 24]. IL-2 and TNF-α levels (both belong to the Th1 pattern) appear lower in HPV lesion than in healthy women [24, 25]. Although IL-4 levels, characteristic Th2 product, seem to increase in low grade squamous intraepithelial lesion (LSIL), as the lesion progresses they decrease slightly. Overall, in HPV lesions both Th1 and Th2 phenotypes are suppressed, especially Th1, presumably due to the activity of the Treg cells.

The expression of CD8 glycoprotein on the surface of a T cell defines the cell as cytotoxic (CTL). CTL is the main agent in antigen specific immunity and recognizes the antigens with the assistance of MHC class I molecules. Cell mediated immunity plays a pivotal role in clearance of HPV lesion. This is substantiated from the observation that HIV positive persons or patients who have undertaken chemotherapy after transplant, with a diminished T-cell number, suffer from persistent HPV infections, either genital warts or intraepithelial lesions and cancer [26, 27]. The most T-cell activation is caused by HPV E6 and E7 proteins, and the destruction is assisted by the upregulation of adhesion molecules like ICAM-1, VCAM-1, and E-selectin in infected cells [28]. Nevertheless, HPV has developed defenses against cytotoxic cells. HPV E7 oncogene downregulates the expression of (antigen peptide transporter-1) TAP-1, which has an essential part in mounting MHC class I with the viral antigen, resulting in suppression in HPV's antigens presentation and offering HPV a great evasion tactic against human cellular defense [29, 30]. Additionally, it is noted that HPV16 E5 downregulates MHC/HLA class I [31].

T-regulatory (Treg) cells are a subset of T cells expressing CD4, CD25, and transcription factor Foxp3, that is normally necessary in the induction of tolerance, but its increase may hinder the immune response and suppress antitumor defense through inhibiting cytokines. Their activation, which is induced by TGF-β and IL-2, is considered as a poor prognostic for malignancy [32-34]. This Treg orchestrated suppression of immunity is still not completely clarified. It is presumed that Tregs reduce proliferation of T-helper and cytotoxic T cells. As for APCs, Tregs also distort their necessary protein expression of CD80 and CD86 and evoke the production of indoleamine 2.3-dioxygenase (IDO) by dendritic cells, which is an enzyme toxic to T-cell populations [35]. The role of TGF-β is still controversial, but it is considered a suppressive factor as it evokes the expression of Foxp3 in CD4+ cells and differentiates them to induced Treg cells [36, 37]. Other Treg products like carbon monoxide, galectins, and IL-10 pleiotropic activity in the tumor microenvironment should be further examined [38-40]. Recent studies have highlighted the part of Treg cell during the HPV infection. TGF-β1 and TGF-β2 levels are reported to increase as the lesion progress from LSIL to invasive cervical cancer; in contrast IL-12 and TNF-α levels (classic Th1 pattern cytokines) drop significantly. IL-10 is also rising as the disease deteriorates, especially in HSILs [24, 40].

B cells are responsible for humoral response, which neutralize and opsonize viral agents. Humoral immunity is stimulated by antigen presenting cells and Th2 cytokine pattern and depends on CD4 helper T cells that assist B cells to mature and produce antibodies against a specific epitope. The antibodies against HPV target mainly the L1 capsid protein although weak antibodies directing against E2, E6, E7, and L2 have been described. The vast majority of these antibodies are IgG1 class, a predictable response against viral antigens [41]. There are two types of neutralizing L1 antibodies. The first class hinders cell surface binding while the second class prevents binding to the basement membrane. Both appear to prevent the viral internalization either by direct binding or by blocking necessary conformational changes. Eight to nine months after natural infection, sero-conversion and neutralizing antibodies can be estimated, but their levels are low and not apparent in all women [88].

The L1 neutralizing antibodies that are produced by virus-like particles (VLP) of prophylactic vaccination belonging to the second class are greater than those created in natural infection, and their serum levels remain high in long-term studies [42].

1.4 Current status of HPV vaccine development

The HPV vaccine was originally developed by the University of Queensland in Australia and the final form was constructed by the groups at the University of Queensland, Georgetown University Medical Center, University of Rochester, and the U.S. National Cancer Institute [89]. Two Researchers from the University of Queensland, Ian Frazer and Jian Zhou have been accorded priority under U.S. patent law for the invention of the HPV vaccine's basis, which is the HPV VLPs [90].

Heretofore, three HPV vaccines have been licensed, and the main component of all of them is a protein subunit of HPV, capsid protein L1, which self-assembles to form VLPs. These three vaccines are multivalent. Gardasil® (2006, Merck & Co.) manufactured in yeast cells (*Saccharomyces cerevisiae*), Cervarix® (2009, Glaxo-SmithKline) manufactured in baculovirus/insect cell expression system, and Gardasil®9 (2014, Merck & Co.) manufactured in *S cerevisiae* yeast cells are quadrivalent (genotypes 6, 11, 16, and 18), bivalent (genotypes 16 and 18), and 9-valent (genotypes 6, 11,18 16, 18, 31, 33, 45, 52, and 58), respectively. The tetravalent Gardasil® has been replaced by nonavalent Gardasil®9 so that Cervarix® and Gardasil®9 are currently used to prevent HPV infections. The second generation of HPV vaccines has been sought and new approaches has been tested such as the inclusion of another capsid protein L2 beside L1 and the addition of other important genotypes (Please see more details in the section “1.10 VLP-based HPV vaccine”).

1.5 Animal models for HPV vaccines

Due to the species-specificity of the papillomaviruses, animal efficacy trials had to be done with the animal equivalent of the vaccine. Firstly, biological effects of non-human papillomaviruses in non-human models were studied to form the groundwork. The vaccine based on bovine papilloma virus (BPV) VLPs was found to protect against the bovine papillomavirus in cattle, and subsequent species-specific versions of the VLP vaccines were tested in rabbits and dogs. The vaccinated animals produced high levels of antibodies and the vaccines were at least 90 percent effective at preventing warts following exposure to papillomavirus. Afterwards, it is confirmed that VLPs of human papillomaviruses induced a sufficient immune response in non-human primates.

1.6 Structure, genome and life cycle of Human immunodeficiency virus (HIV)

HIV-1 is a human enveloped retrovirus belonging to the family Retroviridae and the subfamily lentivirus. The virus has a spherical spike-like structure and is around 100 nm in diameter. HIV-1 has two copies of a positive-sense single stranded ribonucleic acid (RNA) genome, which is reverse transcribed into double-stranded deoxyribonucleic acid (DNA), and subsequently integrated into the DNA of the human chromatin [8] (Figure 7). The HIV-1 genome is about 9800 bp in size and consists of three large open reading frames (Gag, Pol and Env) and six smaller genes that encode regulatory HIV-1 protein expression, Tat (transactivator of transcription) and Rev (regulator of viral protein expression), as well as accessory proteins Vif (viral infectivity factor), Vpr (viral protein R), Vpu (viral protein U) and Nef (negative factor), encoding 9 genes all together [10, 11]. The entire genome is flanked at the 5'and 3' end by long terminal repeats (LTR) which are important for reverse transcription and polyadenelation. The three open reading frames are initially translated as polyprotein precursors encoding structural proteins and enzymes. The polyprotein precursors are processed by viral and cellular proteases to produce mature viral proteins [10].

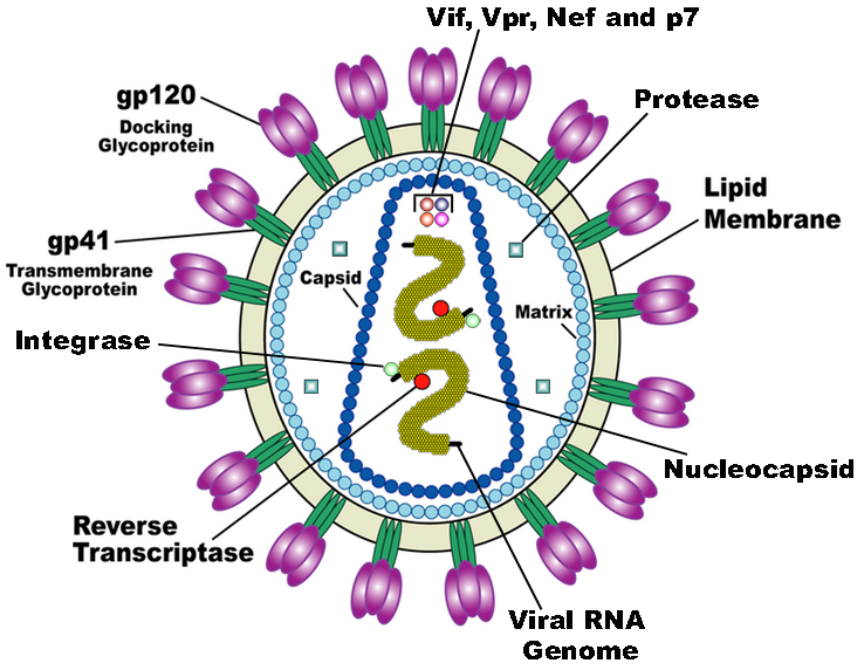

Figure 7. HIV viral structure. Illustration of HIV-1 structure, the membrane and proteins [8].

The Gag open reading frame is translated to produce a 55 kDa precursor protein (Pr55) called assemblin, due to its role in viral assembly. The Pr55 polyprotein is integrated into the budding virus, where it is cleaved by viral protease during and after budding of the virus. This leads to the formation of a myristoylated matrix (p17), which lines the inner envelope of the virus particle: the capsid (p24) which forms the virus core containing the RNA genome, enzymes and accessory proteins; the nucleocapsid (p7), that coats the RNA genome within the virus: a C-terminal domain (p6) which is necessary for budding of the virus and two short spacer peptides SPI (p1) and SP2 (p2) that separate the capsid from the nucleocapsid. While the matrix, capsid and nucleocapsid are common to all retroviruses, the presence of a p6 domain at the C- terminus of the Gag polyprotein is a special feature of HIV-1 and other primate lentiviruses [91].

The Pol gene is translated from a 160 kDa Gag-Pol precursor polyprotein (pr160) produced by a ribosomal frame shift. During viral maturation, the Pol polypeptide is cleaved away from Gag and is digested further into the viral enzymes reverse transcriptase (RT) involved in the transcription of the double stranded DNA (dsDNA) from RNA; Protease (PT) RNAse H and Integrase (IN) which allows the integration of the dsDNA into the host cell genome [92].

The open reading frame of Env is translated into a precursor glycoprotein gp160 which is processed and cleaved by cellular proteolytic enzymes producing the gp41 transmembrane and gp120 external glycoprotein. The Env mediates virus attachment and entry into target cells due to the gp120 surface subunit containing the CD4 receptor binding site. The gp120 is structured as three glycoproteins and is associated non- covalently with three membrane-anchored gp41 subunits [93].

The Tat gene encodes for a 14 kDa protein. It is one the first proteins to be expressed after infection and is a key activator of HIV-1 transcription. It is a RNA binding protein that recognizes a structure known as transactivation response element (TAR) located at the 5' terminus of the viral transcript [10, 11]. Rev gene encodes a 19 KDa phosphoprotein and is an essential viral regulatory factor for HIV protein expression. It acts by binding to the Rev response element (RRE) present on spliced and unspliced transcripts [94]. The RRE is encoded within the Env region and is essential for Rev function [10, 11]. Rev escorts unspliced or incompletely spliced viral pre-mRNA's out of the nucleus of infected cells [10, 11, 95]. Nef gene encodes a 27-35 kDa myristoylated protein. It is one of the first proteins produced in

infected cells and has been shown to downregulate a variety of host receptors, including CD4, Major histocompatibility complex (MHC) class I, CD28 and CXCR4. It is involved in viral replication and pathogenesis [9] (Figure 8).

Vif, Vpr and Vpu are three small genes in HIV-1 expressing accessory proteins. Vif gene encodes a 23 kDa cytoplasmic protein and is essential for viral infectivity. The lack of Vif renders free viruses defective in infecting cells, however cell to cell transmission is not affected [10, 11]. Vpr expresses a 14 kDa protein incorporated into the virion. It increases the rate of viral replication and accelerates the cytopathic effect of the virus on T cells and is essential for viral replication in macrophages. Vpr is associated with the induction of immune activation by depleting regulatory CD4 T cells which have a propagation of CCR5-tropic. Vpu gene encodes a 16 kDa type 1 transmembrane protein that is unique to HIV-1 and some simian immunodeficiency virus (SIV). The Vpu protein downregulates the CD4 receptor in the endoplasmic reticulum and enhances virion release from infected cells [10, 11] (Figure 8).

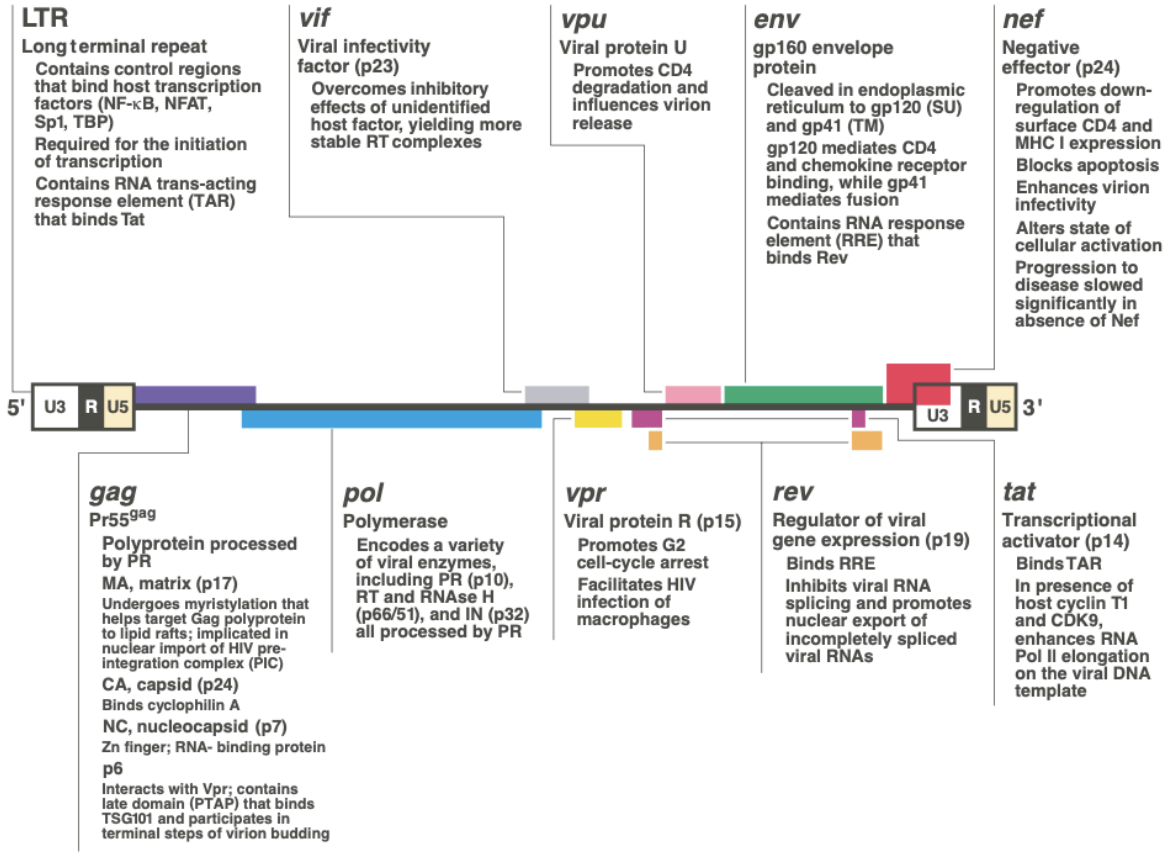

Figure 8. An overview of the organization of the ~9-kilobase genome of the HIV provirus and a summary of the functions of its nine genes encoding 15 proteins [9].

The HIV replication cycle begins when HIV fuses with the surface of the host cell [8] (Figure 9). A capsid containing the virus's genome and proteins then enters the cell. The shell of the capsid disintegrates and the HIV protein called reverse transcriptase transcribes the viral RNA into DNA. The viral DNA is transported across the nucleus, where the HIV protein integrase integrates the HIV DNA into the host's DNA. The host's normal transcription machinery transcribes HIV DNA into multiple copies of new HIV RNA. Some of this RNA becomes the genome of a new virus, while the cell uses other copies of the RNA to make new HIV proteins. The new viral RNA and HIV proteins move to the surface of the cell, where a new, immature HIV forms. Finally, the virus is released from the cell, and the HIV protein called protease cleaves newly synthesized polyproteins to create a mature infectious virus.

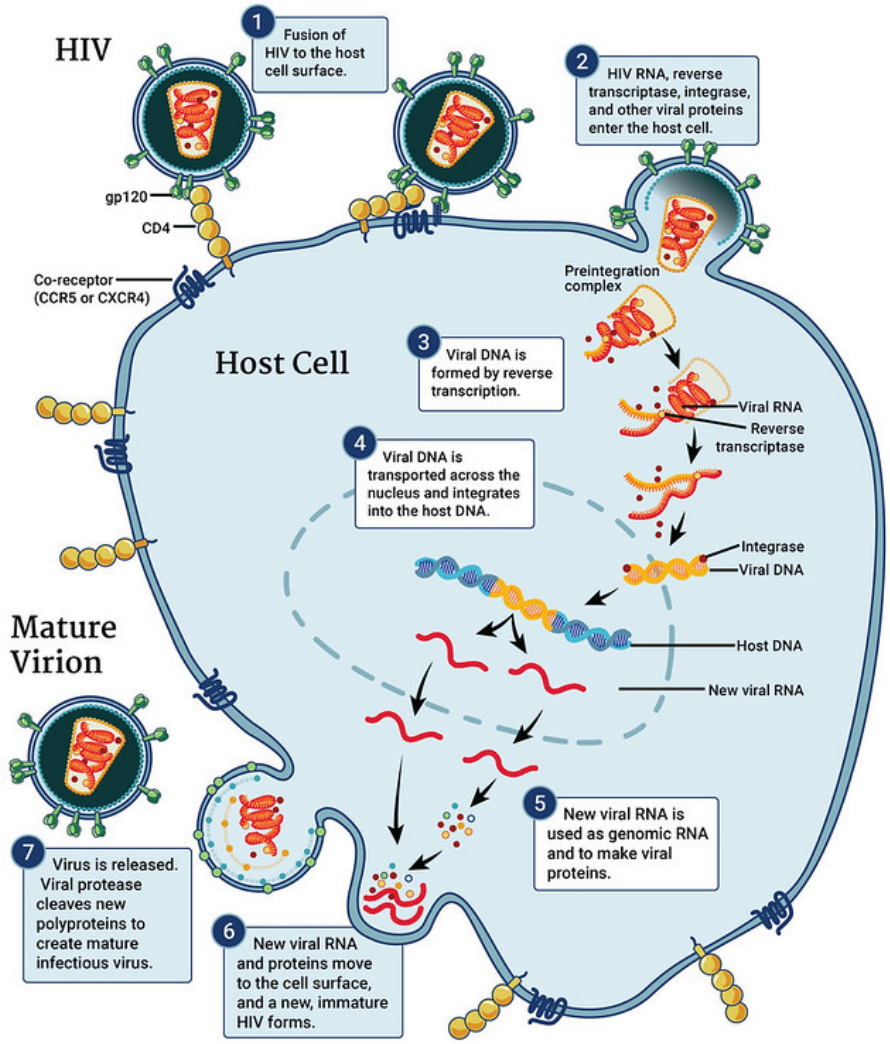

Figure 9. HIV life cycle [8].

1.7 Epidemiology of HIV/Acquired Immunodeficiency Syndrome (AIDS)

In 2019, approximately 38.0 million people globally were living with HIV, 1.7 million people became newly infected with HIV, 690 000 people died from AIDS-related illnesses [12] (Table 4). Since the start of the epidemic until the end of 2019, 75.7 million people have become infected with HIV and 32.7 million people have died from AIDS-related illnesses [12]. 26.0 million people were accessing antiretroviral therapy as of the end of June 2020 [12]. Effective treatment with antiretroviral therapy (ART) besides prevention of new infections among key populations have helped in the fight against the HIV/AIDS pandemic. However, only 67% of HIV-infected individuals were accessing antiretroviral therapy in 2019 [12]. Among 38.0 million people living with HIV, 36.2 million are adults and 1.8 million are children (0–14 years).

81% of all people living with HIV knew their HIV status while about 7.1 million people did not know that they were living with HIV.

	2000	2005	2010	2015	2016	2017	2018	2019/*2020
People living with HIV	**24.0 million** [20.0 million–28.2 million]	**27.3 million** [22.8 million–32.1 million]	**30.7 million** [25.6 million–36.1 million]	**34.9 million** [29.1 million–40.9 million]	**35.7 million** [29.8 million–41.9 million]	**36.5 million** [30.4 million–42.8 million]	**37.3 million** [31.0 million–43.6 million]	**38.0 million** [31.6 million–44.5 million]
New HIV Infections (total)	**2.7 million** [2.0 million–3.7 million]	**2.4 million** [1.8 million–3.2 million]	**2.1 million** [1.6 million–2.9 million]	**1.9 million** [1.4 million–2.5 million]	**1.8 million** [1.3 million–2.4 million]	**1.8 million** [1.3 million–2.4 million]	**1.7 million** [1.2 million–2.3 million]	**1.7 million** [1.2 million–2.2 million]
New HIV infections (aged 15+)	**2.2 million** [1.7 million–3.0 million]	**1.9 million** [1.4 million–2.6 million]	**1.8 million** [1.4 million–2.5 million]	**1.7 million** [1.2 million–2.3 million]	**1.6 million** [1.2 million–2.2 million]	**1.6 million** [1.2 million–2.1 million]	**1.5 million** [1.1 million–2.1 million]	**1.5 million** [1.1 million–2.0 million]
New HIV infections (aged 0–14)	**480 000** [300 000–750 000]	**440 000** [280 000–700 000]	**310 000** [200 000–500 000]	**190 000** [120 000–290 000]	**180 000** [110 000–280 000]	**170 000** [110 000–270 000]	**160 000** [99 000–250 000]	**150 000** [94 000–240 000]
AIDS-related deaths	**1.4 million** [1.0 million–2.0 million]	**1.7 million** [1.2 million–2.4 million]	**1.1 million** [830 000–1.6 million]	**830 000** [610 000–1.2 million]	**800 000** [580 000–1.1 million]	**760 000** [550 000–1.1 million]	**730 000** [530 000–1.0 million]	**690 000** [500 000–970 000]
People accessing antiretroviral therapy*	**590 000** [590 000–590 000]	**2.0 million** [2.0 million–2.0 million]	**7.8 million** [6.9 million–7.9 million]	**17.2 million** [14.7 million–17.4 million]	**19.3 million** [16.6 million–19.5 million]	**21.5 million** [19.5 million–21.7 million]	**23.1 million** [21.8 million-23.4 million]	**25.4 million** [24.5 million-25.6 million]/ **26.0 million** (mid 2020)
Resources available for HIV (low- and middle-income countries)*	**US$ 4.8 billion****	**US$ 9.4 billion****	**US$ 15.0 billion****	**US$ 18.0 billion*****	**US$ 18.4 billion*****	**US$ 19.9 billion*****	**US$ 19.0 billion*****	**US$ 18.6 billion*****

* As of the end of June 2020, 26.0 million [25.1 million–26.2 million] people were accessing antiretroviral therapy.
** Constant 2016 dollars
*** Includes countries classified as low- and middle-income level per the World Bank 2012 classification.
**** Includes countries classified as low- and middle-income level per the World Bank 2013 classification.

Table 4. Global HIV data [12].

By region, HIV infection is most prevalent in "Eastern and southern Africa" followed by "Asia and the Pacific" and "Western and central Africa" [12] (Figure 10).

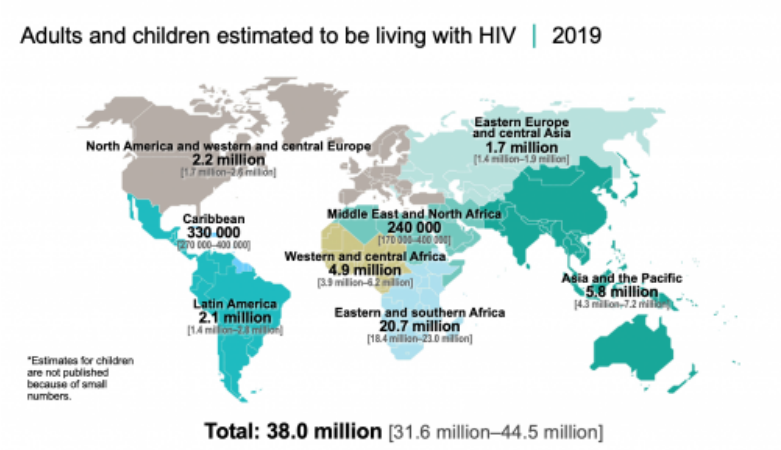

Figure 10. The total number of people living with HIV across the world in 2019 [12].

According to UNAIDS data [43], in 2019, in Spain, people newly infected with HIV were 2700, the number of people living with HIV were approximately 150,000, 130,000 of which are on

antiretroviral therapy (ART), and the deaths due to AIDS were less than 1000. Even locally, in Catalonia, according to data from the Center for Epidemiological Studies on STIs and AIDS in Catalonia (CEEISCAT) [44], an estimated 33,736 people live with HIV throughout the Catalan territory. A total of 471 new HIV cases were diagnosed in Catalonia in 2019 fell by 23.2% compared to 2018. Around 91% of Catalans infected with HIV have been diagnosed, 90% of them are in treatment and 93% have an undetectable viral load.

1.8 HIV-specific immune responses

After HIV infection, there are mainly two different phases, acute phase and chronic phase without any ART treatment. At the acute phase, the number of CD8+ lymphocytes and the plasma virus load increase while the number of CD4+ lymphocytes decrease [45]. And in chronic phase, the number of CD4+ and CD8+ lymphocytes decrease mildly while the plasma virus load stays low until the reach to AIDS (Figure 11).

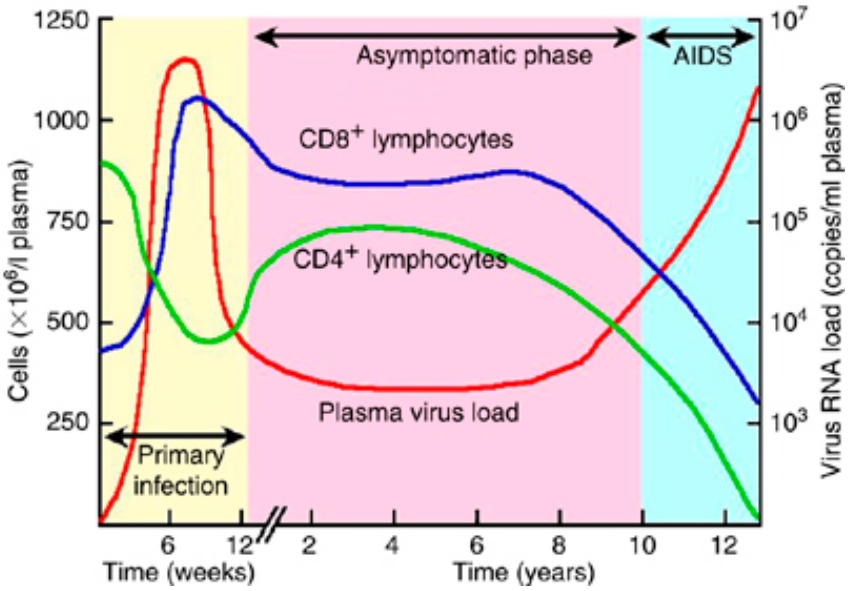

Figure 11. Schematic of typical course of HIV-1 infection showing changes in CD4 and CD8 T-cell counts in peripheral blood and plasma virus RNA load [45].

As for humoral immunity against HIV, during the first weeks of acute infection, HIV envelope-specific IgM and IgG antibodies are produced sequentially to a number of epitopes (gp41, gp120, V3 loop, CD binding site, and MPER) and are non-neutralizing but capable of inducing Fc-mediated functions, such as antibody-dependent cellular cytotoxicity (ADCC) by natural killer (NK) cells [96]. The first neutralizing antibody responses appear after months of infection

and are specific to autologous viral strains. Over the following years, some individuals spontaneously control infection. These individuals harbor innate immune-recruiting antibodies. Broadly neutralizing antibody responses, conversely, evolve largely in individuals who fail to control infection (Figure 12).

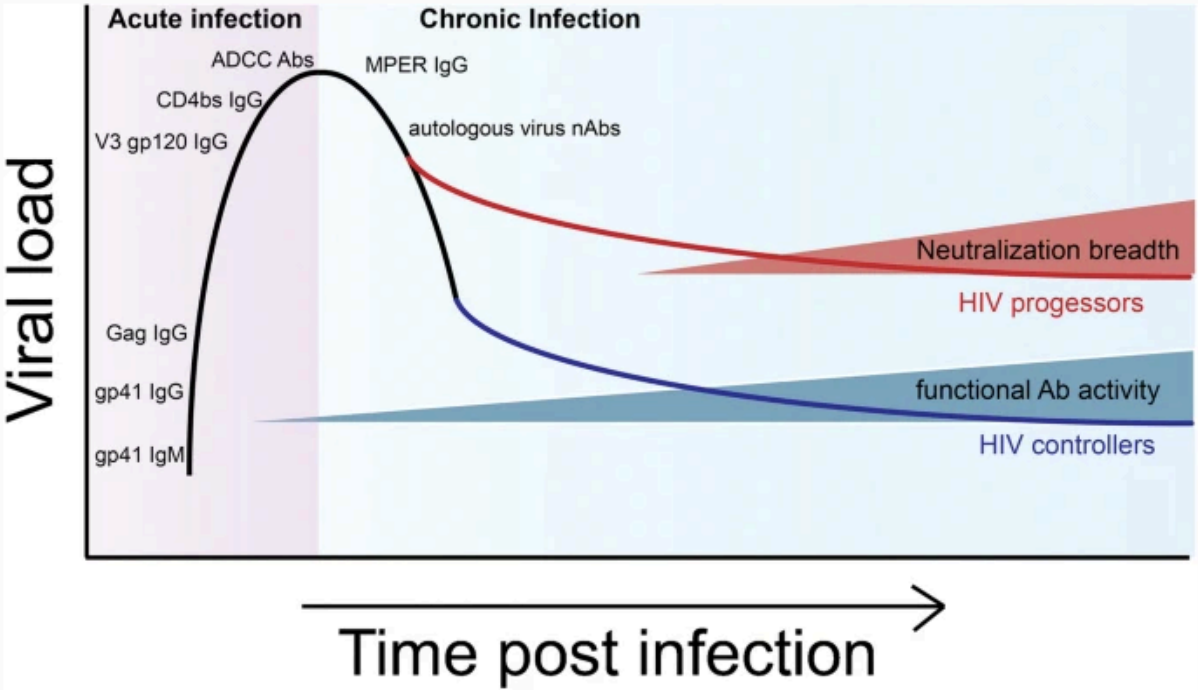

Figure 12 Humoral immunity timeline in HIV [96].

1.8.1 Innate immune response to HIV

Innate immune cells such as dendritic cells and natural killer cells are the first line of defense which HIV encounters upon entry to the body [14]. Tissue macrophages are one of the target cells for HIV. These macrophages harbor the virus and are known to be the source of viral proteins. However, the infected macrophages are shown to lose their ability to ingest and kill foreign microbes and present antigen to T cells. This could have a major contribution in overall immune dysfunction caused by HIV infection. Dendritic cells (DCs) are large cells with dendritic cytoplasmic extensions [52]. These cells present processed antigens to T lymphocytes in lymph nodes. Epidermal DCs, expressing CD1a and Birbeck granules, are probably among the first immune cells to combat HIV at the mucosal surfaces. These cells transport HIV from the site of infection to lymphoid tissue. The follicular DCs, found in lymphoid tissue, are also key antigen-presenting cells that trap and present antigens on their cell surfaces. In the lymph node follicles, DCs provide signals for the activation of B lymphocytes. Natural killer (NK) cells have lytic activity against cells that have diminished

expression of major histocompatibility complex (MHC) I antigens [51]. Because the presence of MHC class I is required for peptide presentation to T cell receptors, NK cells are important line of defense when HIV escapes the cellular immune response. NK cells proliferate in response to type 1 interferon secreted by DCs [51]. These stimulated NK cells release cytokines such as interferon γ (IFN-γ), tumor necrosis factor α (TNF-α), and chemokines to activate T-cell proliferation (cellular immune response) and also inhibit viral replication by releasing IFN-γ [52].

1.8.2 Adaptive immune response to HIV

The cellular immune response to HIV is induced upon the entry of HIV into the target cells (e.g., T cells) and synthesis of viral proteins [14]. MHC class I on the cell surface displays the intracellularly degraded HIV peptide fragments for recognition by T-cell receptors (TCR) on CD8+ T cells. CD8+ T cells lyse HIV infected cells and secrete cytokines, i.e. interferon-γ (IFN-γ), tumor necrosis factor α (TNF-α), and chemokines, i.e. MIP-1 α, MIP β and RANTES, that inhibit virus replication and block viral entry into CD4+ T cells [53]. Development of CD8+ T cells is crucial for control of HIV replication. This results in declining viremia after primary infection. In the early stages of infection, CD4+ T cells lose their proliferative capacity and therefore their contribution to viral control is minor. However, during chronic infection CD4+T cells are present and secrete interleukin-2 (IL-2) or cytokines, such as IFN-γ, to control viremia [51].

The humoral immune response against HIV occurs in 3 months after the infection; therefore, the level of antibodies during the acute infection is very low. Non-neutralizing antibodies to structural proteins (i.e. P17 and P24) are first to appear and generally do not persist. Later neutralizing antibodies specific to proteins, involved in the entry of the virus into the cells, will be generated. These antibodies are specific to: (1) the variable region of gp120 (V3); (2) CD4 binding sites and chemokine receptors (i.e., CXCR4 and CCR5); (3) the transmembrane protein gp41 [55]. Potent neutralizing antibodies have been shown to play a major role in controlling HIV infection in a few symptom-free HIV+ individuals who maintain high level of CD4+ T cells and low viral load. Elite controllers (ECs) are individuals who are not on antiretroviral therapy, but are able to control viral load below the levels of detection of

commercial assays. Autologous neutralizing antibodies are the antibodies generated by infected individuals in response to their own virus. Heterologous neutralizing antibodies are neutralizing antibodies against a more diverse range of viral isolates, which are called broadly neutralizing antibodies (bNAbs). Several bNAbs have been well characterized: three (b12, 447-52D, and 2G12) recognize epitopes on the conformationally conserved outer domain of gp120 [56-58], and the others (2F5, Z13, and 4E10) recognize epitopes on the membrane proximal external region (MPER) of gp41 [59-60] (Table 5).

Table 5. Broadly neutralizing antibodies against HIV [55].

Broadly neutralizing antibody	Epitope recognized	Description of epitope
4E10	MPER of HIV-1 gp41	NWFNIT, may have cross-reactivity with cardiolipin
2F5	MPER of HIV-1 gp41	ELDKWA, may have cross-reactivity with cardiolipin
Z13	MPER of HIV-1 gp41	WNWFDITN
447-52D	gp120	Conformationally conserved epitope on outer domain of gp120
B12	gp120	Conformationally conserved epitope on outer domain of gp120

1.9 Current status of HIV vaccine development

In 1984 HIV was identified as the cause of AIDS and The United States Department of Health and Human Services declared that an AIDS vaccine will be ready for testing within two years [97, 98]. In 1987, The first HIV vaccine clinical trial opened at the National Institutes of Health (NIH) Clinical Center in Bethesda, Maryland. This Phase 1 trial enrolled 138 healthy, HIV-negative volunteers and the gp160 subunit vaccine showed no serious adverse effects [98].

Since then, although HIV vaccine studies have been held over 35 years, none of the HIV vaccine candidates has shown to be protective enough. The best obtained result so far is 31.2% vaccine efficacy in the clinical trial RV 144 [64]. While broadly neutralizing antibodies (bNAbs) against HIV are considered as a crucial factor to prevent HIV infection, it does not seem sufficient and the induction of HIV-specific T-cell-mediated immune responses is also

essential to develop a prophylactic vaccine against HIV. In other words, an optimal HIV vaccine should induce innate mucosal, humoral, and cellular immunity specific for HIV. Another difficulty in developing preventive HIV vaccines is HIV's high mutation rates and genetic diversity so that designing a universal and cross-clade HIV vaccine is extremely challenging. Therefore, several researchers have been currently aiming to select and target more conserved regions/epitopes to their HIV vaccine models. For example, HIV-1 vaccine candidates containing HIV envelope glycoprotein gp120 (bivalent) or gp140 (trimeric) are now being tested in human vaccine efficacy trials [102] and they have great potential to be applied to develop chimeric HPV/HIV VLP-based vaccines by incorporating them into the HPV L1 VLP. In addition, disulfide-stabilized, cleaved trimeric form of HIV-1 gp140, SOSIP, which displays conformational epitopes recognized by bnAbs is going to be tested in Phase I clinical trial [60]. For T-cell immunogens against HIV-1, mosaic immunogens, which were designed to provide maximum coverage of conserved regions of HIV-1, have been studied [61]. Another candidate, the "HIVACAT T-cell immunogen" (HTI), which was designed to cover T-cell targets, against which T-cell responses are predominantly observed in HIV-1-infected individuals with low HIV-1 viral loads, has also been investigated [62].

1.10 Animal model for HIV vaccines

Finding perfect animal models to evaluate protective effect of vaccine candidates is one of other big issues. Several alternative animal models have been developed to study HIV-1 infection *in vivo*. In the case of small animals that are amenable to genetic manipulation, such as mice, efforts have focused on the development of immunodeficient mice engrafted with cells or tissues from the human immune system to provide the virus with susceptible target cells for replication. In the case of larger animals, such as primates, research has focused on the use of simian immunodeficiency virus (SIV) or simian–human immunodeficiency virus (SHIV) recombinants. Thus, there is no single animal model for HIV-1 infection, but rather a variety of host species and viruses that can be used depending on the question to be addressed [65]. Nowadays, the humanized mouse model has also been considered as an alternative animal model to assess immunogenicity and protection as it can mimic the human immune system. Furthermore, the conformational changes and glycan shield of the HIV envelope are other challenges for the development of an effective HIV-1

vaccine. Finally, understanding the immune correlates of protection against HIV-1 would be an important key to develop an efficacious HIV-1 vaccine.

1.11 Expression systems for VLP production

Virus-like particles (VLPs) are a type of subunit vaccine which resembles viruses but do not contain any genetic material so that they are not infectious. VLPs maintain the same antigenic conformation to the original virus, and they could be a better vaccine candidate than live-attenuated and inactivated vaccines. In addition, compared to other subunit vaccines such as soluble protein, VLPs can stimulate both innate and adaptive immune responses effectively and safely against several pathogens by the closer morphology to its native virus. They have already been licensed as vaccines against Hepatitis B virus, human papillomavirus (HPV), and several veterinary diseases. Moreover, it has been investigated to prevent other viral infections including HIV.

There are mainly five different expression systems to produce VLPs: Bacteria (mainly *E. coli*), yeast, insect cells, mammalian cells, and plant cells and each system has merits and demerits [16, 66] (Tables 6, 7). For example, while *E. coli* has low production cost, ease of expression, and ability to scale-up, it does not allow for glycosylation so that it is not ideal to express complex protein [66]. On the other hand, mammalian cells can produce VLPs more accurately as they are more closely related to the natural host, it has higher production cost. Therefore, expression systems for VLP production must be chosen, depending on available equipment, budget and feasibility. In our study, we chose to use one type of yeast, *Pichia pastoris* because *P. pastoris* is a well-studied methylotrophic yeast harboring an extensive toolbox for genetic engineering and is more easily scalable to industrial production than another yeast *S. cerevisiae* [99]. Specifically, it provides high levels of heterologous protein expression and rapid growth on relatively simple defined media to very high cell densities, so that it is cheap to use while it could give a better yield compared to other yeast expression systems thanks to the use of the strong Glyceraldehyde-3-phosphate dehydrogenase (GAP) and the Alcohol oxidase (AOX) promoters. In addition, heterologous gene expression in *P. pastoris* by using DNA expression vectors require less manipulation than the baculovirus expression system, where one step of cell culture growth (sf9 or sf21 cells) and one step of infection and protein harvest are needed [100].

Table 6. Advantages and disadvantages of the different VLP production platforms [16].

VLP expression system	Merits	Demerits
Bacteria	Less expensive; simplicity of expression; fast growth rate; high-level expression; genetic stability; simple process scale-up	Lack mammalian-like PTM; Poor ability on immunogenicity; Presence of host cell-derived contaminants
Yeast	Less expensive; high-density fermentation; modification of the expression protein; moderately rapid expression; support most protein folding and PTM	High mannose modification; some secretory proteins cannot get ideal results; enhanced safety precautions are required
Insect cells	Moderately rapid expression; support most protein folding and eukaryotic-type PTM of the expression protein; works well for non-enveloped and enveloped VLPs, free of mammalian pathogens	High cost; difficult to scale-up; incomplete modification of proteins; low-level expression, contamination of product with enveloped baculovirus particles; perform simpler *N*-glycosylation compared to mammalian cells
Mammalian cells	Perform appropriate complex mammalian-type PTMs; perform authentic assembly and folding of recombinant proteins; works well for non-enveloped and enveloped VLPs	High cost; difficult to scale-up; lengthy expression time; low yield; vulnerable to infection with mammalian pathogens
Plant cells	Rapid expression; highly scalable; less expensive; free of mammalian pathogens; support most protein folding and eukaryotic-type PTM	Low yield; technical and regulatory issues

Table 7. Advantages and disadvantages of the different VLP production platforms [66]

Production platform	Advantages	Disadvantages
E. coli	• Ease of expression • Ability to scale-up • Low production cost	• Does not allow for glycosylation. • Endotoxins
Yeast	• Ease of expression • Ability to scale-up • Low production cost	• Non-appropriate protein glycosylation (i.e. high mannose glycoprotein modification). • Risk of incorrect folding & assembly.
Insect cells	• Can produce large amounts of correctly folded VLP in high density cell culture conditions • Ability to scale-up • The risk of culturing opportunistic pathogens is minimised compared to mammalian cell culture • Host-derived insect cell/baculovirus components may act as vaccine adjuvants, help trigger a more effective immune response	• Limited to high mannose glycoprotein modification. • Baculovirus contaminants may be difficult to remove • Host-derived insect cell/baculovirus components may also mask the immune response against the desired epitope
Mammalian cells	• Producer cells more closely related to the natural host • Appropriate PTMs and authentic assembly of VLPs	• Higher production cost • Lower productivities
Plants	• Ease of expression • Ability to scale-up • No human-derived virus contamination	• Cannot undergo PTMs and VLP assembly • Low expression levels • Stability: antigen degradation

1.12 Current status of VLP-based HPV vaccine

While VLP-based HPV vaccines are already in the market, the second-generation of VLP-based preventive HPV vaccines has been developed and tested preclinically. Regarding the production system, different species of yeast such as *Pichia pastoris* and *Hansenula polymorpha* have potential to produce L1 protein with lower cost and higher yields compared to Saccharomyces cerevisiae used for Gardasil® and Gardasil®9, or compared to the baculovirus/insect cell (Hi-5 Rix4446 cells derived from the insect Trichoplusia ni) expression system used for Cervarix. Based on the fact that the antibodies against minor papillomavirus (PV) capsid protein L2 have a cross-neutralizing activity, monovalent L1 expressing RG1 epitope (aa17-36 of capsid protein L2) might work to protect from other HPV genotype infections [101] (Figure 3). Moreover, Novartis Vaccines and Diagnostics (Emeryville, CA, USA)

stated a method to generate yeast-expressed mosaic VLPs composing both HPV-6 and -16 L1 proteins. Furthermore, as vehicles of edible HPV vaccines, Asahi Glass (Kanazawa, Japan) patented a recombinant yeast *Schizosaccharomyces pombe* expressing HPV-16 L1 protein, and Genome, Inc. (Pohang, Korea) patented transgenic plants expressing recombinant HPV L1. These edible vaccines were developed with the intention of lowering the cost of HPV vaccine and improve its availability regardless of regions and poverty. Ultimately, an ideal preventive HPV vaccine should protect vaccinees from all 15 of the high-risk HPV genotypes.

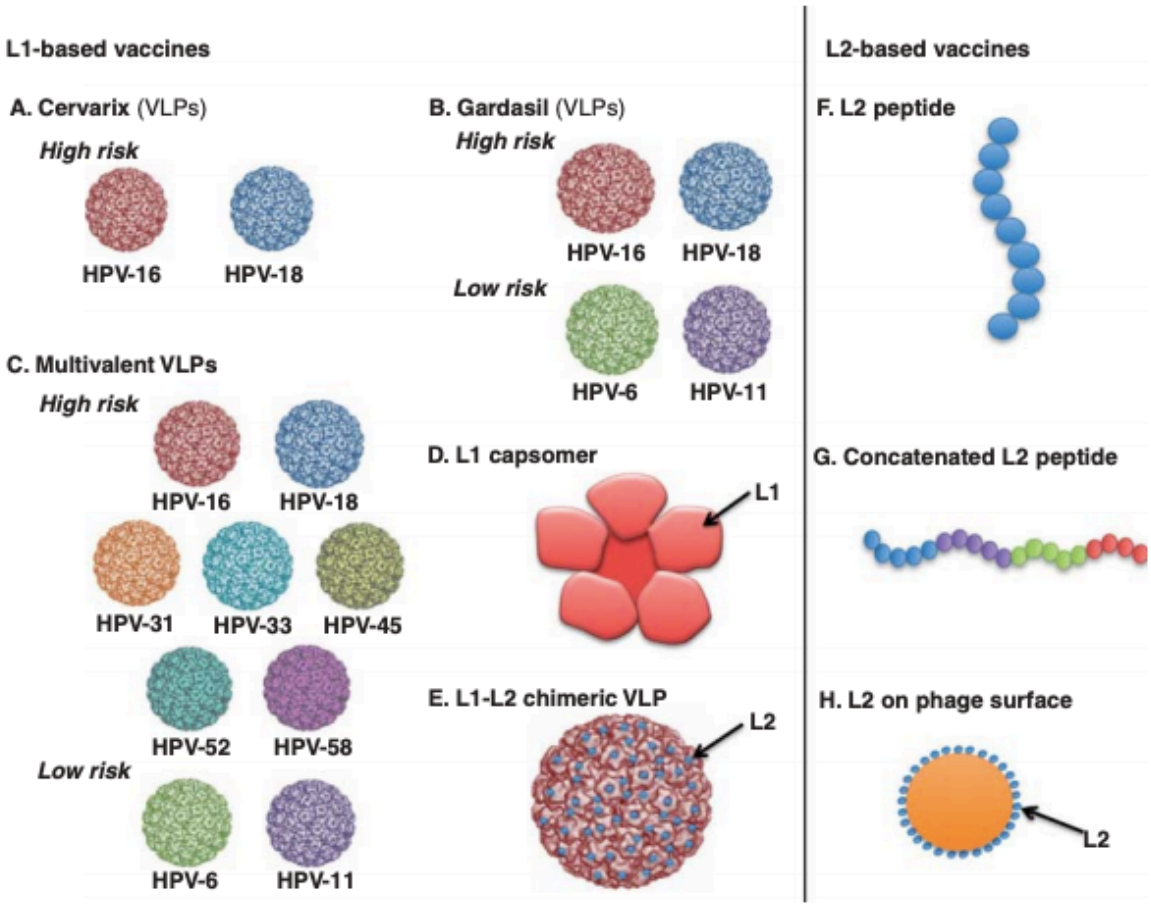

Figure 13. Schematic diagram to depict the next generation of preventive HPV vaccines based on HPV capsid proteins (L1 and/or L2) [101]. A. Cervarix composed of HPV-16 and HPV-18 VLPs. B. Gardasil composed of HPV-6, HPV-11, HPV-16 and HPV-18 VLPs. C. Multivalent VLP vaccines composed of HPV-6, HPV-11, HPV-16, HPV-18, HPV-31, HPV-33, HPV-45, HPV-52 and HPV-58 VLPs (V503 Merck). D. L1 capsomer vaccine. E. Chimeric L1-L2 VLP vaccine with L2 on the surface. F. L2 peptide vaccine. G. Concatenated L2 peptide vaccine. H. L2 peptides displayed on the surface of bacteriophage VLP.

1.13 HPV VLP immunogenicity

All immunogenicity studies have been focused on neutralizing antibodies rather than T-cell mediated immunity because the neutralizing antibodies have been shown to have the main

role in the prevention of HPV infection as considered in the commercial vaccines. Interestingly, both Gardasil® (genotypes 6, 11, 16, and 18) and Cervarix® (genotypes 16 and 18) showed cross-protection against HPV-31 and HPV-45 due to their similarity to HPV-16 and HPV-18. This suggests that Gardasil® 9 and the next generation of HPV VLP vaccines should be evaluated if they can reduce the incidence of infection with other HPV genotypes be- sides the targeted ones by cross-protection. Recently, in 2017, Huber et al. created HPV L1-L2-based VLP targeting cutaneous HPV. Minor capsid protein L2 was considered to extend the genotype- restricted protection generated by the current HPV L1- based vaccine. It showed not only humoral immunity against HPV genotypes included in the VLPs, also had cross protections against other HPV genotypes, and this could be a promising next-generation HPV vaccine candidate. In favor of facilitating vaccine administration, non-needle injection routes such as nasal and oral administration should be considered. In addition, further studies of dose-route responses should be performed and compared with three-dose immunization schedule.

1.14 Current status of VLP-based HIV vaccine

Although VLP-based HIV vaccine studies have been held over 30 years, none of the HIV VLP vaccine candidates has shown to be protective enough. A few of them have successfully reached clinical trials but were not assessed in efficacy trials due to low immunogenicity and safety properties. However, several important factors have been found regarding its immunogenicity in comparison to subunit proteins. In general, HIV VLPs could induce stronger humoral and cellular immunity than HIV recombinant proteins or other Subunit vaccines (SUVs). As HIV-1 polyprotein precursor can form 100 nm to 120 nm VLP, Gag-based and Env-based VLPs were studied separately first, and then chimeric Env-Gag HIV VLPs have been targeted as a vaccine model to improve immunogenicity. Furthermore, chimeric VLPs of HIV and other viruses such as influenza virus, Bovine/HPV (B/HPV), and hepatitis E virus have also been studied. Nowadays, for the sake of enhancing VLP-derived immune responses, especially T-cell mediated immunity, delivering VLPs with different adjuvants such as toll-like receptors have been assessed, and it is known that nonmethylated CG motifs could generate higher T-cell mediated cytotoxicity when they were codelivered with VLPs. Moreover, recent studies suggest that the exposure of highly conserved epitopes

of HIV Env by removing glycosylation sites could improve the production of broadly neutralizing antibodies (bNAbs) by HIV Env-based VLPs. In addition, natural killer cell immune responses were mediated by Gag-VLP through activating and maturating DCs. Furthermore, although DC-based immunization is still intricate, DCs loaded with HIV-1 VLP was suggested to be used as a supplementary boost regimen for HIV-1 VLP vaccination because DCs are potent and indispensable antigen-presenting cells to induce HIV-1 specific humoral immunity. What is more, a few independent non-human primate immunization studies with SIV Gag VLPs demonstrated cross-protection between SIV Env and Gag [15]. All the research groups detected elevated Env-specific or neutralizing antibody responses after SIV or SHIV challenge in rhesus macaques which were immunized with only SIV Gag VLPs. Another series of studies in small animal models demonstrated that membrane-anchored flagellin and CD40 ligand have been shown as effective adjuvants to enhance HIV-1-specific immune responses after incorporating various adjuvants into HIV-1 VLPs [15].

In addition, HIV VLPs have been also generated in several expression systems. Yeast expression system was used to produce HIV VLPs for the first time in 1987 by Adams et al. using the yeast retrotransposon, Ty, that encodes a set of proteins that are assembled into VLPs, Ty-VLPs [103]. They showed that the major structural components of Ty-VLPs were proteolytic products of the primary translation product, p1, and such protein p1 alone can form Ty-VLPs by itself. Moreover, they demonstrated that p1 fusion proteins, consisting of most of p1 and part of HIV-1 gp120 could form hybrid HIV: Ty-VLPs. In 2002, Sakuragi et al. produced HIV-1 p55 (Gag) VLPs by budding from yeast spheroplasts, in other words, yeast cells without cell wall [104]. However, to get spheroplasts, first, the cell walls needed to be gently enzymatically digested by Zymolyase-100T because thick yeast cell walls were considered as one difficulty to secret proper HIV VLP. Baculovirus/insect cell system was mainly chosen to produce HIV VLPs in 1990s and 2000s [105, 106], especially because of higher yields compared to yeast system. Recently, human embryonic kidney cells (HEK) 293 cells have relatively more efficient protein production than baculovirus/insect cell expression system and it has been the main expression system of HIV VLP production. HEK 293 cells have been adapted and can produce 1 mg/L of VLP or more in a few days and can produce gag-env VLPs. For example, Cervera et al. showed HIV-1 VLP production of 2.8 μg of recombinant Gag-GFP/ml of HEK 293 cell culture [107].

1.15 HIV VLP immunogenicity

Tsunetsugu-Yokota et al separated DCs end T cells from fresh peripheral blood mononuclear celle of non-infected and HIV-infected individuals and observed that pulsing DCs with 1 or 10 pg/mL HIV-1 Gag p55 VLP for 2 days induced perforin expression in Gag- specific CD8 T cells [108]. Furthermore, BALB/c mice were inoculated intradermally with 20 pg of HIV-1 Gag p55 VLPS twice at 3-week interval, and statistically significant anti-Gag humoral responses were detected [109]. Immunogenicity data with three types of HIV-1 Env-based VLPs were demonstrated by Crooks et al [110]. Guinea pigs were immunized with (i) "naked VLPs", which do not bear Env, (ii) "SOS-VLPs" bearing disulfide-shackled functional trimers, and (iii) "UNC-VLPs" that present uncleaved nonfunctional Env or soluble monomeric gp120 3 times on days 0, 43, and 97 by a combination of intradermal and intramuscular (i.m.) routes in two locations each. UNC- and SOS-VLPS immediately induced anti-gp120 antibodies while in naked VLP case, humoral immunity was barely detected after third dose. Ultimately, low level of neutralizing activity was found in all candidates. Tagliamonte et al administered 20 ug of HIV Gag p55-based VLPS presenting trimeric HIV-1 gp140 spikes in BALB/c mice subcutaneously twice at the 3-week interval and statistically significant anti-gp140 activity was obtained while anti-Gag activity was not analyzed [111]. Benen et al. assessed HIV Gag VLP-based immunogen presenting membrane proximal external region (MPER) of HIV-1 gp41 [112]. They demonstrated in an immunization study in rabbits that priming with DNA and boosting with VLPS generated that low titers of anti- MPER antibodies and low neutralizing activity. Poteet et al. inoculated HIV-1 Gag/Env VLPS with monophosphoryl lipid A (MPLA) adjuvant to C57BL/6 mice through different routes including a novel oral buccal cheek subcutaneous administration [113]. After trying several combinations of injection routes, they concluded that an intranasal prime sub-cheek boast regimen of HIV-1 Gag/Env VLPS with MPLA adjuvant has a strong potential to induce Env-specific Th1-oriented HIV-specific immune responses. Vzorov et al. specifically modified the transmembrane spanning (TMS) and cytoplasmic tail (CT) domains of HIV-1 Env [114]. They demonstrated that the immunization of guinea pigs by a construct containing a short version of the TMS domain induced the highest titers of anti-Env lgG immune responses. In addition, VLPs with high Env content and containing the CT Trimerization sequence improved neutralization activity and antibody avidity in guinea pig.

Beltran-Pavez et al demonstrated that rabbit immunization with HIV-1-Gag VLPS containing 4E10-selected envelope variant (LR1-C1) induced humoral responses to 4E10-proximal region. Taken as a whole, HIV VLPs can be safe and immunogenic using different immunization routes regardless of coadministration of adjuvants and should be continuously pursued to acquire an effective HIV vaccine.

1.16 Current Status of chimeric VLP-based HPV-HIV vaccine

To the best of our knowledge, the production of chimeric papillomavirus (PV)/HIV VLP was first described by Peng et al., using bovine papillomavirus (BPV)/HIV VLP to present HIV epitopes [116]. Afterward, Chackerian et al. published a research article regarding chimeric BPV VLP containing CCR5 coreceptor, which is required for HIV entry [117] (Table 8 and Figure 14). Henceforth, the production and immunogenicity data of BPV/HIV were introduced by Liu XS et al. [48, 49] and Liu WJ et al [50] and those data of HPV/HIV VLP by Dale et al [118]. In all cases, VLPs were produced by baculovirus/insect sf9 cell expression system. In 2013, Zhai et al. constructed BPV-1 L1 VLP harboring (i) B/T cell conserved epitopes from MPER of HIV-1 gp41 and (ii) the linear epitopes recognized by neutralizing monoclonal antibodies 2F5 and 4B10, which were inserted in D-E loop of L1 protein [119]. While all the previous VLPs were designed to add HIV epitopes into B/HPV L1-based VLPS, in 2009, the incorporation of HPV protein into HIV-1-based VLPS produced in HEK 293 cells was first reported by Bonito et al [120].

Table 8. Chimeric B/HPV-S/HIV VLP production and immunogenicity in small animal and non-human primate models

Year	Expression system	Cells	Recombinant proteins	Animal model	Route	Dose	Schedule	Immunogenicity	
1998	Baculovirus/ insect cells	Sf-9 cells	L1 (BPV-1) + P18-I10(HIV-1)	BALB/c mice	SC	20 μg	0, 2, 4 weeks	Anti-BPV1 VLP Ab and CTL	[116]
1998	Baculovirus/ insect cells	Sf-9 cells	L1 (BPV-1) + P18-I10(HIV-1)	C57BL/6J mice	IN, IM	50 μg × 2	Day 0, 21	IgG, IgA, CTL	[49]
1999	Baculovirus/ insect cells	Sf-9 cells	L1 (BPV-1) + mCCR5	C57BL/6 mice	ID	10 μg × 3	0, 2, 4 weeks	IgG, anti-CCR5 Ab, chemokine	[117]
2000	Baculovirus/ insect cells	Sf-9 cells	L1 (BPV-1) + P18-I10 (HIV-1) + RT (HIV-1) + Nef (HIV-1)	BALB/c mice C57BL/6J mice HLA-A2.1/K^b transgenic ($H\text{-}2^b$) mice	IM	20 μg × 2	Day 0, 21	IgG, CTL	[50]
2002	Baculovirus/ insect cells	Sf-9 cells	L1 (BPV-1) + V3/ P18-I10 (HIV-1)	BALB/c mice	IM, IVA, IR	50 μg × 2	Day 0, 14	IgG, IgA, CTL	[48]
2002	Baculovirus/ insect cells	Sf-9 cells	L1 (HPV6b) + P27 gag (SIV)/ tat (HIV-1)/ rev (HIV-1)	Pigtailed macaques	IM, IR	IM 20 μg × 7 as prime IR 20 μg × 3 as boost	8, 11, 14 weeks	AntiHPV L1 ab, IFN-Y, SHIV challenge	[118]
2004	Baculovirus/ insect cells	Sf-9 cells	L1 (BPV-1) + ptCCR5	C57BL/6 mice, pig-tailed macaques	Mice: SC, Macaques: IM	mice: 5 μg × 3 macaques: 20-25 μg × 9	Mice: 0, 2, 4 weeks Macaques: 9 times during>2 years	IgG, Challenge with S/HIV	[121]
2009	293 GPR HIV-1 inducible packaging cells	293 GPR HIV-1 inducible packaging cells	HIV-1 Nef+HPV16 E7	C57BL/6 mice	SC	10 μg × 3	0, 2, 4 weeks	IFN-Y	[120]
2013	Baculovirus/ insect cells	Sf-9 cells	L1 (BPV-1) + gp41 (HIV-1)	BALB/c mice	Oral	10 μg × 3	0, 2, 4 weeks	mAb, IgG, IgA, HIV neutralizing assay	[119]

SC: subcutaneous, ID: intradermal, IM: intramuscular, IN: intranasal, IP: intraperitoneal, BPV: bovine papillomavirus, HPV: human papillomavirus, SIV: simian immunodeficiency virus.

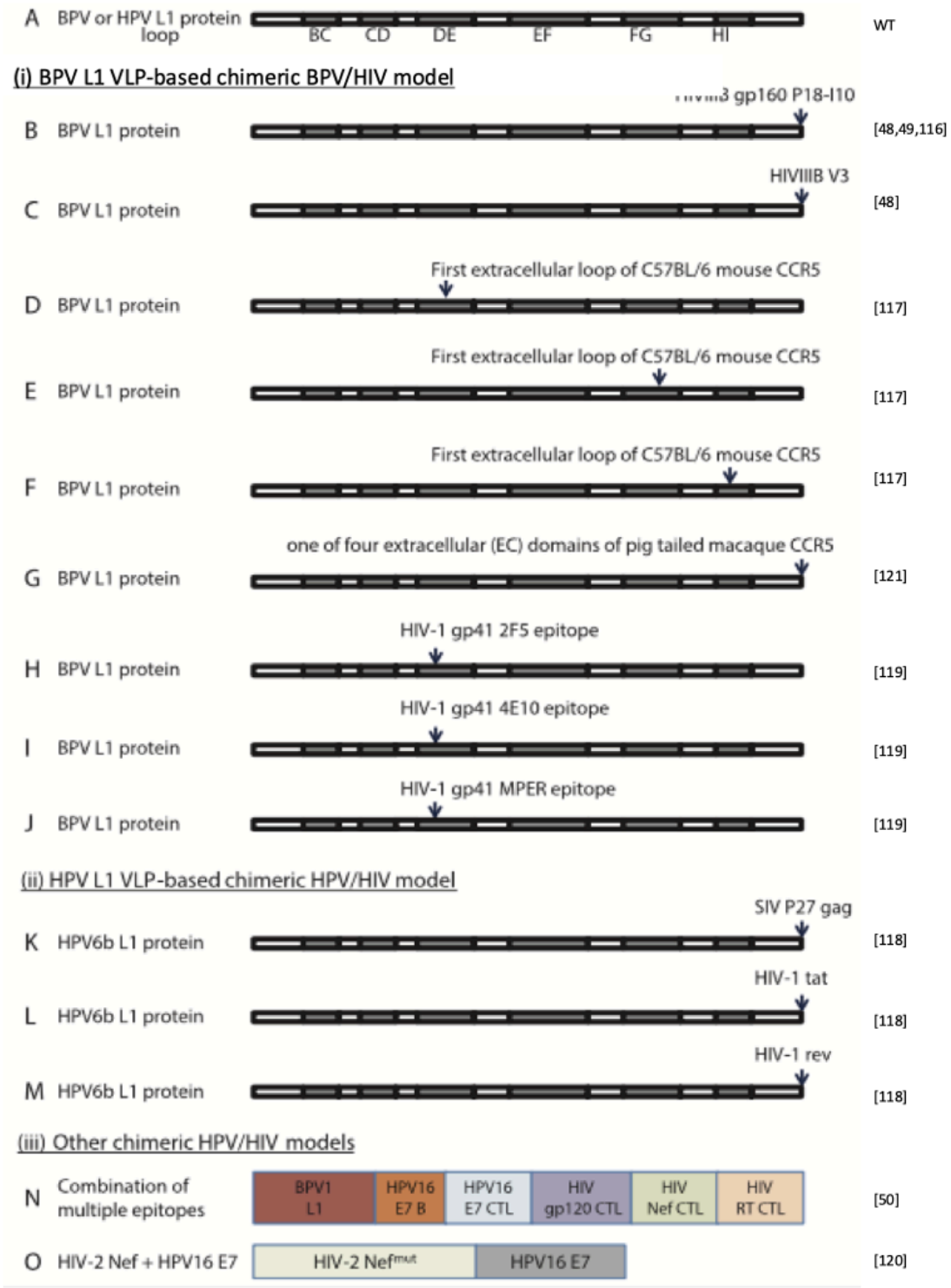

Figure 14. Schematic representation of chimeric B/HPV and S/HIV-1 proteins for virus-like particles (VLP)-based vaccine development (adapted from Sadeyen et al. [122]). A: Wild type model of B/HPV L1 protein. B-M: The insertion point of HIV protein in B/HPV L1 protein is indicated. 360 copies of each protein form a VLP. (i) BPV L1 VLP-based chimeric HPV/HIV model. B and C: HIV protein was inserted at C-terminal. D,H,J: D-E loop 130-136 of BPV1 L1 protein was replaced by mCCR5 or HIV-1 epitope. E: FG loop 275-285 of BPV1 L1 protein was replaced by mCCR5. F: HI loop 344-350 of BPV1 L1 protein was replaced by mCCR5. G: Purified BPV1L1 VLPs were biotinylated and EC domains were bound to those biotins. (ii) HPV L1 VLP-based chimeric HPV/HIV model. K-M: SIV or HIV protein was inserted at C-terminal. (iii) Other chimeric HPV/HIV model. N: BPV1L1, HPV16E7 B, HPV16E7 CTL, HIV1 P18-I10, HIV1 Nef CTL, and HIV RT CTL are combined as seen above. O: gag-pol-nef HIV VLPs with modification at nef c-terminal by HPV16 E7 were produced. BPV: bovine papillomavirus; HPV: human papillomavirus; SIV: simian immunodeficiency virus; WT: wild type.

1.17. Immunogenicity of chimeric HPV-HIV VLPs in small animals and non-human primate model

Liu et al. investigated in BALB/c mice whether mucosal administration of chimeric BPV/HIV VLP could elicit mucosal cellular and humoral immune responses to BPV VLP and incorporated HIV epitopes [48]. They detected specific antibodies for BPV-1 VLP and HIV-1 CTL epitope P18 from gp120 in serum by i.m. administration but not intrarectal (i.r.) or intravaginal (i.va) immunization. Regarding VLP specific IgA, it was higher in the intestine by i.r. than i.va administration, and higher in vaginal by i.m. than i.r. or i.va. administration. CTL precursor cells specific for HIV P18 were found in spleen from all three routes of Immunization but in Peyer's patches only from i.m. or i.r. Immunization. Dale et al. [118] designed HPV genotype 6b L1 VLPS incorporating SIV Gag p27 and HIV-1 tat and vaccinated pigtailed macaques with DNA encoding SIV gag, HIV- 1 tat, and HIV-1 rev or HPV/SHIV VLP prime intramuscularly and with three VLP boosters intrarectally, com- paring DNA prime/HPV VLP boost regimen versus all HPV/SHIV VLPS. However, they could detect only weak antibody or T cell responses to the chimeric SHIV antigen in DNA prime/HPV VLP boost regimen, but not in the all HPV/SHIV VLP group. Di Bonito et al. [120] fused HPV genotype 16 E7 to Nef-mutant, inserted into HIV-1 gag-pol VLP, and vaccinated C57BL/6 mice subcutaneously 3 times over 4 weeks at 2-week interval. The culture of the murine splenocytes demonstrated an anti-E7 CTL activity. Furthermore, the vaccinated mice were challenged with tissue culture number one (TC-1) tumor cells causing HPV-related tumor 2 weeks after the last VLP inoculum. The mice inoculated with the chimeric VLPS were protected after tumor challenge. Furthermore, effective Nef-specific CTL activity was detected. BPV L1 VLPS presenting HIV-1 epitopes from MPER of gp41 constructed by Zhai et al. [119] and were inoculated to BALB/c mice orally, and induced strong vaginal IgG responses against BPV while only weak vaginal HIV-specific secretory IgA responses were detected. They confirmed that IgG and mucosal secretory I9AI were elicited against 2F5 and MPER. The induced antibodies recognized native MPER in HIV-1 infected cells and were able to partially neutralize infectivity from HIV-1 viruses of clade B and C.

1.18 Human clinical trials using VLPs

In the near future, more VLP-based vaccine candidates will enter human clinical trials. After the licensure of three VLP-based HPV vaccines, four clinical trials are currently on-going to follow-up the safety and long- term efficacy [123] (Table 9). Regarding HIV VLP, only a few candidates have been tested in clinical trials. The first candidate, p17/p24:Ty, where yeast-derived Ty protein containing 25% HIV-1 p17 and 79% HIV-1 p24, was tested in Phases I and II [124]. They only induced low level of HIV-specific humoral and cell-mediated immune responses and were discontinued. Another candidate, p24-VLP, which is HIV VLP composed of Gag p24, was reached to Phase II [125]. The VLPs were administered with or without zidovudine, a nucleoside reverse transcriptase inhibitor to asymptomatic HIV-1 infected patients but it could not improve HIV-specific immune responses in them. Finally, DNA and recombinant modified vaccinia virus Ankara (MVA) vaccines expressing HIV-1 VLP were assessed. In Phase I trial for safety and immunogenicity [126]. The MVA vaccine producing HIV-1 VLPS of HIV-1 Gag, PR, RT, and Env was well tolerated and elicited different patterns of T cell and Ab responses when administered alone or in combination with the DNA vaccine producing HIV-1 VLPS composed of HIV-1 HXB2 Gag, HIV-1 BH10, PR and RT, and Env, Tat, Rev, and Vpu derived from a recombinant of the HXB-2 and ADA (V3-ADA) strains of HIV-1. Various chimeric VLP-based vaccine candidates entered clinical trials such as the anti-influenza A M2-HB-cAg VLP vaccine, the anti-HIV p17/p24:Ty VLP, two anti-malaria vaccines, the nicotine-Qb VLP and the anti-Ang II Qb VLP, and other chimeric VLP vaccine candidates went on preclinical trials [127]. Moreover, several clinical trials for other VLP-based vaccines are on-going: Severe acute respiratory syndrome coronavirus 2 (SARS-CoV-2), Norovirus, Chikungunya virus, and Respiratory Syncytial Virus [123] (Table 9).

Table 9. On-going clinical trials of HPV VLP and other VLP models [123].

HPV VLP	**Estimated study completion date**
Immunobridging Study of 9- Valent Human Papillomavirus (9vHPV) Vaccine (V503) in Chinese Females 9 to 45 Years of Age (V503-024)	January 18, 2025
Long-term Follow-up of Broad Spectrum Human Papillomavirus (HPV) Vaccine Study in Women (V503-021)	January 1, 2024
Efficacy Against Oral Persistent Infection, Immunogenicity and Safety of the 9-valent Human Papillomavirus Vaccine (9vHPV) in Men Aged 20-45 Years (V503-049)	August 20, 2024
Cervical Intraepithelial Neoplasm (CIN) in Women (Gardasil) (V501-015)	March 3, 2025
Other VLP models	**Estimated study completion date**
Study of a Severe Acute Respiratory Syndrome CoV-2 (SARS-CoV-2) Virus-like Particle (VLP) Vaccine in Healthy Adults	March 2022
Long-Term Immunogenicity of the Norovirus GI.1/GII.4 Bivalent Virus-like Particle (VLP) Vaccine (NoV Vaccine) in Adults	October 26, 2021
Phase 2 Open-label Study of Alum-adjuvanted Chikungunya Virus-like Particle Vaccine (PXVX0317) (WRAIR)	September 3, 2021
Safety and Tolerability of COVID-19 Vaccine (ABNCoV2) (COUGH-1)	December 20, 2021
Phase 1 Study to Evaluate the Safety and Immunogenicity of a Candidate Vaccine Against Respiratory Syncytial Virus	June 30, 2022
Safety, Tolerability, and Immunogenicity of the COVID-19 Vaccine Candidate (VBI-2902a)	June 2022

1.19 Scientific and technical background of the research team

Joan Joseph, Yoshiki's thesis director, is member of the Microbiology Research Group at Vall Hebron Research Institute (VHIR), led by Dr. Tomas Pumarola. Dr. Pumarola is the head of the Microbiology Service at Hospital Vall Hebron. Dr. Joan Joseph has been working on recombinant BCG based HIV vaccines in the laboratory led by Dr. Barry R Bloom at Albert Einstein College of Medicine, New York (1997) and later in the microbiology laboratory at Harvard School of Public Health, Boston, also directed by Dr. Barry B Bloom (1998-2001). Our

group has been working on recombinant BCG based HIV vaccine development for many years with the aim of inducing protective cell-mediated responses. We have constructed different mycobacterial expression vectors that contained different promoters to regulate the expression of different HIV antigens. We have also shown that when we use a weak promoter and auxotrophic lysine BCG strains we prevent genetic rearrangements and gene expression disruption of HIV-1 gp120 [128]. Our starting platform was based on a heterologous rBCG prime and recombinant modified vaccinia virus Ankara (MVA) boost regimen delivering the HIVA immunogen containing the whole gag protein and different CTL epitopes of gag, envelope and nef of HIV-1, subtype A predominant in Central and Eastern Africa. We have demonstrated in mice, that using a heterologous immunization regimen with BCGHIVA prime and MVAHIVA boost a high-quality and long-lasting specific cellular immune response was induced [129]. We have also collaborated in the evaluation of immunogenicity of BCGHIVA + MVAHIVA in newborn and adult Rhesus macaques [130, 131]. We have also published a paper in the Clinical and Developmental Immunology where we evaluated the influence of age and immunization routes in newborn and adult mice [132]. On the other hand, in the framework of a European EDCTP grant (CT.2006.33111.002) and with the collaboration of COBRA inc., we evaluated in vivo, the immunogenicity in BALB /c mice of BCG.HIVA strain without resistance to antibiotics [133]. In May 2014, we published the construction of a new mycobacterial vaccine design by using an antibiotic-free plasmid selection and maintenance system (J. Joseph et al., 2014). We have demonstrated that, the use of integrative expression vectors and the antibiotic-free plasmid selection system based on “double” auxotrophic complementation are likely to improve the mycobacterial vaccine stability in vivo and immunogenicity [134]. We have recently published a review paper in Expert review of vaccines journal entitled: “Advances and challenges in recombinant Mycobacterium bovis BCG-based HIV vaccine development: Lessons learned“ [135]. Recently, in collaboration with Professor Carlos Martin from University of Zaragoza, and with the aim of using MTBVAC as a vector for a dual TB-HIV vaccine, we constructed the recombinant MTBVAC. HIVA2auxo strain [136]. MTBVAC is the only live-attenuated *Mycobacterium tuberculosis* (Mtb)-based vaccine in clinical development, and it confers superior protection in different animal models compared to the current vaccine, BCG [137]. Moreover, within the European AIDS Vaccine Initiative Consortium, we have constructed the recombinant BCG expressing EAVI 2020 T-cell immunogens and we have recently published the data in Frontiers Immunology and Vaccines

journal [138]. These immunogens are currently tested in Phase I clinical trials in Barcelona and Oxford.

In addition, our group is working in the development of chimeric Virus-like particles-based HPV/HIV vaccines. We are using the insect, mammalian and yeast expression platforms for VLP production. Recently, we have published two review papers: (i) Designing chimeric virus-like particle-based vaccines for human papillomavirus and HIV: lessons learned [47] and (ii) Design Concepts of Virus-Like Particle-Based HIV-1 Vaccines [139]. Therefore, this is the framework of this thesis, testing different expression platforms for VLP production and being one of them *P. pastoris*.

1.20 Abstract of this thesis

In this study, two recombinant *Pichia pastoris* strains producing chimeric HPV-HIV L1P18 protein were constructed. After optimizing the purification methods, the VLPs from the L1P18 protein were purified after cell disruption by a combination of ammonium sulfate precipitation, size exclusion chromatography, ultracentrifugation and ultrafiltration. At the end of purification process, the chimeric VLPs were recovered with 96% purity and 9.2% overall yield, and the morphology of VLPs were confirmed by transmission electron microscopy. This work contributes towards the development an alternative platform for production of a bivalent vaccine against HPV and HIV in *P. pastoris*.

2. Hypothesis

Both HPV and HIV are sexually transmitted infections and still major problem in the world. One of the main access routes for both viruses is the mucosal genital tract. While HPV vaccines are commercialized, there are still not economically reachable, and any HIV vaccines are not developed yet. Thus, the development of a combined vaccine that would protect against HPV and HIV infections is a logical effort in the fight against these two major global pathogens. In addition, *P. pastoris* could be a good alternative in terms of production costs and volume compared to superior eukaryotic expression systems for VLP production.

3. Objectives

The main goal is to develop a chimeric virus-like particle based HPV-HIV vaccine produced in yeast and optimize the purification methods and purify VLPs and confirm the morphology by TEM.

The specific objectives are as follows:

3.1 Construction of the recombinant yeast strain expressing the L1 (HPV):P18I10 (HIV) protein (L1P18)

Recombinant plasmid DNA pGAPZB harboring L1P18 DNA sequence is transformed into *Pichia pastoris* X33 strain by electroporation in order to produce L1P18 protein.

3.2 Genetic and phenotypic characterization of recombinant yeast strains

Recombinant yeast strains are characterized genetically and phenotypically by PCR analysis and Western blotting analysis, enzymatic resistance.

3.3 Selection and optimization of VLP purification methods

Several purification methods such as ultracentrifugation with sucrose cushion, ammonium sulfate precipitation, heparin chromatography, cation exchange chromatography, anion exchange chromatography, size exclusion chromatography, and ultrafiltration are systemically tested based on (a) Product recovery, (b) Product concentration and conditioning, (c) Product purification and refinement. At the end, VLP purification methods are optimized.

3.4 Production and purification of VLPs

L1P18 VLPs are produced by recombinant yeast intracellularly and purified by the optimized purification methods.

3.5 Characterization of VLPs

Purified VLPs are characterized by Coomassie staining for purity, western blot analysis for the confirmation of the existence, the expression and the size of L1P18 protein, and transmission microscopy for the morphology.

4. Materials and methods

4.1 Bacterial and yeast strains, and cultivation media

4.1.1 Bacterial strain

5 ng of the DNA Plasmids were transformed into 100 µL of *Escherichia coli* MAX Efficiency™ DH5α heat-shock competent cells (Thermo Fisher Scientific, USA) in 1.5-mL polypropylene microcentrifuge tubes by heat-shock for exactly 30 seconds in a 42°C water bath. The cells were incubated on ice for 2 minutes. After adding 0.9 mL room-temperature S.O.C. Medium, the cells were shaken at 225 rpm for 1 hour at 37°C. The cells were spread at 6 different concentrations (10^{-1}, 10^{-2}, 10^{-3}, 10^{-4}, 10^{-5}, and 10^{-6} dilutions) on separate low salt Luria-Bertani (LB) medium (1% tryptone, 0.5% NaCl, and 0.5% yeast extract plus 2% agar in plates), and supplemented with 25 µg/mL Zeocin™ (InvivoGen, USA) for the selection of transformants. The plates were inverted and incubated overnight at 37°C. The *E. coli* colonies were used for further analysis. In addition, the *E. coli* colonies were inoculated into 250 mL of low salt LB broth and incubated overnight at 37°C. The cells were centrifuged at 5,000 × g for 10 minutes at room temperature, and the supernatant was discard. Approximately 1 mg of the DNA plasmids were extracted from the cells by PureYield™ Plasmid Maxiprep System (Promega, USA). Extracted DNA were stored in -80°C.

4.1.2 Yeast strain

The methylotrophic yeast *Pichia pastoris* X-33 yeast strain (Thermo Fisher Scientific, USA) was routinely cultured in YPD (yeast extract, peptone, and dextrose) medium (1% yeast extract, 2% peptone, and 2% dextrose, plus 2% agar in plates), BMG (buffered minimal glycerol) medium (100 mM potassium phosphate, pH 6.0, 1.34% yeast nitrogen base with ammonium sulfate and without amino acids (Thermo Fisher Scientific, USA), 0.00004% biotin and 1% glycerol) or BMM (buffered minimal methanol) medium (10% potassium phosphate, pH 6.0, 1.34% yeast nitrogen base with ammonium sulfate without amino acids, 0.00004% biotin, 0.5% methanol), supplemented with 100 µg/mL Zeocin™ for the selection of transformants. Furthermore, the yeast cells were stored at OD_{600}=40~60 in a freezing medium (80% YPD media and 20% glycerol) in -80°C.

4.2 Design and construction of recombinant *P. pastoris* X-33 strain expressing chimeric L1P18 protein

The HIV-1 P18-I10 peptide DNA coding sequence was inserted *in silico* into DNA coding sequence of D-E loop of HPV genotype 16 capsid protein L1. The DNA coding sequence corresponding to the chimeric HPV-HIV protein HPV-16 L1: HIV-1 P18-I10 (L1P18) was codon optimized for *P. pastoris* usage, synthetized by Thermo Fisher Scientific, USA (Figure 15), and cloned into pGAPZB plasmid DNA as a EcoRI-XhoI fragment under the control of glyceraldehyde-3-phosphate dehydrogenase (GAP) promoter by Thermo Fisher Scientific, USA (Figure 16). Alternatively, it was cloned into pPICZαA plasmid DNA as a EcoRI-NotI fragment under the control of Alcohol Oxidase 1 (AOX1) promoter (Figure 17). Both pGAPZ and pPICZα are integrative expression vectors that contain a Zeocin resistance gene as a selectable marker and the expression cassette harboring the multiple cloning site, *myc* epitope tag, Polyhistidine tag, stop codon, and the GAP promoter and AOX1 promoter respectively. Regarding pGAPZ, the restriction site between NotI and the *myc* epitope is different in each version: Apa I in pGAPZA, *Xba I* in pGAPZB, and *SnaB I* in pGAPZC. When it comes to pPICZα, *Pst I* cloning site is only in Version B, and *Cla I* cloning site is only in Version C. Furthermore, pPICZα has α-factor secretion signal for directing secreted expression of the recombinant protein. The construction and DNA sequencing of the recombinant plasmid DNA pGAPZB-L1P18 was performed by Life technologies and the recombinant plasmid DNA pPICZαA-L1P18 was constructed by amplifying L1P18 DNA coding sequence by PCR and inserting it into pPICZαA plasmid DNA by restriction enzymes. The correct insertion was confirmed by enzymatic digestion followed by 0.8% agarose gel electrophoresis with Sybr green staining. 5 µg of the pGAPZB and pGAPZB-L1P18 were linearized at 356 bp of pGAPZB vector, which is located in GAP promoter region, by *Bsp HI* enzyme, 5 µg of pPICZαA and pPICZαA-L1P18 were linearized at 209 bp of pPICZαA, which is located in AOX1 promoter region, by *SacI* enzyme. After the confirming the complete linearization by agarose gel electrophresis, the enzymes were heat-inactivated at 65 °C for 20 minutes. The DNA were precipitated by using 1/10 volume of 3M sodium acetate and 2.5 volumes of 100% ethanol, and pelleted by the centrifuging the solution at 13,000 rpm at room temperature for 3 min. The pellets were washed with 80% ethanol, air-dried, and resuspended in 10 µL sterile,

deionized water. Competent *P. pastoris* cells were prepared by BEDS solution, which is composed of 10 mM bicine-NaOH, pH 8.3, 3% (v/v) ethylene glycol, 5% (v/v) dimethyl sulfoxide (DMSO), and 1 M sorbitol [140]. The linearized plasmid DNAs were transformed into *P. pastoris* X-33 strain by electroporation with an electric field pulse: 1.5 kV/cm, 50 µF and 200 Ω. The wild type X-33 strain and the transformants were plated out at 6 different concentrations (10^{-1}, 10^{-2}, 10^{-3}, 10^{-4}, 10^{-5}, and 10^{-6} dilutions) onto YPD agar plates with or without 100 µg /mL Zeocin™ and incubated for 2–3 days at 30°C. Eight colonies were picked and purified by re-streaking single colonies three times on fresh YPD plates containing 100 µg/mL Zeocin™. In order to verify the correct integration of the expression cassette, the genomic DNA extracted from the isolated colonies were amplified by Polymerase chain reaction (PCR) by using the primers corresponding to L1P18 DNA coding sequence (Fw: 5'-ATGTCTCTTTGGCTGCCTAGTG-3', Rev: 5'-TTACAGCTTACGTTTTTTGCGTTTAG-3').

Sequence Data

```
Molecule:       pGAPZB-L1P18 Yeast Opt EcoRI-XhoI+Kozak,  4407 bps DNA Circular
File Name:      (not saved)
Description:    Ligation of L1-P18 Yeast Opt EcoRi-XhoI+Kozak* into pGAPZ B*
Printed:        398 to 2158 bps,   Translation Frame 3
```

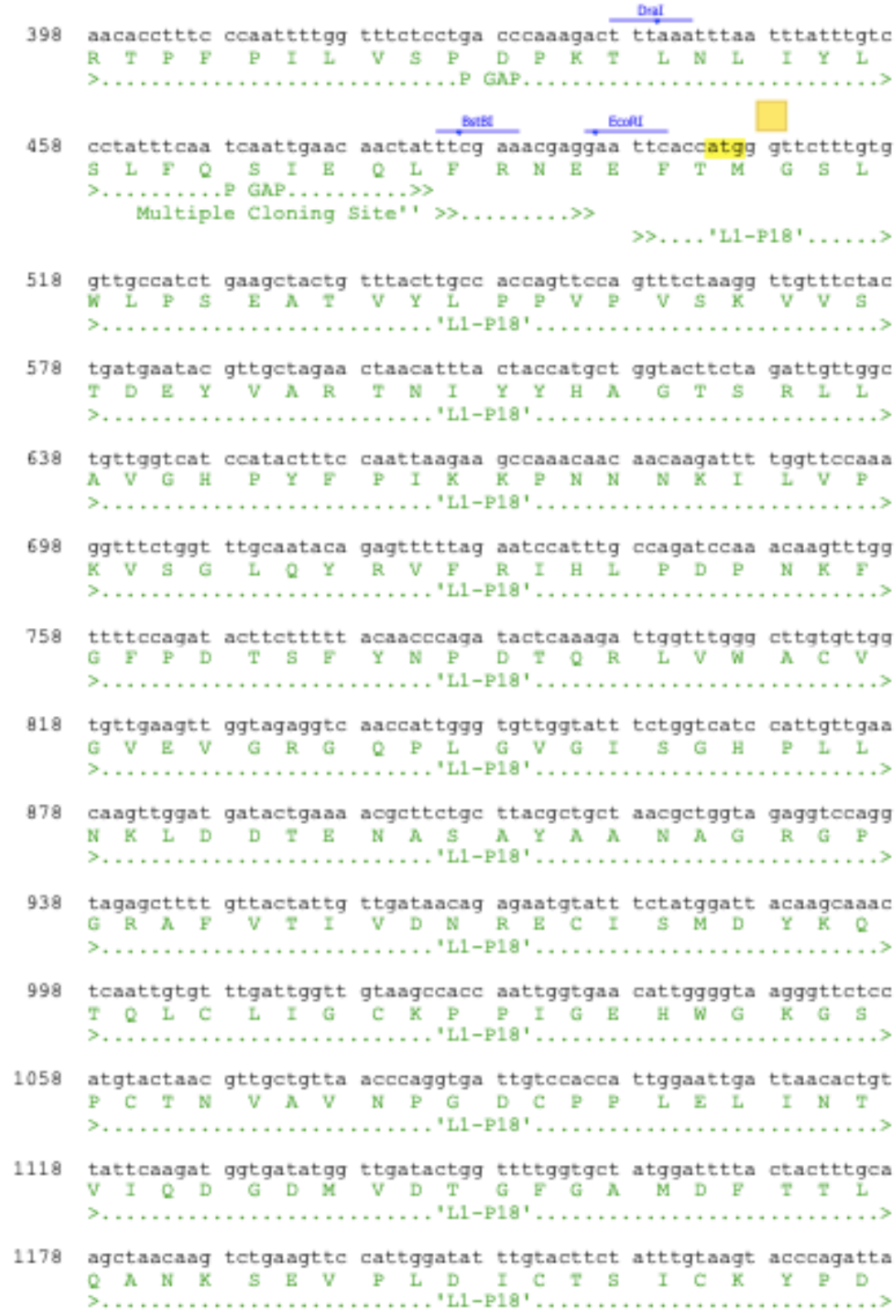

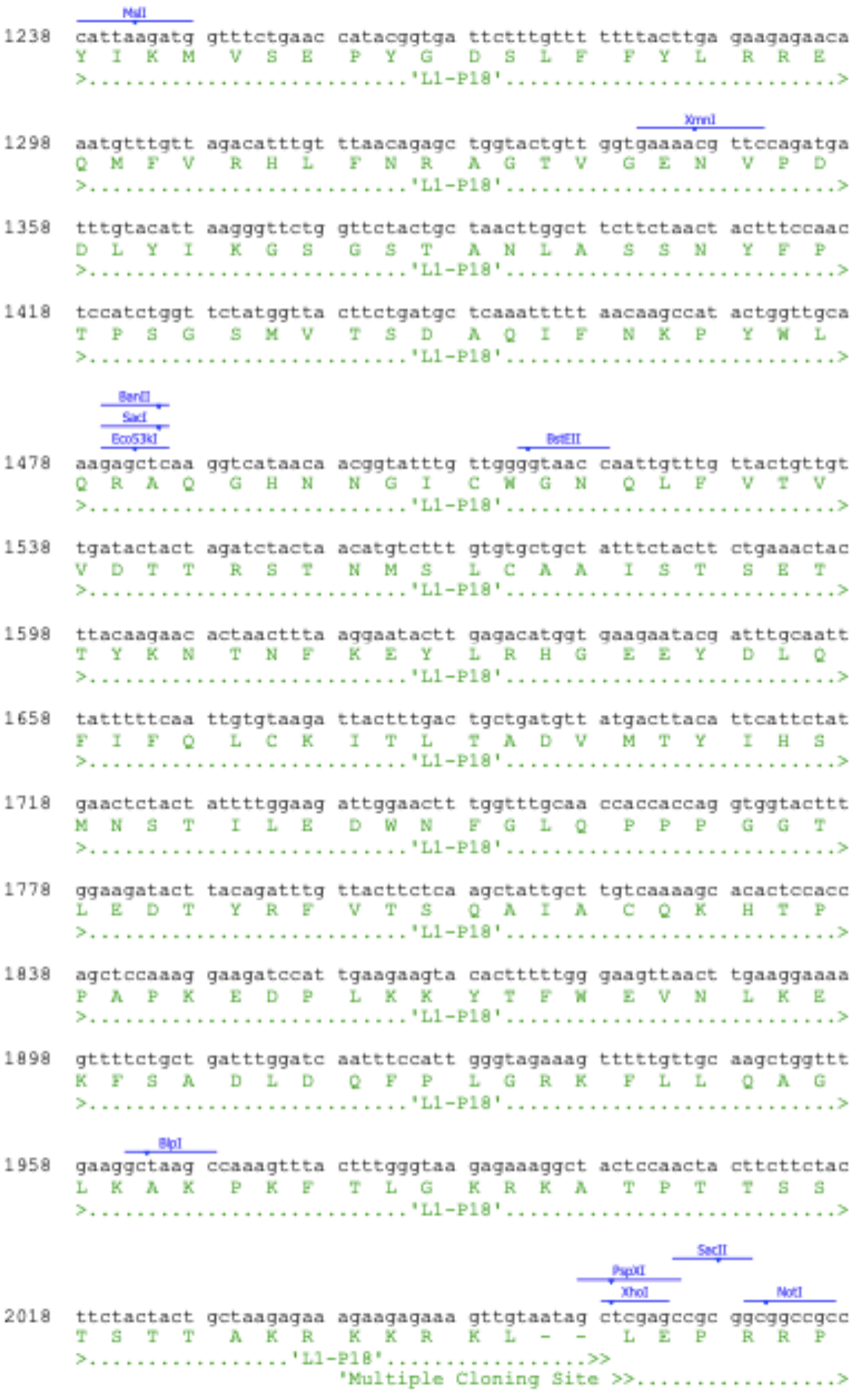
NaiI
1238 cattaagatg gtttctgaac catacggtga ttctttgttt ttttacttga gaagagaaca
Y I K M V S E P Y G D S L F F Y L R R E
>..........'L1-P18'..........>
XmnI
1298 aatgtttgtt agacatttgt ttaacagagc tggtactgtt ggtgaaaacg ttccagatga
Q M F V R H L F N R A G T V G E N V P D
>..........'L1-P18'..........>
1358 tttgtacatt aagggttctg gttctactgc taacttggct tcttctaact actttccaac
D L Y I K G S G S T A N L A S S N Y F P
>..........'L1-P18'..........>
1418 tccatctggt tctatggtta cttctgatgc tcaaattttt aacaagccat actggttgca
T P S G S M V T S D A Q I F N K P Y W L
>..........'L1-P18'..........>
BanII
SacI
Eco53kI
BstEII
1478 aagagctcaa ggtcataaca acggtatttg ttggggtaac caattgtttg ttactgttgt
Q R A Q G H N N G I C W G N Q L F V T V
>..........'L1-P18'..........>
1538 tgatactact agatctacta acatgtcttt gtgtgctgct atttctactt ctgaaactac
V D T T R S T N M S L C A A I S T S E T
>..........'L1-P18'..........>
1598 ttacaagaac actaacttta aggaatactt gagacatggt gaagaatacg atttgcaatt
T Y K N T N F K E Y L R H G E E Y D L Q
>..........'L1-P18'..........>
1658 tatttttcaa ttgtgtaaga ttactttgac tgctgatgtt atgacttaca ttcattctat
F I F Q L C K I T L T A D V M T Y I H S
>..........'L1-P18'..........>
1718 gaactctact attttggaag attggaactt tggtttgcaa ccaccaccag gtggtacttt
M N S T I L E D W N F G L Q P P P G G T
>..........'L1-P18'..........>
1778 ggaagatact tacagatttg ttacttctca agctattgct tgtcaaaagc acactccacc
L E D T Y R F V T S Q A I A C Q K H T P
>..........'L1-P18'..........>
1838 agctccaaag gaagatccat tgaagaagta cacttttgg gaagttaact tgaaggaaaa
P A P K E D P L K K Y T F W E V N L K E
>..........'L1-P18'..........>
1898 gttttctgct gatttggatc aatttccatt gggtagaaag tttttgttgc aagctggttt
K F S A D L D Q F P L G R K F L L Q A G
>..........'L1-P18'..........>
BlpI
1958 gaaggctaag ccaaagttta ctttgggtaa gagaaaggct actccaacta cttcttctac
L K A K P K F T L G K R K A T P T T S S
>..........'L1-P18'..........>
SacII
PspXI
XhoI
NotI
2018 ttctactact gctaagagaa agaagagaaa gttgtaatag ctcgagccgc ggcggccgcc
T S T T A K R K K R K L - - L E P R R P
>..........'L1-P18'..........>>
'Multiple Cloning Site >>..........>

```
                                                                  AccI
                                                                  SalI
2078  agctttctag aacaaaaact catctcagaa gaggatctga atagcgccgt cgaccatcat
      P  A  F  -   N  K  N   S  S  Q   K  R  I  -   I  A  P   S  T  I
      >.........>> 'Multiple Cloning Site
  myc epitope tag >
                                                        Poly-His >

2138  catcatcatc attgagtttt a
      I  I  I  I   I  E  F
               AOX1 TT >>..>
```

Figure 15. L1P18 DNA sequence codon-optimized for *P. pastoris* usage

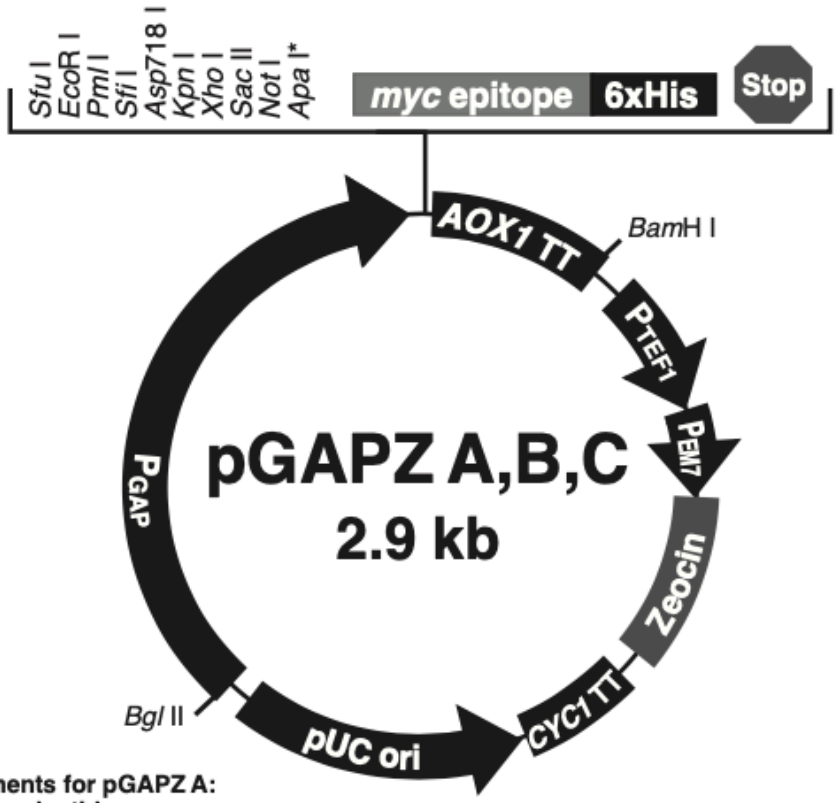

Comments for pGAPZ A:
2884 nucleotides

GAP promoter region: bases 1-483
Multiple cloning site: bases 484-563
myc epitope tag: bases 564-593
Polyhistidine tag: bases 609-626
AOX1 transcription termination region: bases 630-970
Fragment containing *TEF1* promoter: bases 971-1381
EM7 promoter: bases 1382-1449
Sh ble ORF: bases 1450-1824
CYC1 transcription termination region: bases 1825-2142
pUC origin: bases 2153-2826

* The restriction site between *Not* I and the *myc* epitope is different in each version of pGAPZ:

Apa I in pGAPZ A
Xba I in pGAPZ B
*Sna*B I in pGAPZ C

Figure 16. The plasmid map of yeast expression vector pGAPZB

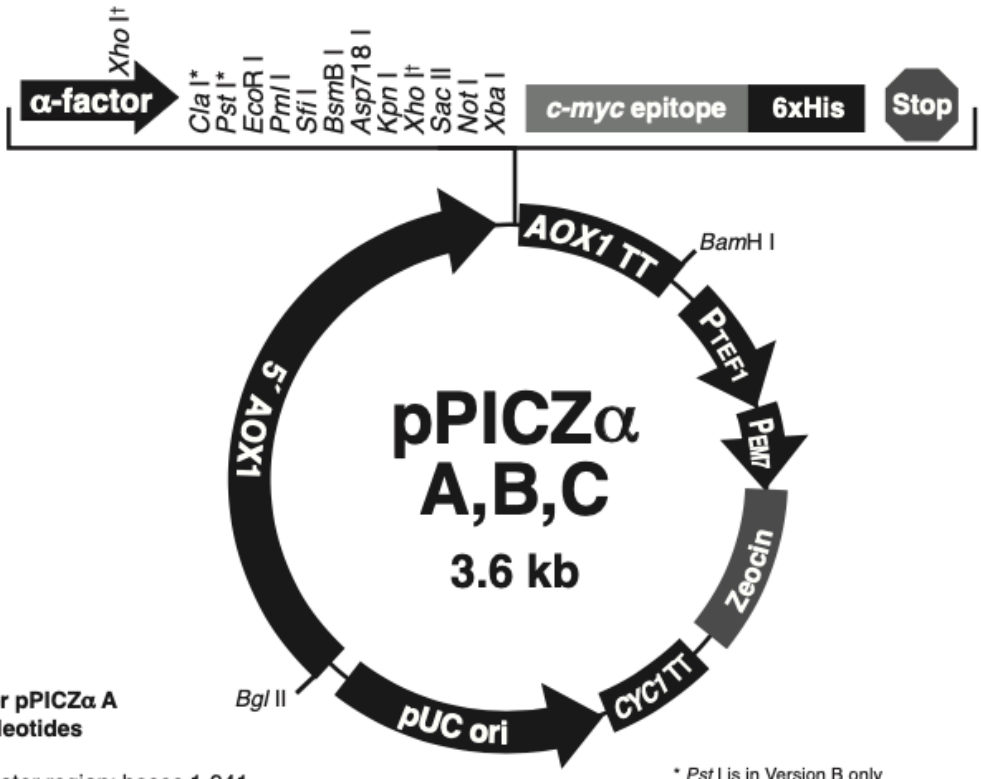

Comments for pPICZα A
3593 nucleotides

5´ *AOX1* promoter region: bases 1-941
5´ *AOX1* priming site: bases 855-875
α-factor signal sequence: bases 941-1207
Multiple cloning site: bases 1208-1276
c-myc epitope: bases 1275-1304
Polyhistidine (6xHis) tag: bases 1320-1337
3´ *AOX1* priming site: bases 1423-1443
AOX1 transcription termination region: bases 1341-1682
TEF1 promoter: bases 1683-2093
EM7 promoter: bases 2095-2162
Sh ble ORF: bases 2163-2537
CYC1 transcription termination region: bases 2538-2855
pUC origin: bases 2866-3539 (complementary strand)

* *Pst* I is in Version B only
Cla I is in Version C only

†The two *Xho* I sites in the vector allow the user to clone their gene in frame with the Kex2 cleavage site, resulting in expression of their native gene without additional amino acids at the N-terminus.

Figure 17. The plasmid map of yeast expression vector pPICZαA

4.3 Cultivation conditions (Production): Cultures in Erlenmeyer shake flasks

A total of 1.75 L YPD broth containing 100 µg /mL Zeocin was used for each production run. This volume was divided into 250 mL fractions, each added to a 1-L volume baffled flasks. These were inoculated directly from frozen working cell stocks of the selected yeast transformant harboring pGAPZB-L1P18. Cultures were grown on a shaker at 150 rpm for 40 hours at 30 °C (final OD_{600} ≈20). The working stock of the yeast transformant harboring pPICZαA-L1P18 plasmid DNA was grown in 100 mL BMG broth containing 100 µg /mL Zeocin in baffled flasks on a shaker at 150 rpm for 16 hours at 30 °C (OD_{600} ≈5) and then grown in 1 L BMM broth in baffled flasks on a shaker at 150 rpm for 48 hours at 30 °C (OD_{600} ≈20) by

adding 100% methanol to a final concentration of 0.5% methanol every 12 hours to maintain induction of gene expression. For the *P. pastoris* harboring pGAPZB-L1P18, the cells were harvested by centrifugation at 5000 ×g for 5 min at 4 °C and washed by PBS twice to remove YPD broth. For the *P. pastoris* harboring pPICZαA-L1P18, the supernatant was collected by centrifugation at 10,000 ×g for 10 min at 4 °C.

4.4 Purification of L1P18 Virus-like particles (VLPs)

4.4.1 Primary recovery and concentration of HPV-HIV L1P18 protein from *P. pastoris* cells.

For the *P. pastoris* harboring pGAPZB-L1P18 plasmid DNA, the cells harvested from a shake culture production run (see section 4.3) were resuspended in 100 mL of ice-cold lysis buffer (20 mM sodium phosphate, pH 7.2, 100 mM NaCl, 1.7 mM EDTA, 0.01%, Tween 80) containing two cOmplete™ protease inhibitor cocktail tablets (#11697498001, Roche, USA). After the cell lysis by cell high pressure disruption (Constant System, UK) at 2 kbar by two cycles, the sample was centrifuged at 10,000 xg for 30 min at 4 °C. The cell lysate supernatant was adjusted to 45% saturated ammonium sulfate and left stirred for 1 hour at 4 °C; the precipitated protein was pelleted at 12,000 xg for 10 min at 4 °C. The pellet was resuspended in 10 mL of PBS + 0.01% Tween 80. To remove further contaminants, the ammonium sulfate precipitate was dialyzed against PBS + 0.01% Tween 80 and diluted 10 times in incubation buffer (10 mM sodium phosphate, pH 7.2, 150 mM NaCl + 0.01% Tween 80) [141]. This suspension was incubated at room temperature for 24 hours, and the precipitated protein was removed by centrifugation at 12,000 xg for 10 min at 4 °C, and the supernatant was obtained.

4.4.2 Purification of HPV-HIV L1P18 protein and VLP by chromatography

Chromatography conditions are summarized in table 10.

4.4.2.1 Heparin chromatography (HC)

The supernatant obtained at the end of the recovery and concentration step (section 4.4.1) or the sample obtained from another chromatography purification step was dialyzed against

binding buffer (2.68 mM KCl, 1.47 mM KH_2PO_4, 8.1 mM Na_2HPO_4, 0.33 M NaCl, pH 7.0 + 0.01% Tween 80) for 3 hours at 4 °C. The dialyzed sample was further microfiltrated at 0.45 µm, and then loaded onto a HiTrap Heparin HP column (GE Healthcare, USA), prepacked with 5 mL of resin (10 mg heparin/1 mL resin) equilibrated with the same buffer, and the column was washed with five column volumes of the binding buffer. To remove contaminants, the column was eluted with a linear gradient from 0.33 to 0.66 M NaCl, and this was followed by a linear gradient from 0.66 to 2 M NaCl to elute L1P18 protein. The fractions containing L1P18 protein (eluting between 0.6 and 1.2 M NaCl) were collected and dialyzed against the binding buffer used for heparin chromatography.

Chromatography condition: Running buffer - 2.68 mM KCl, 1.47 mM KH_2PO_4, 8.1 mM Na_2HPO_4, 0.33 M NaCl, pH 7.0 + 0.01% Tween 80 250 cm/h; Wash buffer -2.68 mM KCl, 1.47 mM KH_2PO_4, 8.1 mM Na_2HPO_4, 0.33 M NaCl, pH 7.0 + 0.01% Tween 80, 150 cm/h; Elution - linear gradient from 0.33 to 2 M NaCl, 150 cm/h, Cleaning in place (CIP) - 1 M NaOH, 100 cm/h

4.4.2.2 Cation exchange chromatography (CEC)

The supernatant obtained at the end of the recovery and concentration step (section 4.4.1) or the sample obtained from another chromatography purification step was dialyzed against binding buffer (2.68 mM KCl, 1.47 mM KH_2PO_4, 8.1 mM Na_2HPO_4, 0.5 M NaCl, pH 7.2 + 0.01% Tween 80) for 3 hour at 4 °C. HiScreen Capto SP ImpRes 4.7 mL column (GE) was equilibrated with binding buffer, and the dialyzed sample was further microfiltrated at 0.45 µm, and then loaded onto the column. This was washed with five column volumes of binding buffer, followed by elution with a linear gradient from 0.5 to 1 M NaCl. The fractions containing L1P18 protein were collected, and dialyzed against the binding buffer for heparin chromatography.

Chromatography condition: Running buffer - 2.68 mM KCl, 1.47 mM KH_2PO_4, 8.1 mM Na_2HPO_4, 0.5 M NaCl, pH 7.2 + 0.01% Tween 80, 250 cm/h; Wash buffer -2.68 mM KCl, 1.47 mM KH_2PO_4, 8.1 mM Na_2HPO_4, 0.5 M NaCl, pH 7.2 + 0.01% Tween 80, 150 cm/h; Elution - a linear gradient from 0.5 to 1 M NaCl, 150 cm/h, Cleaning in place (CIP) - 1 M NaOH, 100 cm/h

4.4.2.3 Anion exchange chromatography (AEC)

The supernatant obtained at the end of the recovery and concentration step (section 4.4.1) or the sample obtained from another chromatography purification step was dialyzed for disassembly condition by incubating with 20 mM DTT for 15 min at room temperature. The dialyzed sample was further microfiltrated at 0.45 µm, and then loaded onto and gone through HiScreen Capto Q ImpRes 4.7 mL column (GE) equilibrated with the same buffer, and the column was washed with five column volumes of the binding buffer. Then, the column was eluted with a Step gradient to 9.3%, 16.5%, and 100% 20 mM Tris, 1 M NaCl, 20 mM DTT, pH 8.5. The fractions containing L1P18 protein was collected.
Chromatography condition: Running buffer - 20 mM Tris, 100 mM NaCl, 20 mM DTT, pH 8.5, 250 cm/h; Wash buffer -20 mM Tris, 100 mM NaCl, 20 mM DTT, pH 8.5, 150 cm/h; Elution - Step gradient to 9.3%, 16.5%, and 100% 20 mM Tris, 1 M NaCl, 20 mM DTT, pH 8.5, 150 cm/h, Cleaning in place (CIP) - 1 M NaOH, 100 cm/h

4.4.2.4 Size exclusion chromatography (SEC)

The supernatant obtained at the end of the recovery and concentration step (section 4.4.1) was dialyzed for reassembly condition (PBS pH 7.2 with 0.01% Tween 80%) at 4 ^{o}C. HiScreen Capto™ Core 700 4.7 mL column (GE) was equilibrated with binding buffer, the dialyzed sample was further microfiltrated at 0.45 µm, and then loaded onto the column. This was washed with five column volumes of binding buffer, followed by CIP buffer 1 M NaOH, 30% 2-propanol and then 2 M NaCl. The flow-through fractions containing L1P18 VLPs were collected.
Chromatography condition: Running buffer - 20 mM Tris, 300 mM NaCl, pH 8.5, 200 cm/h; Wash buffer - 20 mM Tris, 300 mM NaCl, pH 8.5, 150 cm/h; CIP buffer - 1 M NaOH, 30% 2-propanol followed by 2 M NaCl, 60 cm/h.

Table 10. Summary of chromatography conditions

Chromatography type	Heparin	Cation exchange	Anion exchange	Size exclusion
Column	HiTrap Heparin HP 5 mL column (GE)	HiScreen Capto SP ImpRes 4.7 mL column (GE)	HiScreen Capto Q ImpRes 4.7 mL column (GE)	HiScreen Capto Core 700 4.7 mL column (GE)
Sample load speed	150 cm/h	150 cm/h	150 cm/h	150 cm/h
Running buffer	2.68 mM KCl, 1.47 mM KH2PO4, 8.1 mM Na2HPO4, 0.33 M NaCl, pH 7.0 + 0.01% Tween 80	2.68 mM KCl, 1.47 mM KH2PO4, 8.1 mM Na2HPO4, 0.5 M NaCl, pH 7.2 + 0.01% Tween 80	20 mM Tris, 100 mM NaCl, 20 mM DTT, pH 8.5, 250 cm/h	20 mM Tris, 300 mM NaCl, pH 8.5, 200 cm/h
Wash	2.68 mM KCl, 1.47 mM KH2PO4, 8.1 mM Na2HPO4, 0.33 M NaCl, pH 7.0 + 0.01% Tween 80	2.68 mM KCl, 1.47 mM KH2PO4, 8.1 mM Na2HPO4, 0.5 M NaCl, pH 7.2 + 0.01% Tween 80	20 mM Tris, 100 mM NaCl, 20 mM DTT, pH 8.5, 250 cm/h	20 mM Tris, 300 mM NaCl, pH 8.5, 150 cm/h
Elution	linear gradient from 0.33 to 2 M NaCl	linear gradient from 0.5 to 1 M NaCl	Step gradient to 9.3%, 16.5%, and 100% 20 mM Tris, 1 M NaCl, 20 mM DTT, pH 8.5, 150 cm/h	-
Cleaning in place	1 M NaOH, 100 cm/h	1 M NaOH, 100 cm/h	1 M NaOH, 100 cm/h	1 M NaOH, 30% 2-propanol followed by 2 M NaCl, 60 cm/h
Chromatography system	ÄKTA pure	ÄKTA pure	ÄKTA pure	ÄKTA pure

4.4.3 VLP purification by ultracentrifugation with sucrose cushions

The cell lysate after cell disruption, the supernatant obtained at the end of the recovery and concentration step (section 4.4.1) or the pooled flow-throughs from size exclusion chromatography was ultracentrifuged at 28,000 xg for 4 hours at 4 °C with 25% and 70% sucrose cushions. The fraction where the sample was originally loaded (top fraction), the interface fraction between the top fraction and 25% sucrose cushion, 25% sucrose cushion fraction, interface fraction between 25% and 70% sucrose cushions, 70% sucrose cushion fraction the pellet fraction resuspended with 50 µL PBS were collected.

4.4.4 Disassembly and reassembly of VLPs by dialysis

Disassembly of VLPs was carried out by dialyzing the aliquots containing the VLPs against a solution of PBS, pH 8.2, containing 0.166 M NaCl, 2 mM DTT and 2 mM EDTA. For the

reassembly procedure, samples were dialyzed against 2 L of PBS, pH 7.0, containing 0.5 M NaCl at 4°C with four changes of buffer. Both the disassembly and reassembly procedures were performed in the presence of 0.01% polysorbate 80 (Sigma).

4.4.5 Final purification and concentration by ultrafiltration

The samples were centrifuged at 5,000 x g at 4 ^{o}C and concentrated about 10 times with a centrifugal filter device, Vivaspin 20 centrifugal concentrator 1,000 kDa (Santorius, Germany).

4.5 Immunodot analysis

The fractions collected after size exclusion chromatography or ultracentrifugation were loaded on methanol-activated PVDF membrane as a dot and left until it gets soaked. The membrane was blocked with 5 % skim milk in TBS-T (tris-buffered saline, 0.05% tween 20) for 1 hour at room temperature. The membrane was probed with Anti-HPV16 L1 antibody [CamVir 1] (ab69, Abcam, USA) at dilution of 1:2000 with TBS-T for 1 hour at room temperature. After the membrane was washed with 5 % skim milk in TBS-T for 5 minutes 3 times, a secondary antibody directed against mouse IgG conjugated to Peroxidase at lilution of 1:4000 with TBS-T for 1 hour. After the membrane was washed with 5 % skim milk in TBS-T for 5 minutes 3 times, bound antibodies were detected using an enhanced chemiluminescence detection kit (ECL, GE Health care). Recombinant HPV-16 L1 protein (ab119880, Abcam, USA) was used as positive controls.

4.6 Sodium dodecyl sulphate–polyacrylamide gel electrophoresis (SDS-PAGE) and Western Blot analysis

Yeast cell lysate supernatants or purified VLP samples were diluted in sodium dodecyl sulfate polyacrylamide gel electrophoresis (SDS-PAGE) sample buffer, boiled at 100 °C for 10 min, electrophoresed through 10 % TGX Stain-Free SDS-PAGE gel (Bio-rad) and proteins were detected by Stain-Free technology (Bio-rad). Then gel was transferred to a PVDF membrane using a Bio-Rad semi-dry apparatus. The membrane was probed with Anti-HPV16 L1 antibody [CamVir 1] (ab69, Abcam) at dilution of 1:2000 with TBS-T for 1 hour at room temperature.

After the membrane was washed with 5 % skim milk in TBS-T for 5 minutes 3 times, a secondary antibody directed against mouse IgG conjugated to Peroxidase at lilution of 1:4000 with TBS-T for 1 hour. After the membrane was washed with 5 % skim milk in TBS-T for 5 minutes 3 times, bound antibodies were detected using an enhanced chemiluminescence detection kit (ECL, GE Health care). Recombinant HPV-16 L1 protein (ab119880, Abcam, USA) was used as positive controls.

4.7 Total protein quantification

The total amount of L1P18 protein in each purification step was quantified by densitometry of the dots after immunoblot analysis, using several concentrations of recombinant HPV-16 L1 protein (ab119880, Abcam, USA) as positive controls. The total protein of the sample after ultrafiltration step was analyzed by using Pierce™ BCA (bicinchoninic acid) Protein Assay Kit and the L1P18 protein obtained after all the purification steps in this study was quantified by comparing the total protein and the purity.

4.8 Transmission electron microscopy of L1P18 VLPs

The sample concentrated by ultrafiltration was fixed with 20% paraformaldehyde to the final concentration of 4% paraformaldehyde for overnight. Then, the sample was negatively stained on carbon-only 200 mesh grids (20 nm) with 2% phosphotungstic acid at pH 7.2. The stained grids were left to air-dry prior to examination for overnight. The prepared grids were observed by Spirit TWIN (FEI) 120 kV LaB6 Tecnai transmission electron microscope (TEM) operated at Electron Microscopy unit in Science and Technology Centres, University of Barcelona.

5. Results

5.1 Construction of recombinant *P. pastoris* X-33-L1P18 strains

HPV L1 VLPs have been already used as HPV vaccines and the vaccinations led to the stimulation of HPV-specific humoral immune responses. HIV-1 P18-I10 is a gp160 envelope-derived epitope of HIV-1 IIIB isolate and a well-known immunodominant HIV-1 CTL epitope [145]. The HIV-1 P18I10 peptide was inserted into in the loop D-E of the HPV-16 L1 protein because Sadeyen et al [122] showed that Hepatitis B virus capsid (HBc) protein was more immunogenic when it was inserted in the D-E loop of HPV-16 L1 compared to other loops (Figure 18A and 18B). The D-E loop is exposed to the exterior when 360 L1 proteins form a VLP so that the inserted HIV-1 P18I10 proteins are supposed to be situated on the surface of the chimeric HPV-HIV VLP (Figure 18C and 18D). Using this design, the P18 immunogen is supposed to be presented 360 times in each VLP particle in a highly exposed location.

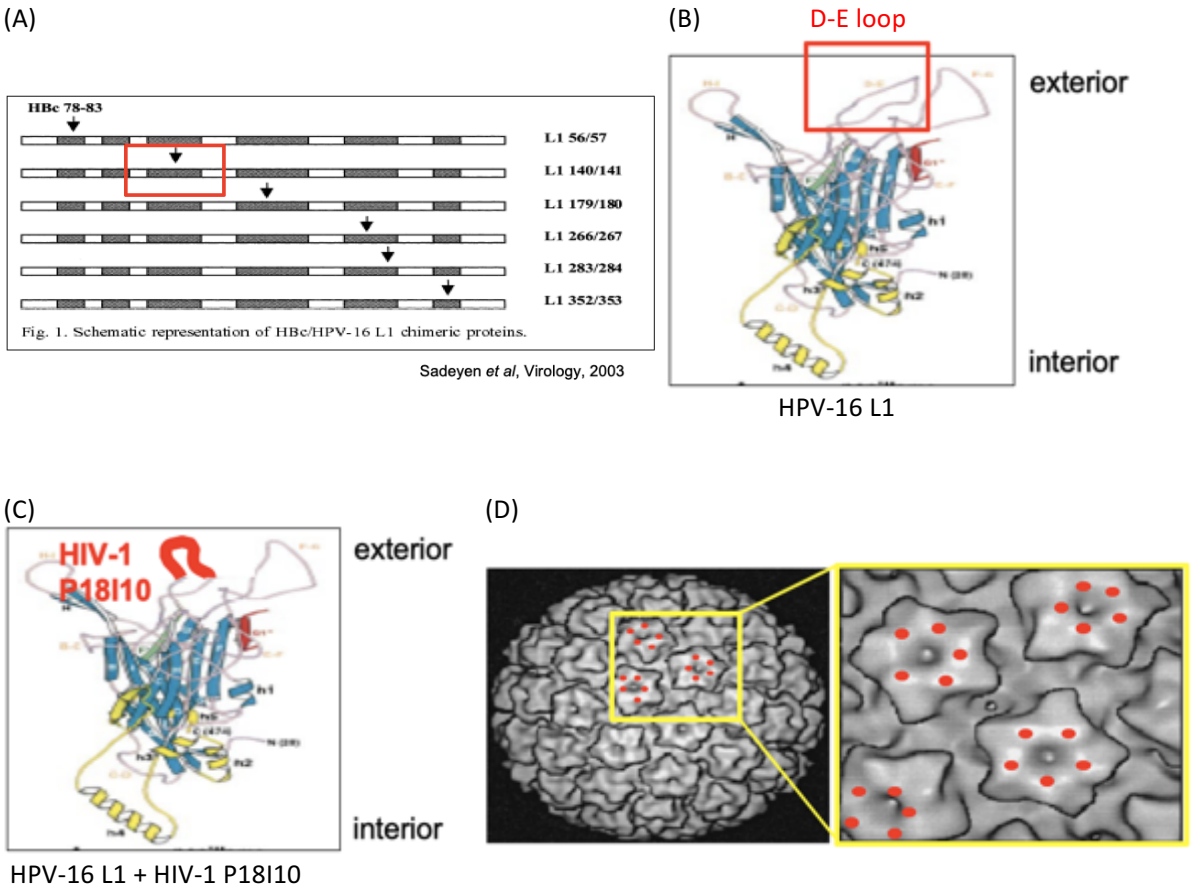

Figure 18. Immunogen design and construction of chimeric HPV-HIV VLP. (A) Schematic representation of HBc/HPV-16 L1 chimeric protein (6) (B) HPV-16 L1 model (C) HPV-16 L1 + HIV-1 P18I10 model (D) chimeric HPV-HIV VLP model

5.1.1 Construction of recombinant *P. pastoris* X-33 harboring pGAPZB-L1P18

The DNA fragment containing the L1P18 coding sequence was inserted into the integrative plasmid pGAPZB (Figure 19A), which constitutively drives production of proteins intracellularly, as a EcoRI-XhoI fragment under the control of glyceraldehyde-3-phosphate dehydrogenase (GAP) promoter. The constructed recombinant plasmid DNA was confirmed by Sanger sequencing (data not shown). The recombinant plasmid DNA was first transformed into *E. coli* by heat-shock for the amplification and purification of the plasmid DNA, and then transformed into the *P. pastoris* X-33 by electroporation. The integration of the expression vector into the genome of the transformants was verified by PCR analysis using a pair of primers flanking the L1P18 gene (Figure 19B) and L1P18 protein expression was further confirmed by western blot analysis (Figure 19C).

(A)

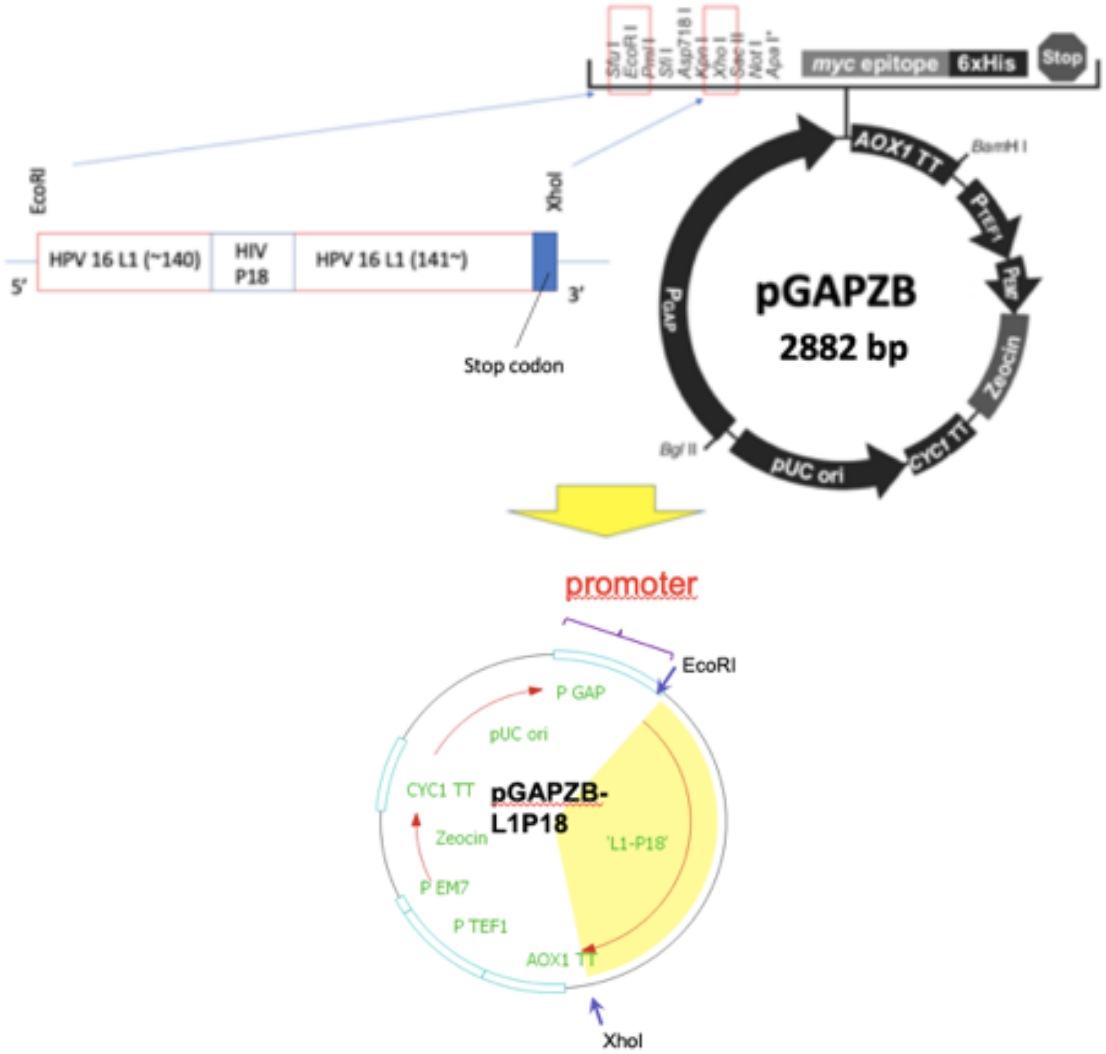

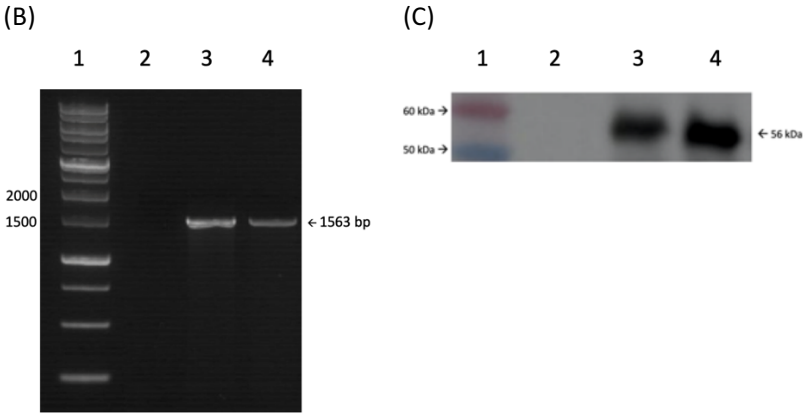

Figure 19. Construction of recombinant X-33-L1P18 yeast strain. (A) Cloning of L1P18 DNA coding sequence into yeast plasmid DNA pGAPZB. (B) PCR analysis of genomic DNA isolated from recombinant *P. pastoris* clone. Amplification of a 1563-bp DNA fragment containing L1P18 reveals positive clones. Lane 1, molecular weight markers; lane 2, Recombinant *P. pastoris* X-33 harboring the pGAPZB without heterologous DNA insert (negative control); lane 3, *P. pastoris* X-33 harboring the pGAPZB-L1P18 expressing the gene encoding the L1P18 protein; lane 4, pGAPZB-L1P18 plasmid (positive control) (C) Western blot analysis of recombinant *P. pastoris* cell lysate. Lane 1, molecular weight markers (50 kDa and 60 kDa); lane 2, Recombinant *P. pastoris* X-33 harboring the pGAPZB without heterologous DNA insert (negative control); lane 3, P. pastoris X-33 harboring the pGAPZB-L1P18 expressing the gene encoding the L1P18 protein; lane 4, abcam HPV16 L1 protein 100 ng (positive control, 56 kDa)

The recombinant clones were isolated by Zeocin antibiotic selection system (Figure 20A). Since pGAPZB is an integrative plasmid DNA, the genomic DNA was extracted from the cell culture, and the integration of the expression vector containing the L1P18 DNA coding sequence in the recombinant yeast colonies was confirmed by performing PCR analysis on purified genomic DNA from the transformants (Figure 20B).

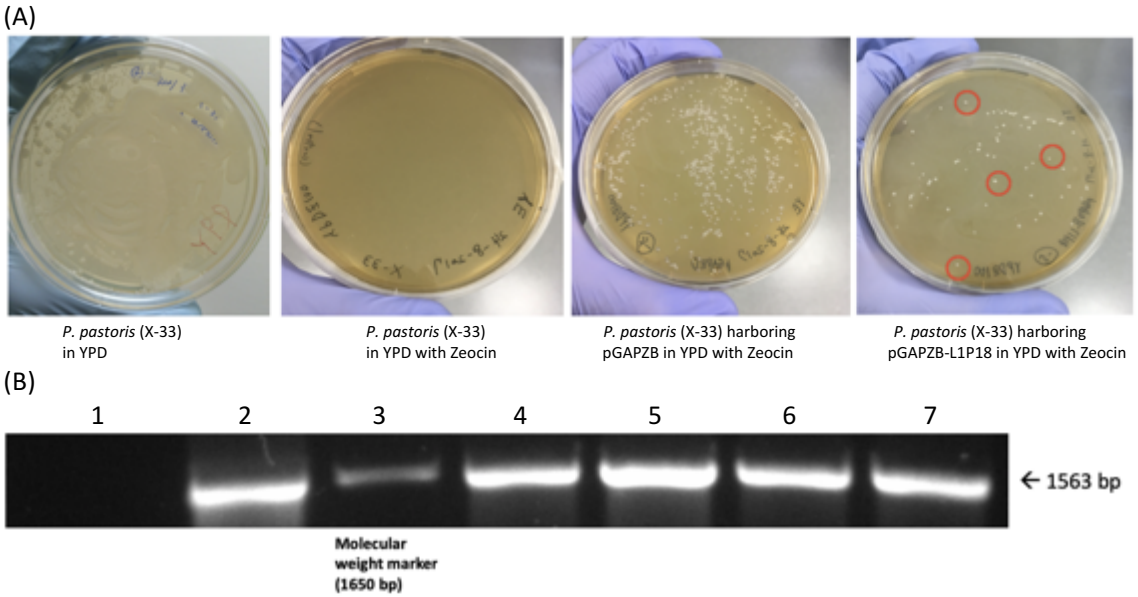

Figure 20. Genetic characterization of recombinant P. pastoris X-33-L1P18 strains. (A) antibiotic selection of recombinant strains. 4 colonies *P. pastoris* (X-33) harboring pGAPZB-L1P18 (red circled) were used for yeast colony PCR. (B) PCR analysis of genomic DNA isolated from recombinant *P. pastoris* clones. Lane 1. X-33 harboring the pGAPZB without DNA insert (negative control); lane 2, plasmid pGAPZB-L1P18 (positive control); lane 3. Molecular weight marker (Invitrogen 1kb plus DNA ladder, 1650 bp); lanes 4-7: Recombinant yeast strains containing the pGAPZB-L1P18 carrying the DNA coding sequence L1P18 (1563 bp).

5.1.2 Construction of recombinant *P. pastoris* X-33 harboring pPICZαA-L1P18

L1P18 DNA coding sequence was inserted into the integrative plasmid pPICZαA (Figure 21A and 21B), which drives production and secretion of proteins by methanol induction, as a EcoRI-NotI fragment under the control of Alcohol Oxidase 1 (AOX1) promoter. The correct insertion of the L1P18 DNA coding sequence was confirmed by enzymatic digestion of the recombinant plasmid pPICZαA-L1P18 (Figure 21C and 21D). The recombinant plasmid DNA was first transformed into *E. coli* by heat-shock for the amplification and purification of the plasmid DNA and then transformed into the *P. pastoris* X-33 by electroporation. The integration of the expression vector into the genome of transformants was verified by PCR analysis (Figure 21E) but the L1P18 protein expression was not detected by western blot analysis while it was detected by dot blot analysis (Figure 21F and 21G).

(A)

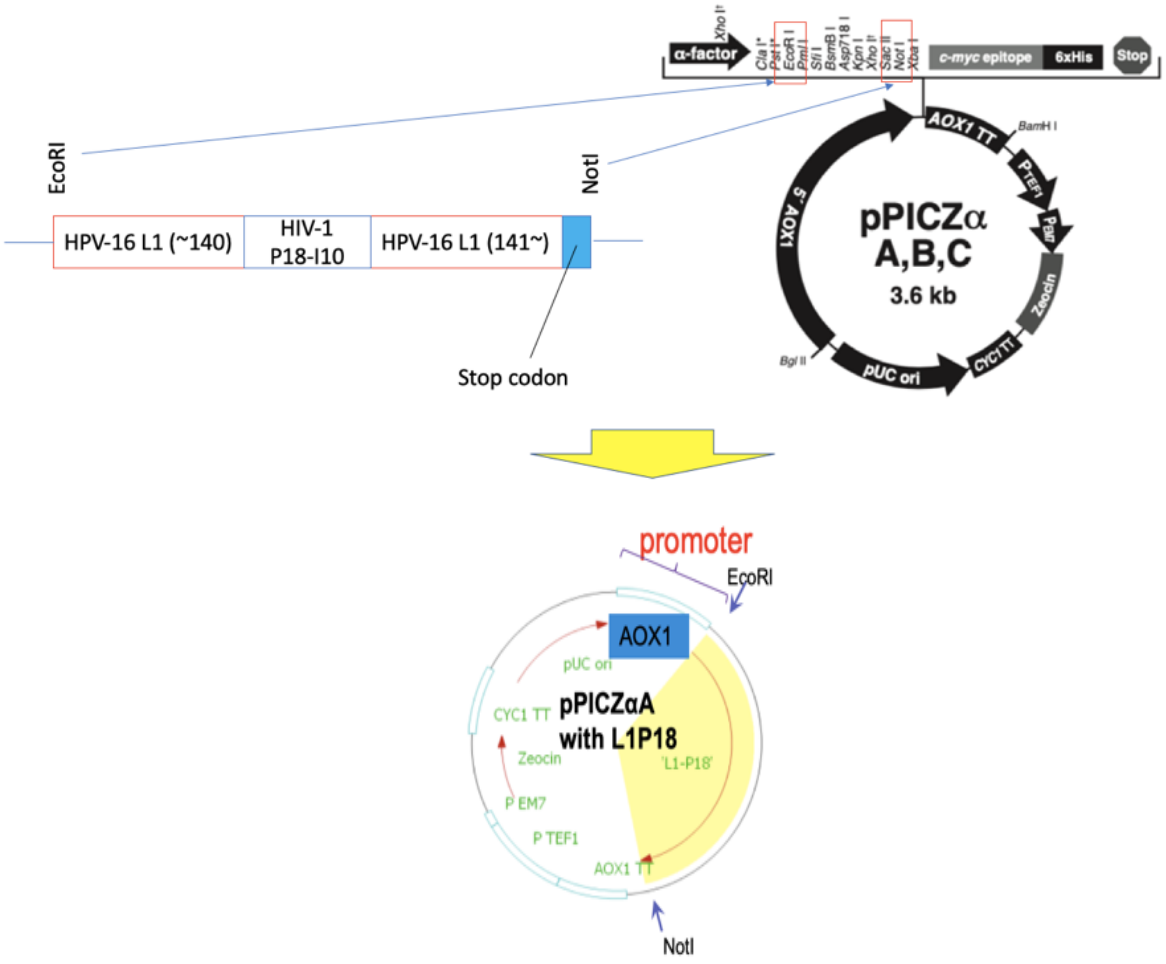

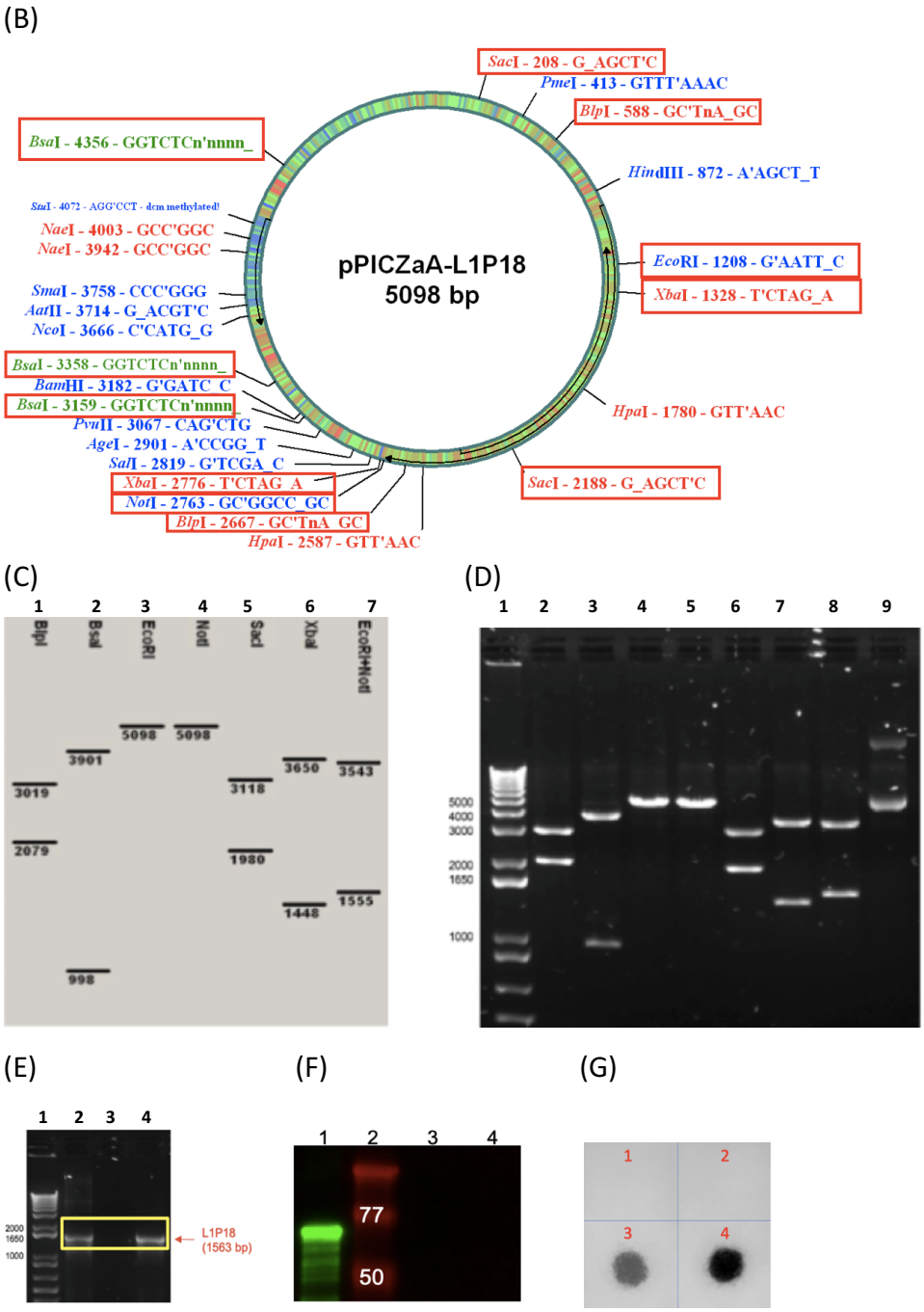

Figure 21. Construction of recombinant X-33-L1P18 yeast strain. (A) Cloning of L1P18 DNA coding sequence into yeast plasmid DNA pPICZαA. (B) enzymatic restriction sites on plasmid DNA pPICZαA-L1P18. (C) Expected size of DNA fragments generated after enzymatic digestions of the recombinant DNA plasmid pPICZαA-L1P18. Lane 1, BlpI; lane 2, BsaI; lane 3, EcoRI; lane 4, NotI; lane 5, SacI; lane 6, XbaI; lane 7 EcoRI+NotI (D) Enzymatic digestions of the recombinant DNA plasmid pGAPZαA-L1P18. Lane 1, molecular weight markers; lane 2, BlpI; lane 3, BsaI; lane 4, EcoRI; lane 5, NotI; lane 6, SacI; lane 7, XbaI, lane 8, EcoRI+NotI; lane 9, without enzyme (no digestion) (E) PCR analysis of genomic DNA isolated from recombinant *P. pastoris* clone. Amplification of a 1563-bp DNA fragment containing L1P18 reveals positive clones. Lane 1, molecular weight markers; lane 2, *P. pastoris* X-33 harboring the pPICZαA-L1P18 expressing the gene encoding the L1P18 protein lane 3, Recombinant *P. pastoris* X-33 harboring the pPICZαA without heterologous DNA insert (negative control); lane 4, pGAPZB-L1P18 plasmid (positive control, 1563 bp). (F) Western blot analysis. Lane 1, abcam HPV16 L1 protein 100 ng (positive control, 56 kDa); lane 2, molecular weight markers; lane 2, *P. pastoris* X-33 harboring the pPICZαA-L1P18 expressing the gene encoding the L1P18 protein lane 3, Recombinant *P. pastoris* X-33 harboring the pPICZαA without heterologous DNA insert (negative control) (G) Dot blot analysis. Dot 1, PBS; dot 2, Recombinant *P. pastoris* X-33 harboring the pPICZαA without heterologous DNA insert (negative control); lane 3, *P. pastoris* X-33 harboring the pPICZαA-L1P18 expressing the gene encoding the L1P18 protein lane 3,) Dot 4, abcam HPV16 L1 protein 1 ng (positive control)

The recombinant clones were isolated by Zeocin antibiotic selection system (Figure 22A). Since pPICZαA is an integrative plasmid DNA, the genomic DNA was extracted from the cell culture, and the integration of the expression vector containing the L1P18 DNA coding sequence in the recombinant yeast colonies was confirmed by performing PCR analysis on purified genomic DNA from the transformants (Figure 22B).

(A)

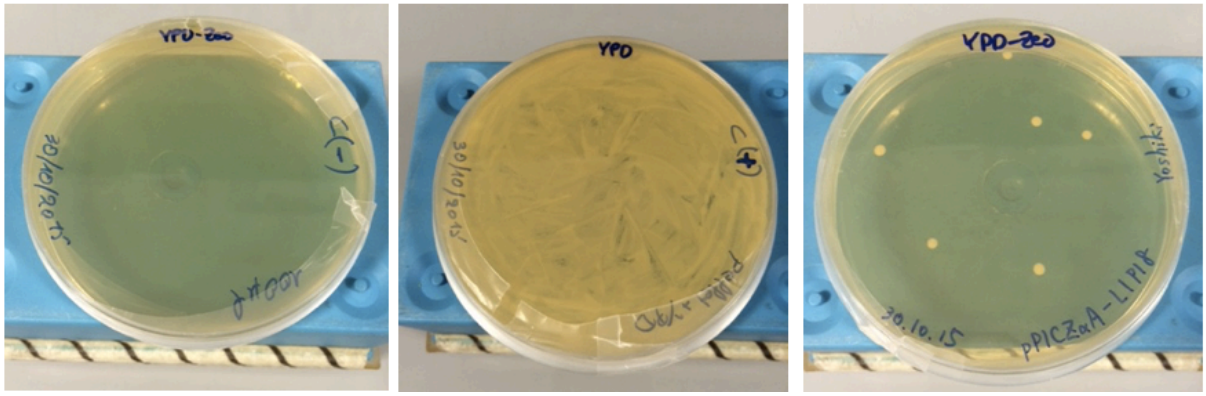

P. pastoris X-33 in YPD with Zeocin

P. pastoris X-33 harboring pPICZαA in YPD with Zeocin

P. pastoris X-33 harboring pPICZαA-L1P18 in YPD with Zeocin

(B)

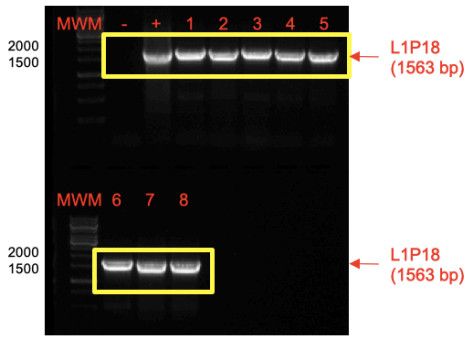

Figure 22. Genetic characterization of recombinant P. pastoris X-33-L1P18 strains. (A) antibiotic selection of recombinant strains (B) Yeast colony PCR. MWM: molecular weight markers, -: water (negative control) +: plasmid DNA pPICZαA-L1P18; lanes 1-8, DNA extracted from 8 colonies.

5.2 Phenotypic characterization of recombinant *P. pastoris* X-33-L1P18 strains

5.2.1 Small-scale screening of L1P18 production by *P. pastoris* X-33/pGAPZB-L1P18 clones

In order to take into account clone heterogeneity, a phenomenon commonly found when transforming *P. pastoris* (e.g. due to seldom integration of multiple copies of the expression vector, ectopic integration events or post transformation recombination events), four independent clones harboring pGAPZB-L1P18 were selected (see Section 5.1.1). These were further analyzed to test L1P18 production levels. To this end, clones were picked up from the agar plate and were grown in 25 mL YPD broth 100 µg /mL containing Zeocin in 250 mL baffled shake flasks as described in the Materials and Methods section. At the end of the culture, cells were harvested and after cell lysis by means of a high-pressure cell disruptor, L1P18 protein production was confirmed by western blot analysis (Figure 23). L1P18 production level among four clones were the same so that they were stored as working stocks for further use.

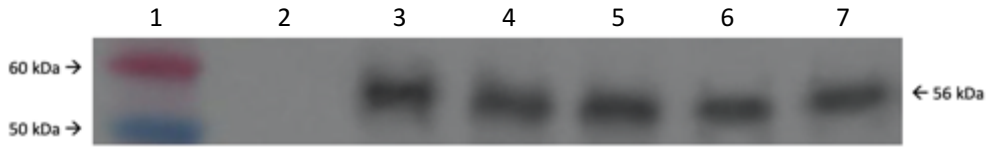

Figure 23. Phenotypic characterization of recombinant *P. pastoris*. Western blot analysis of 4 recombinant P. pastoris cell lysates. Lane 1. Molecular weight markers (50 kDa and 60 kDa); lane 2, Recombinant *P. pastoris* X-33 harboring the pGAPZB without heterologous DNA insert (negative control); lane 3, abcam HPV16 L1 protein 75 ng (positive control, 56 kDa); lanes 4-7, 4 recombinant *P. pastoris* X-33 colonies harboring the pGAPZB-L1P18 expressing the L1P18 protein.

5.2.2 Small-scale screening of L1P18 production by *P. pastoris* X-33/pPICZαA-L1P18 clones

In order to In order to take into account clone heterogeneity, a phenomenon commonly found when transforming *P. pastoris* (e.g. due to seldom integration of multiple copies of the expression vector, ectopic integration events or post transformation recombination events), four independent clones harboring pPICZαA-L1P18 were selected (see Section 5.1.2). These were further analyzed to test L1P18 production levels. To this end, clones were picked up from the agar plate and were incubated in 25 mL YPD broth 100 µg /mL containing Zeocin in 250 mL baffled shake flasks at 30 °C at 150 rpm for 12 hours. For the other half of culture, the yeast cells were grown in BMG media and then in BMM containing methanol for the protein induction. The L1P18 protein expression was confirmed by dot blot analysis (Figure 24). L1P18 production level among eight clones were the same so that they were stored as working stocks for further use.

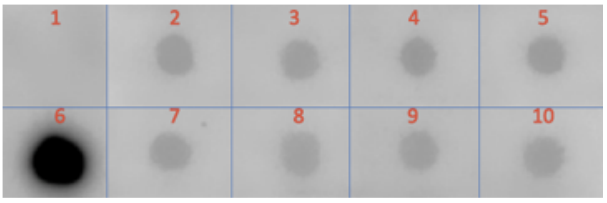

Figure 24. Phenotypic characterization of recombinant *P. pastoris.* Immunodot analysis of 8 recombinant *P. pastoris* supernatants. Dot 1, Supernatant from X-33 harboring pPICZαA (negative control); Dots 2-5 and 7-10, Supernatants of 8 independent cultures of X-33 harboring pPICZαA-L1P18; dot 6, abcam HPV16 L1 protein 20 ng (positive control)

5.3 Production of L1P18 protein

5.3.1 L1P18 production by *P. pastoris* X-33/pGAPZB-L1P18 in large scale culture

The cells of *P. pastoris* X-33 harboring pGAPZB-L1P18 were cultured at 30 °C at 150 rpm for 48 hours in 1.75 L of YPD media at final OD_{600}=20. The cells were processed as described in materials and methods. The cell lysate pellets were rususpended with SDS-PAGE sample buffer and boiled at 100 °C for 10 min. The production level of L1P18 protein was estimated by immunodot analysis (Figure 25). The estimated amount of L1P18 in the soluble fraction of 1.75 L culture was 81.3 μg and the estimated amount of L1P18 in the insoluble fraction was 755.5 μg.

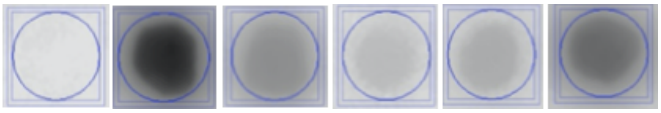

	1	2	3	4	5	6
densitometry of dots	0	20.3	2.13	0.531	0.689	6.44
amount (ng)/4 μL breaking buffer or SDS-PAGE buffer	0	10	1	0.25	0.325	3.02
amount (μg)/1.75 L culture					81.3	755.5

Figure 25. Quantification of L1P18 protein. Immunodot analysis of soluble and insoluble fractions from 1.75 L culture. Every dot is of 4 μL. Dot 1, 10^{-1} dilution of cell lysate from X-33 harboring pGAPZB (negative control); dot 2, abcam HPV16 L1 protein 10 ng (positive control); dot 3, abcam HPV16 L1 protein 1 ng (positive control); dot 4, abcam HPV16 L1 protein 0.25 ng (positive control); dot 5, 10^{-1} dilution of cell lysate supernatant from X-33 harboring pGAPZB-L1P18; dot 6, 10^{-1} dilution of resuspended cell lysate pellet of X-33 harboring pGAPZB-L1P18 with SDS-PAGE buffer.

5.3.2 L1P18 production by *P. pastoris* X-33/pPICZαA-L1P18 in large scale culture

The cells of *P. pastoris* X-33 harboring pPICZαA-L1P18 were cultured at 30 °C at 150 rpm for 16 hours in 100 mL BMG media at final OD_{600} =5 and then cultured at 30 °C at 150 rpm for 48 hours in 1 L of BMM media at final OD_{600} =20 by adding 100% methanol to a final concentration of 0.5% methanol every 12 hours to maintain induction of gene expression. The supernatant was collected by centrifugation at 10,000 ×g for 10 min at 4 °C. The cells were processed as described in materials and methods. The production level of secreted L1P18 protein was estimated by immunodot analysis (Figure 26). The estimated amount of secreted L1P18 from 1 L culture was 167 μg and the estimated amount of L1P18 in the intracellular soluble fraction was 1412.5 μg.

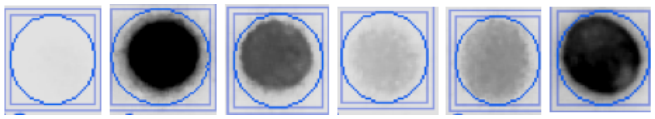

	1	2	3	4	5	6
densitometry of dots	0	24.9	5.13	0.62	1.73	14.1
amount (ng)/4 μL supernatant or breaking buffer	0	10	2	0.25	0.668	5.65
amount (μg)/1 L culture					167	1412.5

Figure 26. Quantification of L1P18 protein. Immunodot analysis of secreted L1P18 protein and intracellular L1P18 protein in the soluble fraction from 1 L culture. Every dot is of 4 μL. Dot 1, 10^{-1} dilution of cell lysate from X-33 harboring pPICZαA (negative control); dot 2, abcam HPV16 L1 protein 10 ng (positive control); dot 3, abcam HPV16 L1 protein 2 ng (positive control); dot 4, abcam HPV16 L1 protein 0.25 ng (positive control); dot 5, Supernatant from the cell culture of X-33 harboring pPICZαA -L1P18; dot 6, 10^{-1} dilution of cell lysate supernatant from X-33 harboring pPICZαA-L1P18.

In order to find the reason why western blot analysis did not work for the strain, the supernatant containing secreted L1P18 protein was concentrated 10 times by tangential flow filtration system with 0.45 μm filter and then immunodot analysis was performed on the secreted L1P18 after three different treatments, on ice for 10 min, at 37 °C for 10 min and at 100 °C for 10 min (Figure 27). In this analysis, the densitometry of secreted L1P18 protein was less in the treatment of 37 °C for 10 min compared to the treatment on ice for 10 min and when it comes to the treatment of 100 °C for 10 min, the signal was almost disappeared.

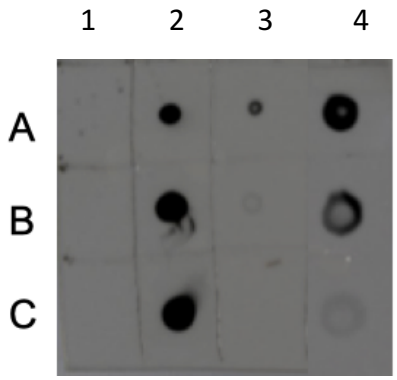

Figure 27. Immunodot analysis of L1P18 protein. Immunodot analysis of secreted L1P18 protein after three different treatment. Every dot is of 4 μL. Lane A, on ice for 10 min; lane B, 37 °C for 10 min; lane C, 100 °C for 10 min; lane 1, 10^{-1} dilution of cell lysate from X-33 harboring pPICZαA (negative control); lane 2, abcam HPV16 L1 protein 1 ng (positive control); lane 3, Supernatant from the cell culture of X-33 harboring pPICZαA -L1P18; lane 4, 10x concentrated supernatant from the cell culture of X-33 harboring pPICZαA -L1P18.

Furthermore, the secretion capacity of *P. pastoris* X-33 harboring pPICZαA-L1P18 was analyzed at Autonomous University of Barcelona, Faculty of Engineering, Department of Chemical, Biological and Environmental Engineering by labeling green fluorescent protein (GFP) on L1P18 protein inside the cells of *P. pastoris* X-33 harboring pPICZαA-L1P18 in BMM media. This analysis detected that L1P18 protein was not secreted properly because the size of L1P18 protein is beyond the secretion capacity of *P. pastoris* X-33 with α secretion signal.

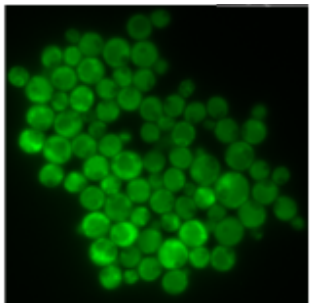

Figure 27. immunofluorescence staining of L1P18 protein with GFP inside the cells of P. pastoris X-33 harboring pPICZαA-L1P18 in BMM media.

Due to the heat sensitivity and the limitation of secretion capacity, the project with *P. pastoris* X-33 harboring pPICZαA-L1P18 became on hold.

5.4 Downstream process development: Selection and optimization of VLP purification methods

5.3.1 General strategy

Given the extremely limited capacity of *P. pastoris* to produce secrete L1p18 VLPs, our study focused on the development of a downstream process for recovery, purification of L1P18 protein intracellularly produced in *P. pastoris* and subsequent generation of VLPs.

In addition to choosing the type and sequence of recovery and purification steps, we also aimed at optimizing the operating conditions for each one of them.

In order to select the best product recovery and purification strategy, an important goal of this study was to establish a series of analytical methods and key indicators for assessment and selection of the optimal purification process alternatives. For product quantity, total protein quantitation and dot blot analysis for L1 quantitation were performed. For product quality and purity, SDS-PAGE, Coomassie staining, and Western blot analysis were conducted. For final assembled product identity (structural initial characterization), Transmission electron microscopy (TEM) was used.

The purification process was divided into three different stages: (a) product recovery, (b) product concentration and conditioning, and (c) product purification. Product purification was essentially done by a series of chromatographic techniques and comprised a minimum of two steps: a capturing and refinement step (Figure 28). Initially, heparin chromatography and cation exchange chromatography were tested as a capturing step based on literature [6, 7]. However, the yield and purity was lower than described in those previous studies, so alternative techniques were sought. In particular, the use of a special type of size exclusion chromatography was explored as a capturing step based on a recent GE application note [8]. Unlike conventional size exclusion typically used for polishing after capturing, this type of size exclusion chromatography can be used for capturing, followed by anion exchange chromatography as a polishing step. In addition, two additional alternatives were tested as alternative polishing steps, namely heparin chromatography and ultracentrifugation with sucrose cushion.

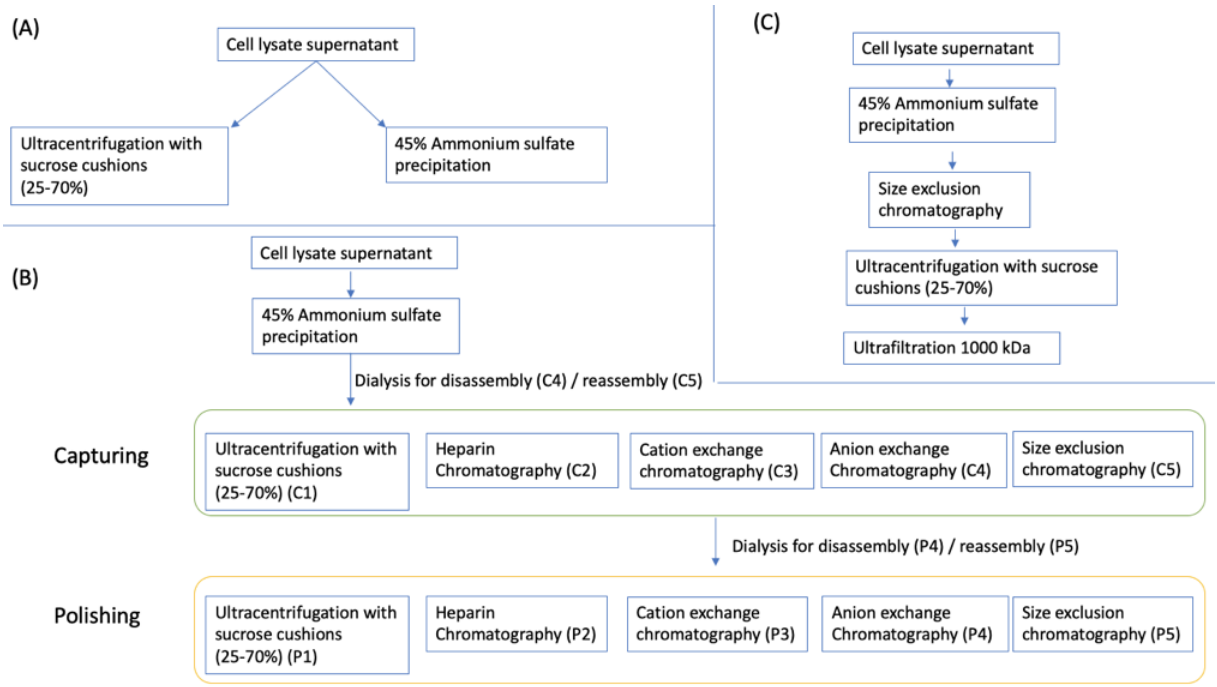

Figure 28. Optimization of HPV-HIV VLP purification procedures. (a) Ultracentrifugation with sucrose cushions and 45% ammonium sulfate precipitation are compared as the first part of secondary purification step. (b) Ultracentrifugation with sucrose cushions, heparin chromatography, cation exchange chromatography, anion exchange chromatography, size exclusion chromatography and several combinations of them were tested as the second and third parts of the secondary purification step (capturing and polishing). (c) Optimized purification procedure for chimeric HPV-HIV VLPs.

(a) **Product recovery**: First, the lysis step was optimized. Cells were lysed by enzyme lyticase, glass beads, and French press. Taking into account the ease, efficiency and cost of the disruption, French press was chosen. While L1P18 proteins were mostly seen in the insoluble fraction after the cell lysis, the use of Tween 80 in lysis buffer helped to solubilize approximately 30% of L1P18 protein in the insoluble fraction. Also, the use of protease inhibitors reduced the degradation of L1P18 due to the yeast enzymes activated by lysis.

(b) Product concentration and conditioning: the main purpose of this process was to concentrate our product from the soluble cell extract with minimum loss and degradation, efficiently by a simple procedure, as well as allowing a first elimination of impurities prior to further purification step such as chromatography. In our study, based on published methods [6,7], ultracentrifugation with sucrose cushions and 45% ammonium sulfate precipitation were compared.

The cell lysate supernatant containing L1P18 protein was ultracentrifuged at 28,000 xg for 4 hours at 4 °C with 25% and 70% sucrose cushions. However, this method did not efficiently separate L1P18 from other contaminants and was difficult to process (Figure 29).

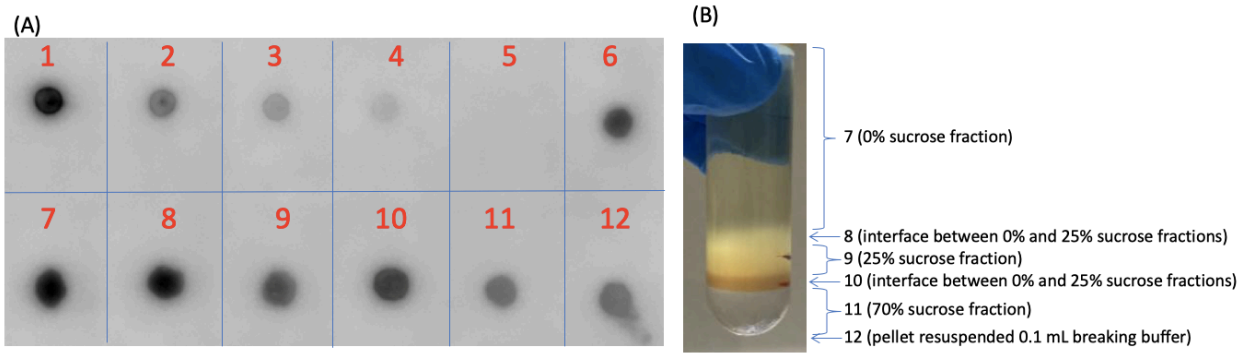

Figure 29. Ultracentrifugation of cell lysate supernatant. (A) Dot blot analysis of ultracentrigugated fractions. Dot 1, abcam HPV-16 L1 20 ng (+ control); dot 2, abcam HPV-16 L1 10 ng (+ control); dot 3, abcam HPV-16 L1 5 ng (+ control); dot 4. abcam HPV-16 L1 2.5 ng (+ control); dot 5, PBS; dot 6, Cell lysate supernatant; dot 7, 0% sucrose; dot 8, Interface between 0% and 25%; dot 9, 25% sucrose; dot 10, Interface between 25% and 70%; dot 11, 70% sucrose; dot 12, Pellet resuspended with 0.1 mL breaking buffer. (B) Ultracentrifuge tube after ultracentrifugation. The numbers are matched with the lane numbers in (A).

On the other hand, the cell lysate supernatant was adjusted to 45% saturated ammonium sulfate and left stirred for 1 hour at 4 °C, and the precipitated protein was pelleted at 12,000 xg for 10 min at 4 °C. The pellet was resuspended in 10 ml of PBS + 0.01% Tween 80. To remove further contaminants, the ammonium sulfate precipitate was dialyzed against PBS + 0.01% Tween 80 and diluted 10 times in incubation buffer (10 mM sodium phosphate, pH 7.2, 150 mM NaCl + 0.01% Tween 80). This suspension was incubated at room temperature for 24 hours, the precipitated protein was removed by centrifugation at 12,000 xg for 10 min, and the supernatant subsequently obtained. Finally, ammonium sulfate precipitation was chosen as the first purification step because this method concentrated our product and removed contaminants better than ultracentrifugation with sucrose cushions.

(c) Product purification and refinement: First, the aim was to select the most efficient capturing chromatographic step (C1-C5, Figure 29B) as well as the sequence of the subsequent purification/polishing steps (P1-P5, Figure 29B). Initially, ultracentrifugation with sucrose cushion (C1) and heparin chromatography (C2) were tested as capturing step [6, 7], but the yield of purified VLP recovery was less than 10%. Thus, alternative chromatography purification methods, namely cation exchange chromatography (CEC) (C3) [7], anion exchange chromatography (AEC) (C4) and size exclusion chromatography (SEC) (C5) were tested. As a result, SEC itself was selected as the most suitable purification step after ammonium sulfate precipitation because SEC showed most stable, higher recovery yield and higher selectivity.

Once the capturing step was selected, the next aim was to obtain the best sequence of intermediate and final polishing steps after SEC. To this end, two additional chromatographic steps (P2 and P4) were systematically evaluated as intermediate steps as well as ultracentrifugation (P1) followed by ultrafiltration 1000 kDa as final polishing step. As a result, the ultracentrifugation (P1) proved to be more efficient.

5.4.2 Systematic optimization of capturing and polishing steps

Different alternatives for product capturing and polishing purification steps were tested following a systematic step-by-step approach.

5.4.2.1 Assessment of alternative capturing steps.

[C1] Ultracentrifugation

The sample obtained after ammonium sulfate precipitation was filtered by 0.45 µm and ultracentrifuged at 28,000 xg for 4 hours at 4 °C with 25% and 70% sucrose cushions. However, this method also did not efficiently separate L1P18 protein and L1P18 protein was detected in every fraction by dot blot analysis (Figure 30).

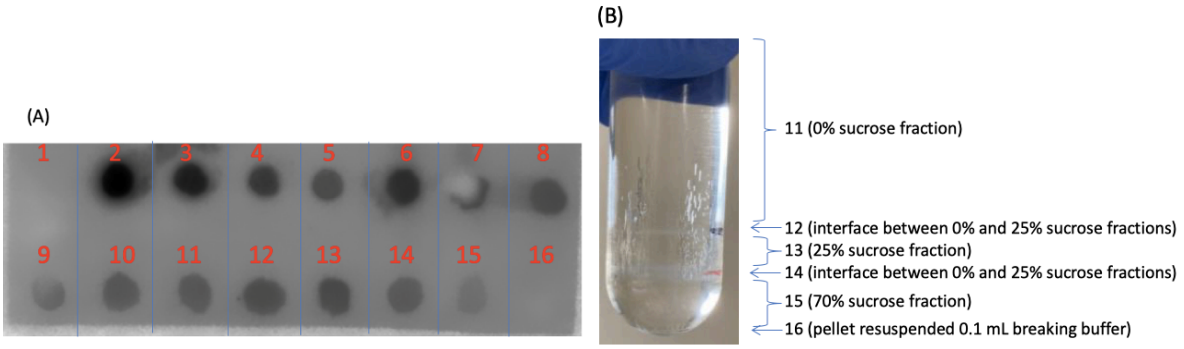

Figure 30. Ultracentrifugation after ammonium sulfate precipitation (ASP). (A) Dot blot analysis of ultracentrigugated fractions. Dot 1, PBS; dot 2, abcam HPV-16 L1 20 ng (+ control); Dot 3, abcam HPV-16 L1 10 ng (+ control); Dot 4, abcam HPV-16 L1 5 ng (+ control); dot 5, abcam HPV-16 L1 2.5 ng (+ control); dot 6, cell lysate; dot 7, ASP pellet resuspended; dot 8, ASP supernatant, lane 9, sample after 24 h incubation; dot 10; 0.45 um filtered sample (pre UC sample); dot 11, 0% sucrose; dot 12, Interface between 0% and 25%; dot 13, 25% sucrose; dot 14, Interface between 25% and 70%; dot 15, 70% sucrose; dot 16, Pellet resuspended with 0.1 mL breaking buffer. (B) Ultracentrifuge tube after ultracentrifugation. The numbers are matched with the lane numbers in (A).

[C2] Heparin chromatography

The sample obtained after ammonium sulfate precipitation was filtered by 0.45 µm and further purified by heparin chromatography with HiTrap Heparin HP 5mL column (GE) on ÄKTA pure (GE) according to the standard setting described in the column instructions. L1P18 was seen as double band in several fractions in elution over two peaks so alternative method was sought (Figure 31).

(A)

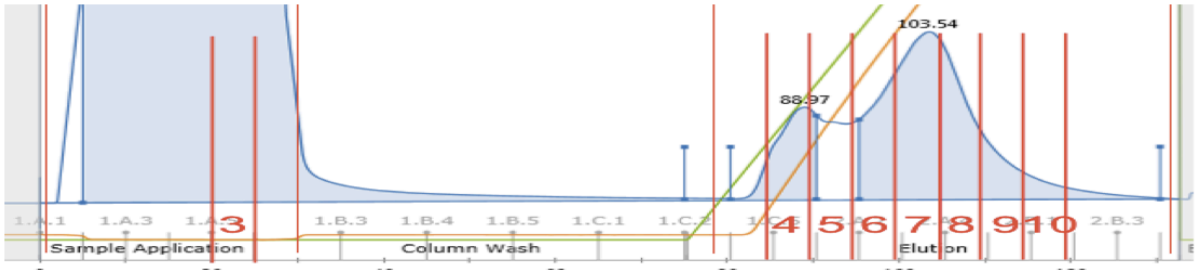

(B)

Figure 31. Western blot analysis after heparin chromatography. (A) Heparin chromatogram of the sample after ASP. The numbers are matched with the lane numbers in (B). (B) Western blot analysis. Lane 1, L1 standard 100 ng (abcam) (56 kD); lane 2, molecular weight marker (Bio-Rad); lane 3, 5th fraction in sample application; lane 4, 3rd fraction in elution; lane 5, 4th fraction in elution; lane 6, 5th fraction in elution; lane 7, 6th fraction in elution; lane 8, 7th fraction in elution; lane 9, 8th fraction in elution; lane 10, 9th fraction in elution

[C3] Cation exchange chromatography

The sample after ammonium sulfate precipitation was gone through HiScreen Capto SP ImpRes cation exchange chromatography column (GE) according to the standard setting described in the column instructions, but the yield of L1P18 protein recovery was very low while containing huge amount of contaminants (Figure 32).

(A)

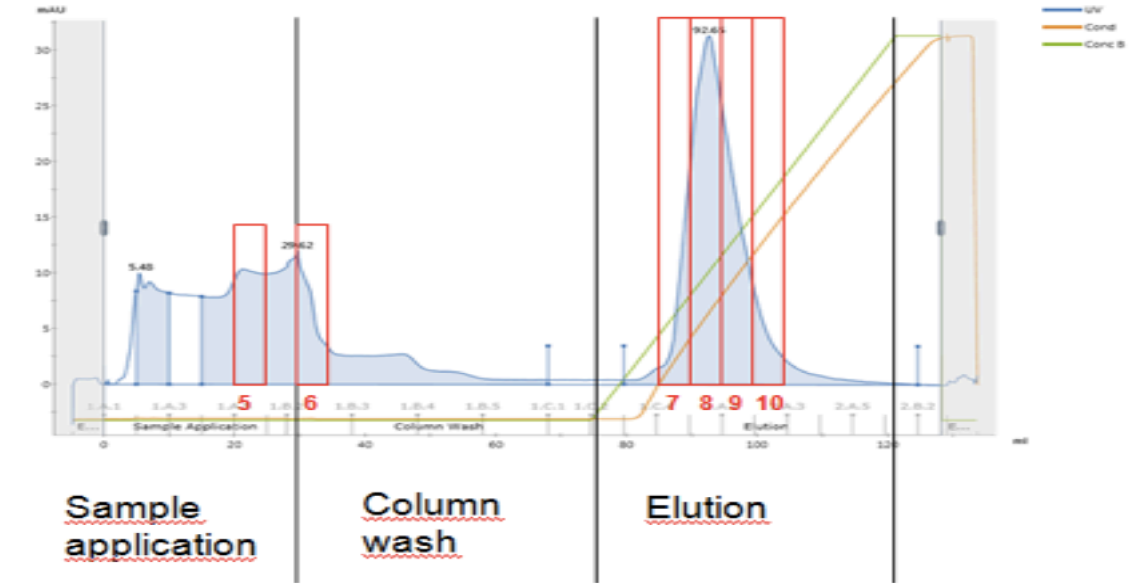

(A) (C)

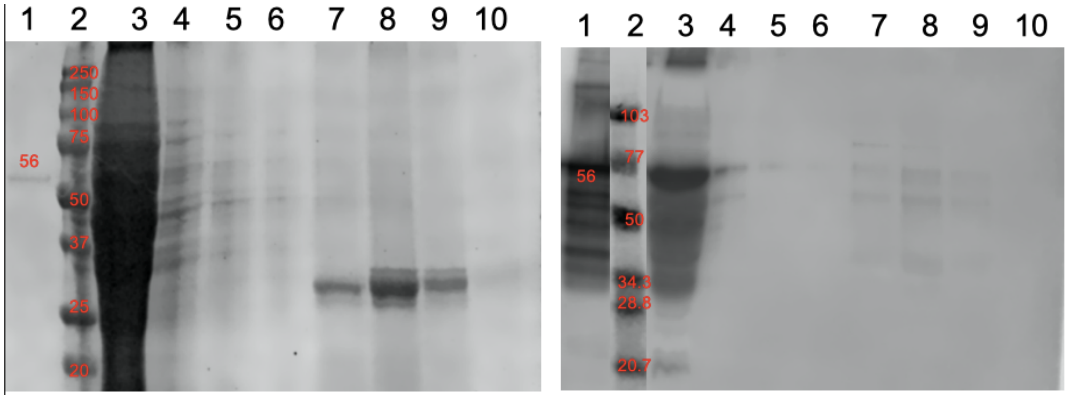

Figure 32. Coomassie staining and western blot analysis after cation chromatography. (A) Cation chromatogram of the sample after ASP. The numbers are matched with the lane numbers in (B) and (C). (B) Coomassie staining. Lane 1, L1 standard 900 ng (abcam) (56 kD); lane 2 : molecular weight marker (Bio-Rad); lane 3, recombinant yeast cell lysate supernatant; lane 4, sample applied to cation exchange chromatography ; lane 5, 5th fraction in sample application; lane 6, 1st fraction in wash; lane 7, 3rd fraction in elution; lane 8, 4th fraction in elution; lane 9, 5th fraction in elution; lane 10, 6th fraction in elution (C) Western blot analysis. Lane 1, L1 standard 900 ng (abcam) (56 kD); lane 2 : molecular weight marker (Bio-Rad); lane 3, recombinant yeast cell lysate supernatant; lane 4, sample applied to cation exchange chromatography ; lane 5, 5th fraction in sample application; lane 6, 1st fraction in wash; lane 7, 3rd fraction in elution; lane 8, 4th fraction in elution; lane 9, 5th fraction in elution; lane 10, 6th fraction in elution.

5.4.2.2. Combined assessment of capturing and polishing steps

[C2P2] Heparin chromatography followed by heparin chromatography

The elution fractions from C2 were gone through HiTrap Heparin HP 5mL column (GE) on ÄKTA pure (GE) again according to the standard setting described in the column instructions. However, no flowthough product were seen during the sample application and eventually the elution fractions were almost the same as the ones in C2.

[C5P4] Size exclusion chromatography followed by Anion exchange chromatography

According to GE application note (6), the sample after ammonium sulfate precipitation was dialyzed for reassembly condition at 4 ^{o}C and gone through Capto™ Core 700 size exclusion chromatography column (GE) (Figure 33). Then the flowthroughs were pooled, incubated with 20 mM DTT for 15 min at room temperature for disassembly and loaded to a HiScreen Capto Q ImpRes anion exchange chromatography column (GE) . Disassembly and reassembly process was described in Figure 34 (68). While L1P18 protein was detected by western blot, one smaller bands (~41 kD) besides L1P18 bands (56 kD) were detected (Figure 35). In addition, the purity estimated by SDS-PAGE was roughly 30% and still not ideal (Figure 33 B).

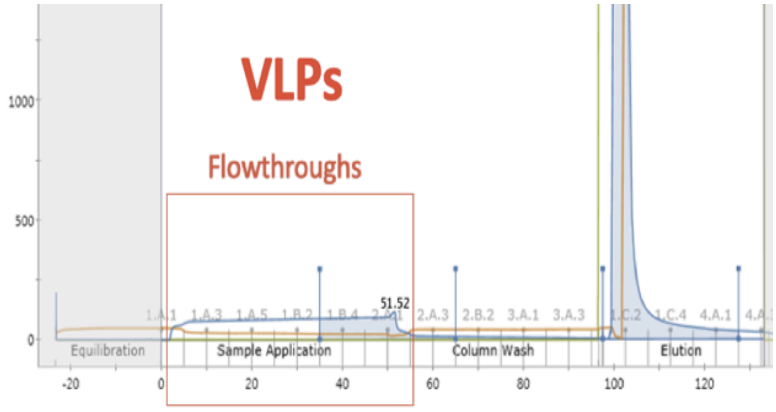

(B)

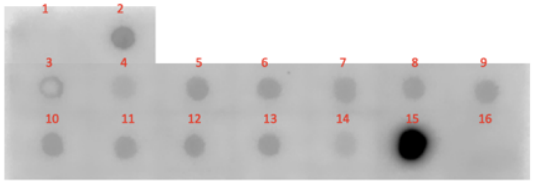

Figure 33. Dot blot analysis of L1P18 protein after size exclusion chromatography (C5). (A) Size exclusion chromatogram after removal of precipitated contaminants. (B) Immunodot analysis of flowthrough and elution fractions after size exclusion chromatography. Dot 1, PBS (negative control); dot 2, 2.5 ng L1 protein (positive control); dot 3. Pre-size exclusion chromatography sample; dots 4-14 flowthrough fractions; dots 15 and 16. Elution fractions. The extremely high intensity of dot 15 is due to the sample concentration at elution. L1P18 monomers and pentamers in 50 mL sample were eluted in 5 mL sample.

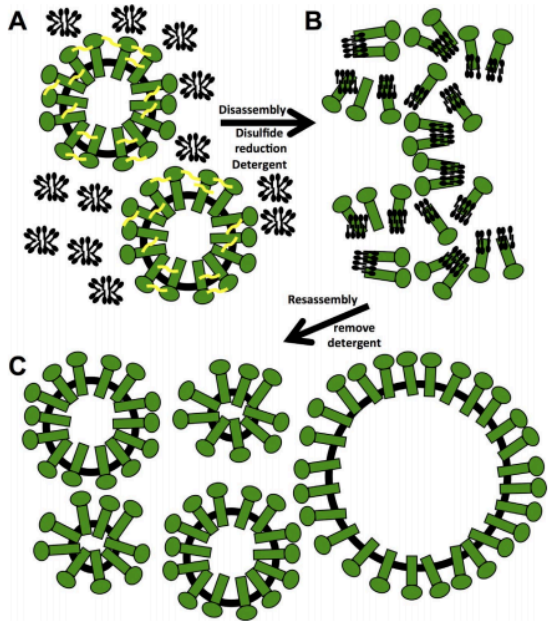

Gallagher et al (2017)

Figure 34. Schematic model for the in vitro disassembly and reassembly of surface antigen glycoprotein nanoparticles (68). (A) Schematic of intact particles (green) with schematics of nonbound detergent molecules as micelles (black). Disulfide bonds are represented by yellow connecting curve segments (yellow). (B) Particles are disassembled into protein-detergent complexes by reduction of disulfide bonds and incubation with detergents, which bind hydrophobic transmembrane regions of the surface antigen (sAg) proteins. (C) Reassembly of particles occurs after removal of detergent. Assembled particles have more variable sizes with smaller and larger particles suggesting a model of plasticity in that hydrophobic interactions drive reassembly and particle integrity (For interpretation of the references to color in this figure legend, the reader is referred to the web version of this article.).

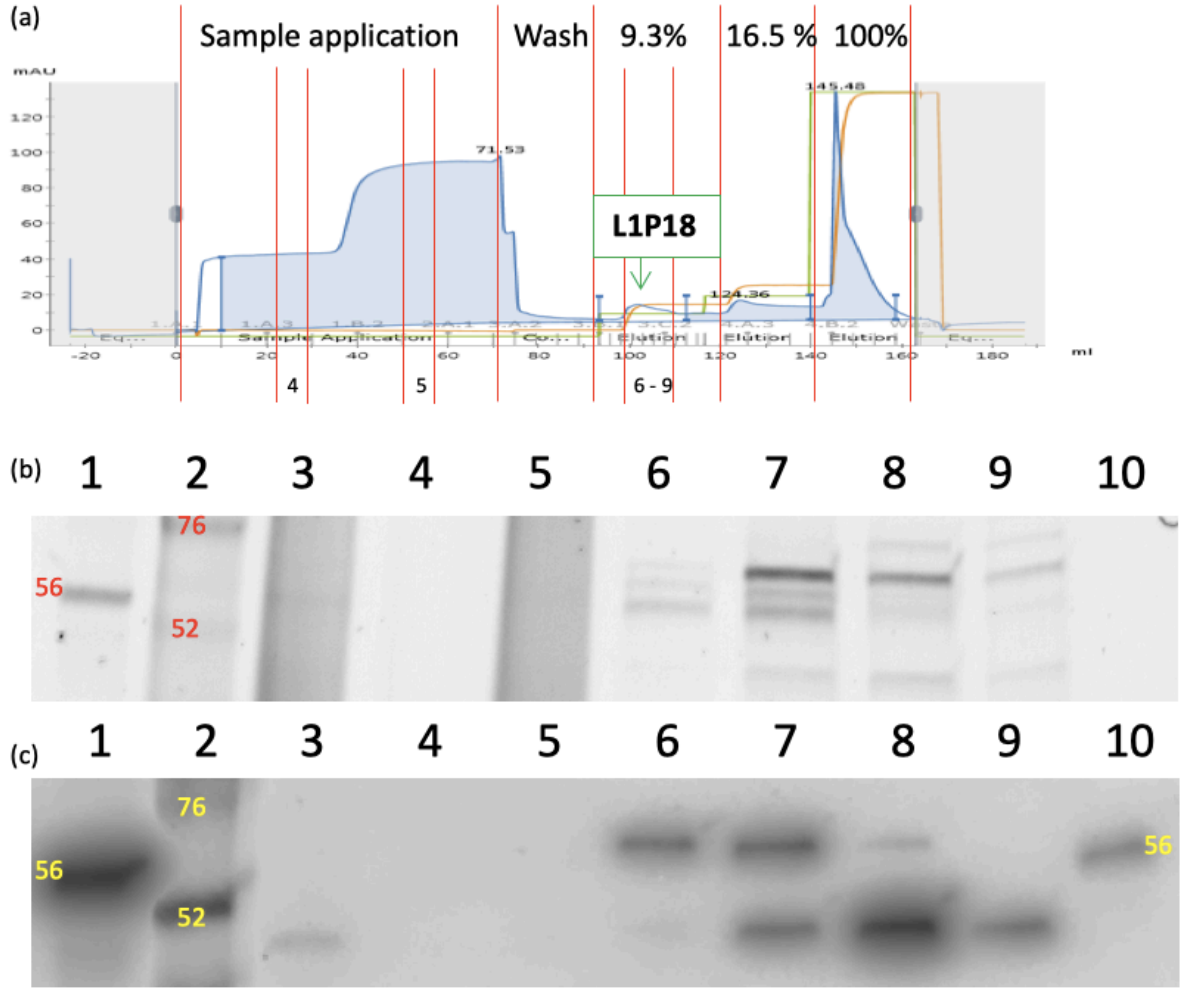

Figure 35. Protein detection analysis and western blot analysis of L1P18 protein after anion exchange chromatography (C5P4). (a) anion exchange chromatograph, (b) Coomassie staining of anion exchange chromatography fractions (c) western blot analysis of anion exchange chromatography fractions. Lane 1, abcam HPV-16 L1 100 ng (+control); lane 2, Amersham ECL Rainbow Marker; lane 3, Pre-anion exchange chromatography sample; lane 4, sample application fraction #3; lane 5, sample application fraction #5; lane 6, elution fraction #3; lane 7, elution fraction #4; lane 8, elution fraction #5; lane 9, elution fraction #6; lane 10 abcam HPV-16 10 ng (+control)

[C5P2] Size exclusion chromatography followed by heparin chromatography

According to GE application note (6), the sample after ammonium sulfate precipitation was dialyzed for reassembly condition 4 ^{o}C and gone through Capto™ Core 700 size exclusion chromatography column (GE). Then the flowthroughs were pooled and gone through HiTrap Heparin HP 5mL column (GE). While L1P18 protein was detected by western blot as a single band, the purity observed in Coomassie staining was still not ideal (Figure 36).

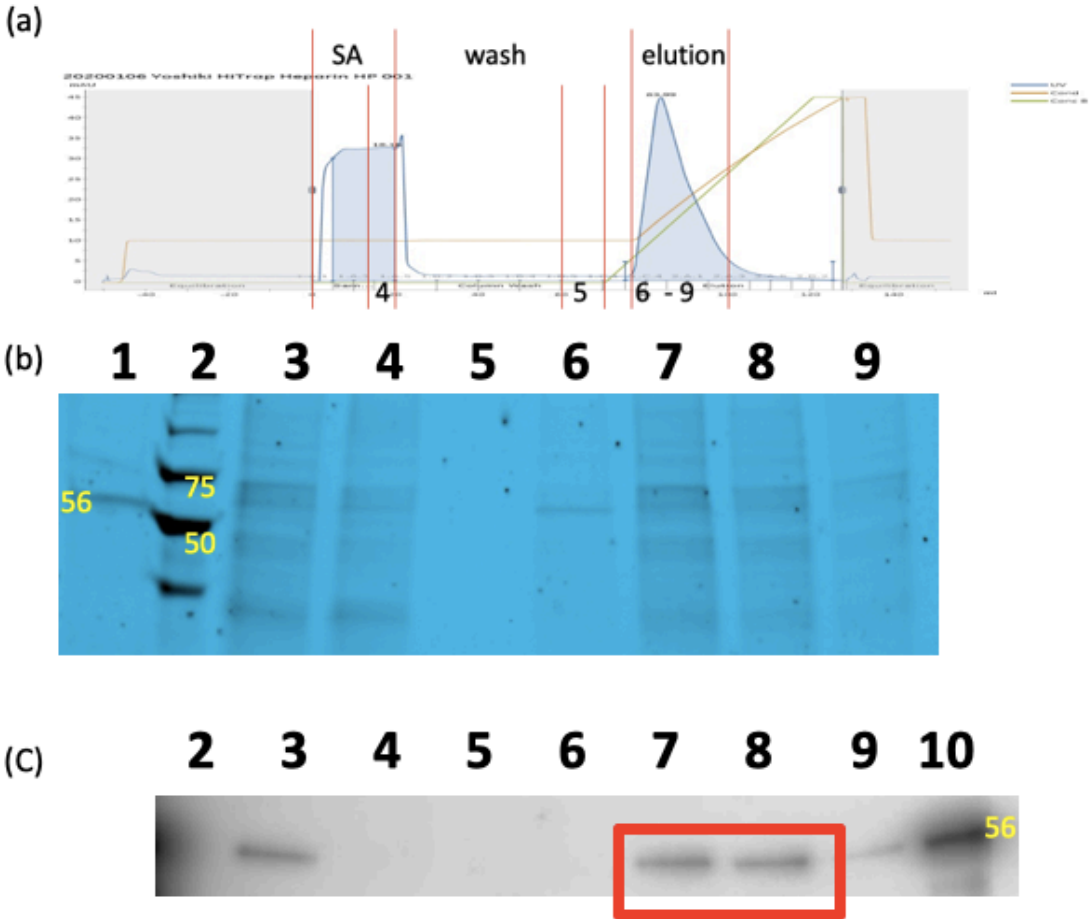

Figure 36. Protein detection analysis and western blot analysis of L1P18 protein after heparin exchange chromatography (C5P2). (a) heparin exchange chromatograph, (b) Coomassie staining of heparin chromatography fractions (c) western blot analysis of heparin chromatography fractions. Lane 1, abcam HPV-16 L1 ug (+control); lane 2, Precision Plus Protein Unstained Protein standard; lane 3, Pre-heparin chromatography sample; lane 4, sample application fraction #4; lane 5, wash fraction #4; lane 6, elution fraction #1; lane 7, elution fraction #2; lane 8, elution fraction #3; lane 9, elution fraction #4; lane 10 abcam HPV-16 75 ng (+control)

[C5P1] Size exclusion chromatography followed by ultracentrifugation

According to GE application note (6), the sample after ammonium sulfate precipitation was dialyzed for reassembly condition at 4 ^{o}C and gone through Capto™ Core 700 size exclusion chromatography column (GE). The flowthrough samples were pooled and ultracentrifuged at 28,000 xg for 4 hours at 4 ^{o}C with 25% and 70 % sucrose cushions. L1P18 protein was captured in 25% sucrose fraction and the interface between 25% and 70 % sucrose cushions (Figure 37A and 37B).

Ultrafiltration after [C5P1] (Size exclusion chromatography followed by ultracentrifugation)

The VLP containing 25% fraction and the interface fraction between 25% and 70% were further purified and concentrated about 10 times with a centrifugal filter device, Vivaspin 20 centrifugal concentrator 1,000 kDa.

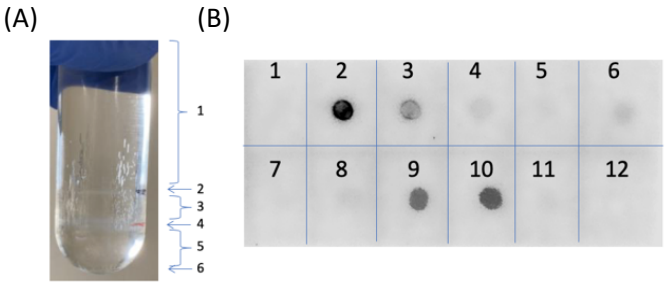

Figure 37. Dot blot analysis of Ultracentrifuged fractions. (A) Fractions after ultracentrigufation. Fraction 1, 0% sucrose; fraction 2, interface between 0% and 25% sucrose; fraction 3, 25% sucrose; fraction 4, interface between 0% and 25% sucrose; fraction 5, 70% sucrose; fraction 6, pellet resuspended 0.1 mL breaking buffer. (B) Immunodot analysis of post-ultracentrifugation fractions. Dot 1, PBS; dot 2, abcam HPV-16 L1 20 ng (+ control); dot 3, abcam HPV-16 L1 10 ng (+ control); dot 4, abcam HPV-16 L1 5 ng (+ control); dot 5, abcam HPV-16 L1 2.5 ng (+ control); dot 6. Pre-ultracentrifugation sample; dot 7, 0% sucrose; dot 8, Interface between 0% and 25%; dot 9, 25% sucrose; dot 10, Interface between 25% and 70% sucrose cushions; dot 11, 70% sucrose; dot 12, pellet resuspended with 0.1 mL breaking buffer.

The Coomassie staining of SDS-PAGE analyses showed that the contaminants seen in the 25% sucrose fraction and the interface fraction between 25% and 70% sucrose cushions (Figure 38A, lanes 4-6) were removed by ultrafiltration and L1P18 was also concentrated and purified (Figure 38A, lane 2). The estimated purity of L1P18 (Figure 38A, lane 2) is 96%.

The purified and concentrated sample after ultrafiltration was 10 times diluted with PBS. Western blot analysis confirmed the heterologous L1P18 protein expression in the sample after ultrafiltration (Figure 38B, lane 2) which is similar in size (56 kDa) with the positive control abcam HPV16-L1 (Figure 38B, lane 3). The sample after ultrafiltration was analyzed by BCA protein assay and the concentration of total protein was 78.1 µg/mL. Therefore, the total amount of protein is 7.81 µg. As the purity of L1P18 was 96% according to Coomassie staining result, 7.50 µg of HPV-HIV L1P18 VLPs was purified from 1.75 L YPD culture. Considering that the amount of L1P18 protein in the cell lysate supernatant was 81.3 µg, the recovery rate was 9.23 % (Table 11).

(A) (B)

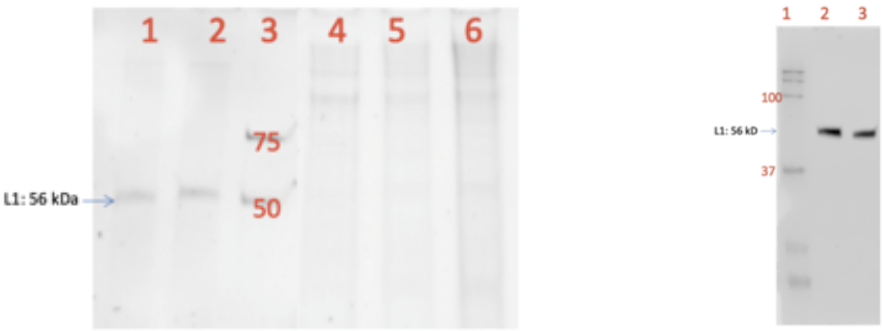

Figure 38. Coomassie staining and western blot analysis of purified L1P18 VLPs. (A) Coomassie staining of purified L1P18 VLPs. Lane 1, abcam HPV-16 L1 1 µg (+ control); lane 2, purified L1P18; lane 3, BIO-RAD Precision Plus Protein™ WesternC™ Standards 1 µL; lane 4; 25% sucrose fraction after ultracentrifugation; lane 5, Interface fraction between 25% and 70% sucrose cushions after ultracentrifugation; lane 6, mixture of 25% sucrose fraction and the interface fraction between 25% and 70% sucrose fractions after ultracentrifugation. (B) Western blot analysis of purified L1P18 VLPs. lane 1, BIO-RAD Precision Plus Protein™ WesternC™ Standards 5 µL; lane 2, 10x diluted purified L1P18 VLPs; lane 3, abcam HPV-16 L1 100 ng (+ control).

Table 11. Purification of recombinant L1P18 protein

Step	Total protein (µg)[a]	Total L1P18 (µg)	Recovery (%)	Purity (%)[c]
Cell lysate supernatants	-	**81.3**[b]	**100**	-
Ammonium sulfate precipitation / removal of precipitated contaminants	-	**46.2**[b]	**56.8**	-
Size exclusion chromatography	-	**12.4**[b]	**15.3**	-
Ultracentrifugation	-	**9.57**[b]	**11.8**	-
Ultrafiltration	**7.81**	**7.50**[d]	**9.23**	**96%**

a: determined by BCA protein assay
b: determined by densitometry of dot blot analysis
c. determined by densitometry of Coomassie-stained SDS-PAGE gel
d: determined by total protein and purity

5.5 Morphology of purified L1P18 VLPs

The morphology of the chimeric L1P18 VLPs was observed under transmission electron microscope at magnification of 54,000x. Identical particles of diameter of ~50 nm were observed (Figure 39).

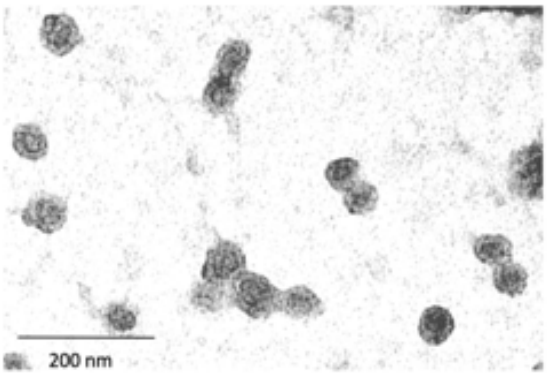

Figure 39. Morphology of purified L1P18 VLPs. Transmission electron microscopy of purified HPV-HIV L1P18 VLPs (magnification 54,000x and bar 200 nm)

6. Discussion

Even though HPV vaccines have already been developed and commercialized, the high cost is still an existing problem not only in developing countries but also in industrialized nations. The treatment for HIV infection has been greatly improved over the last few decades and a great percentage of HIV-infected patients nowadays can survive for many years thanks to antiretroviral therapy (ART). However, the access to health care and ART in developing countries is still far to meet the UNAIDS goals. Thus, the development of an affordable, safe and effective preventive vaccine against HPV and HIV is still an urgent need. In this study, i) a recombinant *P. pastoris* strain expressing the gene encoding for the chimeric HPV-HIV L1P18 protein was constructed and genetically and phenotypically characterized, thereby confirming the intracellular production of heterologous L1P18 protein; ii) the chimeric HPV-HIV VLPs were successfully generated by using this yeast cell factory; iii) the selection and optimization of the intracellularly produced L1P18 protein purification methods and VLPs generation was a great challenge and was successfully solved after overcoming several hurdles; iv) the chimeric HPV-HIV L1P18 VLPs were obtained after purification by ammonium sulfate precipitation, size exclusion chromatography, ultracentrifugation and ultrafiltration;

v) the recovery yield and purity of the overall downstream process were assessed, obtaining a 9,23 % yield and 96% purity; vi) purified chimeric VLPs were characterized and the morphology and size of the chimeric VLPs was confirmed by TEM. The recombinant *P. pastoris* X-33 strain producing the chimeric L1P18 protein was developed under Good Laboratory Practices (GLP)-compatible conditions, preserved according to the seed-lot system, and was genetically and phenotypically verified. Overall, we have demonstrated that chimeric HPV-HIV VLPs can be successfully produced and purified from *P. pastoris*. Thus, this study provides a baseline strategy that may be worthy to improve further and deliver a robust and cost-efficient platform to support the global efforts to develop novel chimeric VLP vaccines for controlling HPV and HIV infections.

As a HPV VLP, we chose HPV genotype 16 (HPV-16) L1 capsid protein because HPV-16 is the most prevalent in the world and responsible for the highest percentage of cervical cancers [1]. In addition, all three licensed HPV VLP-based vaccines include this genotype in their vaccine design.

As an HIV epitope, a gp160 envelope-derived epitope of HIV-1 IIIB isolate and a well-known immunodominant HIV-1 CTL epitope, HIV-1 P18-I10, was selected because this epitope had been previously tested in small animal models by using recombinant Bacillus Calmette–Guérin (BCG) and Modified Vaccinia Ankara (MVA) as a vaccine vehicle in our group as well as many other groups, and we were familiar with the expected results of immunogenicity studies on the mouse major histocompatibility complex (MHC) class I molecule H-2Dd with HIV-1 P18-I10 antigen [71]. Moreover, considering the fact that an HIV epitope is inserted into HPV-16 L1 protein, the size of the HIV epitope needed to be relatively smaller than the HPV L1 protein in order to maintain the morphology of HPV VLP.

Hitherto, several chimeric bovine papillomavirus (BPV)-HIV and HPV-HIV VLP models have been designed but in many of those studies, an HIV epitope was simply added to the C-terminal of BPV/HPV capsid protein L1 [47]. However, it has been shown that when Hepatitis B core (HBc) antigen was inserted into HPV-16 L1 protein, the immunogenicity towards HBc varied according to the insertion point [68]. When HBc was inserted into D-E loop of HPV-16 L1 protein, the highest humoral response was obtained presumably because the D-E loop is exposed outside when L1 proteins form VLPs [68]. Therefore, we decided to insert our HIV epitope P18-I10 into this D-E loop of HPV-16 L1 protein.

All three commercialized HPV VLP vaccines, Cervarix, Gardasil, and Gardasil 9, are based on baculovirus or yeast expression system. The use of yeast expression systems are an attractive alternative because of their ease of handling and less cost compared to baculovirus/insect cells. Recently, human embryonic kidney cells (HEK) 293 cells and *E. coli* have been also explored for HPV VLP production, showing a great potential for future production of HPV VLP vaccines and HPV-HIV chimeric VLP vaccines [47].

While Gardasil and Gardasil 9 have been produced in one type of yeast *Saccharomyces cerevisiae*, we decided to use another type of yeast *Pichia pastoris* because this methylotrophic yeast strain has shorter and less immunogenic glycans, can easily growth at higher cell densities (i.e. an interesting trait for intracellular recombinant protein production) and higher secreted protein yields than *S. cerevisiae* [67]. Furthermore, another reason we chose this yeast strain is that the group of my thesis co-director Dr. Pau Ferrer has been working on *P. pastoris* for several years and has great experience in recombinant protein production using this yeast expression system, all the facilities for the experiments were available, and fundamental methods were already established [69, 70].

In this study, we encountered the following limitations, which would be considered as targets for improvement in future studies: (i) It was difficult to recover L1P18 protein right after cell lysate as most of the protein (close to 90%) stayed in insoluble fraction; (ii) The attempt to secrete L1P18 protein from *P. pastoris* resulted in extremely low level of the protein secretion (less than 10%); (iii) ammonium sulfate precipitation had a lower recovery yield (56.8 %) when applied to our recombinant strain expressing L1P18 protein, compared to previously published similar studies (78.3% [142] and 88% [141]); (iv) it was challenging to reproduce results regarding protein purification from previously published similar studies [12, 14] with our recombinant protein, denoting the lack of robustness of such strategies.

The large fraction (close to 90%) of the intracellularly produced L1P18 protein that remained in the insoluble fraction after cell disruption poses a major bottleneck in the development of an efficient production process; to this end, several attempts to solubilize and purify them showed that it was difficult to significantly increase recovery yields. The only effective way to extract L1P18 protein was the use of strong detergents such as SDS, which are very difficult to eliminate and could interfere with VLP assembly. The optimization of this step is not straightforward because any reagent or method available cannot be used, and it has to be compatible with preservation of functionality of our protein and its ability to assemble into

VLPs, as well as compatibility with downstream purification steps. However, about 10% of L1P18 proteins were soluble and was enough to develop a proof-of-concept method for VLP production. In order to explore the capability of *P. pastoris* to secrete L1P18 protein/VLPs, we also constructed a recombinant *P. pastoris* harboring the integrative plasmid vector pPICZαA-L1P18, which contains a secretion signal coding sequence for protein secretion. In this strain, L1P18 gene expression was regulated by the stronger methanol-inducible promoter AOX. However, a major challenge for efficient production of VLP in yeast is the inability to efficiently secrete large protein complexes (nanobodies). While a low level of secreted L1P18 proteins were detected in liquid culture media, the majority of L1P18 protein were trapped inside the cells based on dot blot analysis. We suppose that L1P18 protein is presumably too big in size for efficient secretion, in other words, beyond *P. pastoris'* secretion capacity. According to the data of Dr. Pau Ferrer's group, the L1P18 protein is likely to block some step along the protein secretory pathway (either translocation into the ER, and/or traffic from ER to Golgi) and most of the produced L1P18 proteins with the secretion signal ends up being accumulated inside the yeast cells. In an attempt to circumvent a potential bottleneck in the ER translocation step, an alternative secretory signal was pOst1 tested [143]. Preliminary data showed an increased amount of product in the soluble fraction, but with a slightly higher molecular weight, probably indicating misprocessing of the secretion signal and accumulation of product in the ER. Nonetheless, these exploratory experiments have set the pathway for future cell engineering efforts towards VLP production in *P. pastoris*, which are being pursued by Dr. Ferrer's group. Besides, although secreted L1P18 protein was detected by immunodot analysis, somehow it could not be detected by western blot. We believe that this failure in western blot analysis could be due to insufficient concentrations to detect L1P18 protein or the degradation of L1P18 protein by heating in the sample preparation step. Therefore, at the end we decided to continue to use the expression vector pGAPBZ, which drives production the recombinant protein intracellularly.

Once focused in the intracellular production, as a first VLP purification step, we chose ammonium sulfate precipitation instead of ultracentrifugation in order to have higher L1P18 protein recovery rates, and to be able to handle large volumes, thinking of possible scaling up. Park *et al* (16) stated that the VLP purification by ammonium sulfate precipitation showed maximally 15 times greater yields compared to the one by ultracentrifugation on sucrose cushion. Moreover, we assessed several published purification methods [141, 144], and it was

difficult to reproduce the expected results by those methods and achieve a high purification yield and purity. For instance, Kim et al [141] demonstrated that the recovery rate of L1 protein produced in another yeast *saccharomyces cerevisiae* by "ammonium sulfate precipitation and removal of precipitated protein" after cell lysate supernatant was 88%. However, our recovery yield of L1P18 protein produced in *P. pastoris* reached only 56.8%. This lower recovery yield could be caused by the variation of yeast production system or the addition of HIV-1 P18-I10. We also tried other concentrations of ammonium sulfate besides 45% for the precipitation, but it did not improve the recovery. In addition, heparin chromatography, cation exchange chromatography, and anion exchange chromatography and combinations of them besides size exclusion chromatography were tested in order to optimize L1P18 protein and its VLP purification. While they seem ideal for purification of larger amount of HPV L1 proteins and the VLPs compared to ultracentrifugation, it was not successful to reproduce the results reported in the published articles [141, 144] with our recombinant L1P18 protein. This could be caused by the incorporation of HIV-1 P18-I10 into HPV L1 protein.

Therefore, we have systematically searched alternative methods for each of the stages, from early recovery to purification and final polishing. We have introduced changes in the sequence of VLP purification steps and adding alternative steps, tested changes one by one in a systematic way in terms of introduction / substitution of conditioning stages (e.g. dialysis, UF), operating conditions (e.g. flow rates, elution gradients) and introduction/substitution of chromatographic steps, and characterized each alternative process in terms of purity, quantity and yields. Finally, we have achieved a process that meets at least two of the objectives: 1) minimum degree of purity in order to reconstitute proper VLPs and 2) reproducible and robust process.

Overall, while our purification method reached 96% purity, the recovery rate was only 9.23 %. Therefore, new purification methods must be investigated in order to improve the yield of recovery and the recovery rate. For instance, we cannot ignore the loss of a significant amount (approximately 65 %) of L1P18 monomers and pentamers during the size exclusion chromatography step. Thus, a method with which these monomers and pentamers could be also purified and collected must be sought.

Considering the fact that ultracentrifugation cannot be carried out on an industrial scale, an alternative polishing purification process needs to be implemented such as heparin,

cation exchange, and anion exchange chromatographies by finding an optimal condition for chimeric protein L1P18.

In conclusion, we successfully constructed, purified and characterized a VLP-based chimeric HPV-HIV vaccine candidate generated by using the *Pichia pastoris* expression system. To the best of our knowledge, this is the first time that a systematic optimization of purification methods for chimeric HPV-HIV VLPs produced in *Pichia pastoris* was described. Although the yield must be improved, our optimized purification method showed 96% purity, which was enough to confirm the morphology of the chimeric VLPs. This approach can be applied to construct chimeric VLP vaccine candidates for other major pathogens.

7. Conclusions

1) The recombinant yeast strains expressing chimeric HPV-HIV immunogen L1P18 was constructed and genetically and phenotypically characterized. The intracellular L1P18 protein expression in the yeast strain harboring pGAPZB-L1P18 was confirmed by western blot analysis, and the secretion of expressed L1P18 protein in the yeast strain harboring pPICZαA-L1P18 by immunodot analysis, and the presence of the L1P18 DNA coding sequence integrated into the expression vectors pGAPZB and pPICZαA was detected by yeast colony PCR.
2) The chimeric HPV-HIV VLPs were successfully generated by using the yeast expression system harboring pGAPZB-L1P18.
3) The selection and optimization of the VLPs purification methods were a great challenge and were successfully solved after overcoming several hurdles: (i) difficulty to recover L1P18 protein right after cell lysate; (ii) low level of secreted L1P18 protein from *P. pastoris*; (iii) struggle to reproduce the data similar with the published papers for HPV L1 protein in our study on chimeric HPV-HIV L1P18 protein.
4) Several VLP purification methods have been tested alone or in combination with others and validated, and an optimal method was established.
5) The recombinant yeast strain expressed the L1P18 protein and chimeric HPV-HIV L1P18 VLPs were purified by ammonium sulfate precipitation, size exclusion chromatography, ultracentrifugation and ultrafiltration and the recovery rate was 9.23%.
6) The purity of L1P18 protein was 96% was based on by Coomassie staining and chimeric VLPs were characterized by western blot analysis.
7) The morphology of purified chimeric VLPs was confirmed by TEM and the approximate amount of VLPs obtained by this method is 7.50 μg from 1.75 L culture.
8) Our highly purified chimeric HPV-HIV VLPs can be used for further analysis such as small-scale animal studies.

8. References

1. José Veríssimo Fernandes and Thales Allyrio Araújo de Medeiros Fernandes (January 20th 2012). Human Papillomavirus: Biology and Pathogenesis, Human Papillomavirus and Related Diseases - From Bench to Bedside - A Clinical Perspective, Davy Vanden Broeck, IntechOpen, DOI: 10.5772/27154. Available from: https://www.intechopen.com/chapters/26297

2. Kirnbauer, R., et al. "Papillomavirus L1 Major Capsid Protein Self-Assembles into Virus-Like Particles That Are Highly Immunogenic." *Proceedings of the National Academy of Sciences of the United States of America*, vol. 89, no. 24, 1992, pp. 12180–12184. *JSTOR*, www.jstor.org/stable/2360881.

3. Hagensee, M. E., Yaegashi, N., & Galloway, D. A. (1993). Self-assembly of human papillomavirus type 1 capsids by expression of the L1 protein alone or by coexpression of the L1 and L2 capsid proteins. *Journal of virology*, *67*(1), 315-322. https://doi.org/10.1128/jvi.67.1.315-322.1993

4. C.M. D'Abramo, J. Archambault. Small molecule inhibitors of human papillomavirus protein–protein interactions. Open Virol J, 5 (2011), pp. 80-95 http://doi.org/10.2174/1874357901105010080

5. JA Kahn. HPV Vaccination for the Prevention of Cervical Intraepithelial Neoplasia. N Engl J Med 2009; 361:271-278 DOI: 10.1056/NEJMct0806938

6. C de Martel, M Plummer, J Vignat, et al. Worldwide burden of cancer attributable to HPV by site, country and HPV type. Int J Cancer. 2017 Aug 15;141(4):664-670.

7. Deligeoroglou et al. HPV Infection: Immunological Aspects and Their Utility in Future Therapy. Infectious Diseases in Obstetrics and Gynecology, vol. 2013, Article ID 540850, 9 pages, 2013. https://doi.org/10.1155/2013/540850

8. US National Institute of Health, www.niaid.nih.gov Retrieved 22 March 2021

9. Greene, W., Peterlin, B. Charting HIV's remarkable voyage through the cell: Basic science as a passport to future therapy. *Nat Med* **8,** 673–680 (2002). https://doi.org/10.1038/nm0702-673

10. A.M. Lever, HIV: the virus. Medicine. 2005, 33(6), 1–3. DOI: https://doi.org/10.1383/medc.33.6.1.65999

11. Sierra S, Kupfer B, Kaiser R. Basics of the virology of HIV-1 and its replication. Journal of Clinical Virology : the Official Publication of the Pan American Society for Clinical Virology. 2005 Dec;34(4):233-244. DOI: 10.1016/j.jcv.2005.09.004.

12. "Global HIV & AIDS statistics — 2020 fact sheet". www.unaids.org. Retrieved 22 March 2021.

13. Unicef press release 25 November. www.unicef.org Retrieved 22 March 2021

14. S Makvandi-Nejad. Human Immunodeficiency Virus (HIV). British Society for Immunology. https://www.immunology.org/ Retrieved 22 March 2021

15. C Zhao et al, Current Advances in Virus-Like Particles as a Vaccination Approach against HIV Infection. Vaccines (Basel). 2016 Jan 22;4(1):2.

16. MG Masavuli et al., Preclinical Development and Production of Virus-Like Particles As Vaccine Candidates for Hepatitis C. 2017 December, Frontiers in Microbiology 8:2413. https://doi.org/10.3389/fmicb.2017.02413

17. HPV information centre: Human Papillomavirus and Related Diseases Report Spain Version posted at www.hpvcentre.net on 17 June 2019. Retrieved 22 March 2021

18. https://hospital.vallhebron.com/en/diseases/human-papillomavirus-hpv Retrieved 22 March 2021

19. J. Mazibrada, M. Rittà, M. Mondini et al., “Interaction between inflammation and angiogenesis during different stages of cervical carcinogenesis,” *Gynecologic Oncology*, vol. 108, no. 1, pp. 112–120, 2008.

20. T. R. Mosmann, H. Cherwinski, M. W. Bond, M. A. Giedlin, and R. L. Coffman, “Two types of murine helper T cell clone—I. Definition according to profiles of lymphokine activities and secreted proteins. 1986,” Journal of immunology, vol. 175, no. 1, pp. 5–14, 2005.

21. J. Zhu and W. E. Paul, “CD4 T cells: fates, functions, and faults,” Blood, vol. 112, no. 5, pp. 1557–1569, 2008.

22. J. C. Steele, C. H. Mann, S. Rookes et al., “T-cell responses to human papillomavirus type 16 among women with different grades of cervical neoplasia,” British Journal of Cancer, vol. 93, no. 2, pp. 248–259, 2005.

23. M. Clerici, M. Merola, E. Ferrario et al., “Cytokine production patterns in cervical intraepithelial neoplasia: association with human papillomavirus infection,” Journal of the National Cancer Institute, vol. 89, no. 3, pp. 245–250, 1997.

24. B. C. Peghini, D. R. Abdalla, A. C. Barcelos, L. Teodoro, E. F. Murta, and M. A. Michelin, “Local cytokine profiles of patients with cervical intraepithelial and invasive neoplasia,” Human Immunology, vol. 73, no. 9, pp. 920–926, 2012.

25. A. Kobayashi, V. Weinberg, T. Darragh, and K. Smith-McCune, “Evolving immunosuppressive microenvironment during human cervical carcinogenesis,” Mucosal Immunology, vol. 1, no. 5, pp. 412–420, 2008.

26. K. D. Chirgwin, J. Feldman, M. Augenbraun, S. Landesman, and H. Minkoff, “Incidence of venereal warts in human immunodeficiency virus-infected and uninfected women,” Journal of Infectious Diseases, vol. 172, no. 1, pp. 235–238, 1995.

27. R. G. Fruchter, M. Maiman, C. D. Arrastia, R. Matthews, E. J. Gates, and K. Holcomb, “Is HIV infection a risk factor for advanced cervical cancer?” Journal of Acquired Immune Deficiency Syndromes and Human Retrovirology, vol. 18, no. 3, pp. 241–245, 1998.

28. M. Scott, M. Nakagawa, and A.-B. Moscicki, “Cell-mediated immune response to human papillomavirus infection,” Clinical and Diagnostic Laboratory Immunology, vol. 8, no. 2, pp. 209–220, 2001.

29. A. Vambutas, J. DeVoti, W. Pinn, B. M. Steinberg, and V. R. Bonagura, “Interaction of human papillomavirus type 11 E7 protein with TAP-1 results in the reduction of ATP-dependent peptide transport,” Clinical Immunology, vol. 101, no. 1, pp. 94–99, 2001.

30. P. J. Keating, F. V. Cromme, M. Duggan-Keen et al., “Frequency of down-regulation of individual HLA-A and -B alleles in cervical carcinomas in relation to TAP-1 expression,” British Journal of Cancer, vol. 72, no. 2, pp. 405–411, 1995.

31. M. S. Campo, S. V. Graham, M. S. Cortese et al., “HPV-16 E5 down-regulates expression of surface HLA class I and reduces recognition by CD8 T cells,” Virology, vol. 407, no. 1, pp. 137–142, 2010.

32. A. Correll, A. Tüettenberg, C. Becker, and H. Jonuleit, “Increased regulatory T-cell frequencies in patients with advanced melanoma correlate with a generally impaired T-cell responsiveness and are restored after dendritic cell-based vaccination,” Experimental Dermatology, vol. 19, no. 8, pp. e213–e221, 2010.

33. J. D. French, Z. J. Weber, D. L. Fretwell, S. Said, J. P. Klopper, and B. R. Haugen, “Tumor-associated lymphocytes and increased FoxP3+ regulatory T cell frequency correlate with more aggressive papillary thyroid cancer,” Journal of Clinical Endocrinology and Metabolism, vol. 95, no. 5, pp. 2325–2333, 2010.

34. J. Fu, D. Xu, Z. Liu et al., “Increased regulatory T cells correlate with CD8 T-cell impairment and poor survival in hepatocellular carcinoma patients,” Gastroenterology, vol. 132, no. 7, pp. 2328–2339, 2007.

35. C. Oderup, L. Cederbom, A. Makowska, C. M. Cilio, and F. Ivars, “Cytotoxic T lymphocyte antigen-4-dependent down-modulation of costimulatory molecules on dendritic cells in CD4+ CD25+ regulatory T-cell-mediated suppression,” Immunology, vol. 118, no. 2, pp. 240–249, 2006.

36. K. Nakamura, A. Kitani, and W. Strober, “Cell contact-dependent immunosuppression by CD4+CD25+ regulatory T cells is mediated by cell surface-bound transforming growth factor β,” Journal of Experimental Medicine, vol. 194, no. 5, pp. 629–644, 2001.

37. L. W. Collison, C. J. Workman, T. T. Kuo et al., “The inhibitory cytokine IL-35 contributes to regulatory T-cell function,” Nature, vol. 450, no. 7169, pp. 566–569, 2007.

38. M. I. Garín, N.-C. Chu, D. Golshayan, E. Cernuda-Morollón, R. Wait, and R. I. Lechler, “Galectin-1: a key effector of regulation mediated by CD4+CD25+ T cells,” Blood, vol. 109, no. 5, pp. 2058–2065, 2007.

39. S. S. Lee, W. Gao, S. Mazzola et al., “Heme oxygenase-1, carbon monoxide, and bilirubin induce tolerance in recipients toward islet allografts by modulating T regulatory cells,” FASEB Journal, vol. 21, no. 13, pp. 3450–3457, 2007.

40. S. Mocellin, F. M. Marincola, and H. A. Young, “Interleukin-10 and the immune response against cancer: a counterpoint,” Journal of Leukocyte Biology, vol. 78, no. 5, pp. 1043–1051, 2005.

41. R. P. Viscidi, M. Schiffman, A. Hildesheim et al., “Seroreactivity to human papillomavirus (HPV) types 16, 18, or 31 and risk of subsequent HPV infection: results from a population-based study in Costa Rica,” Cancer Epidemiology Biomarkers and Prevention, vol. 13, no. 2, pp. 324–327, 2004.

42. J. J. Carter, L. A. Koutsky, J. P. Hughes et al., “Comparison of human papillomavirus types 16, 18, and 6 capsid antibody responses following incident infection,” Journal of Infectious Diseases, vol. 181, no. 6, pp. 1911–1919, 2000.

43. https://www.unaids.org/en/regionscountries/countries/spain Retrieved 22 March 2021

44. http://www.ceeiscat.cat Retrieved 22 March 2021

45. M L Munier, A D Kelleher. Acutely dysregulated, chronically disabled by the enemy within: T-cell responses to HIV-1 infection Immunol Cell Biol. 2007 Jan;85(1):6-15. doi: 10.1038/sj.icb.7100015. Epub 2006 Dec 5.

46. Stuart Z Shapiro. HIV Vaccine Development: 35 Years of Experimenting in the Funding of Biomedical Research.Viruses. 2020 Dec 19;12(12):1469. doi: 10.3390/v12121469.

47. Eto Y, Saubi N, Ferrer P, Joseph J. Designing Chimeric Virus-like Particle-based Vaccines for Human Papillomavirus and HIV: Lessons Learned. AIDS Reviews, 01 Jan 2019, 21(4):218-232 DOI: 10.24875/aidsrev.19000114

48. Liu XS, Liu WJ, Zhao KN, Liu YH, Leggatt G, Frazer IH, et al. Route of administration of chimeric BPV1 VLP determines the character of the induced immune responses. Immunol Cell Biol. 2002;80:21-9.

49. Liu XS, Abdul-Jabbar I, Qi YM, Frazer IH, Zhou J. Mucosalimmunisation with papillomavirus virus-like particles elicits systemic and mucosal immunity in mice. Virology. 1998;252:39-45.

50. Liu WJ, Liu XS, Zhao KN, Leggatt GR, Frazer IH. Papillomavirusvirus-like particles for the delivery of multiple cytotoxic T cell epitopes. Virology. 2000;273:374-82.

51. George M Bahr. Immune deficiency in HIV-1 infection: novel therapeutic approaches targeting innate and adaptive responses. Expert Rev Clin Immunol. 2005 Nov;1(4):529-47. doi: 10.1586/1744666X.1.4.529.

52. Marcus Altfeld, Michael Gale Jr. Innate immunity against HIV-1 infection. Nat Immunol. 2015 Jun;16(6):554-62. doi: 10.1038/ni.3157.

53. Arnaud Moris, Mathias Pereira, Lisa Chakrabarti. A role for antibodies in natural HIV control. Curr Opin HIV AIDS. 2019 Jul;14(4):265-272. doi: 10.1097/COH.0000000000000554.

54. Teena Mohan, Santwana Bhatnagar, Dablu L Gupta, D N Rao. Current understanding of HIV-1 and T-cell adaptive immunity: progress to date. Microb Pathog. 2014 Aug;73:60-9. doi: 10.1016/j.micpath.2014.06.003. Epub 2014 Jun 12.

55. Linda L Baum. Role of humoral immunity in host defense against HIV. Curr HIV/AIDS Rep. 2010 Feb;7(1):11-8. doi: 10.1007/s11904-009-0036-6.

56. Gorny MK, Moore JP, Conley AJ, et al. Human anti-V2 monoclonal antibody that neutralizes primary but not laboratory isolates of human immunodeficiency virus type 1. J Virol. 1994;68:8312–8320.

57. Trkola A, Purtscher M, Muster T, et al. Human monoclonal antibody 2G12 defines a distinctive neutralization epitope on the gp120 glycoprotein of human immunodeficiency virus type 1. J Virol. 1996;70:1100–1108.

58. Burton DR, Pyati J, Koduri R, et al. Efficient neutralization of primary isolates of HIV-1 by a recombinant human monoclonal antibody. Science. 1994;266:1024–1027.

59. Muster T, Steindl F, Purtscher M, et al. A conserved neutralizing epitope on gp41 of human immunodeficiency virus type 1. J Virol. 1993;67:6642–6647. [PMC free article] [PubMed] [Google Scholar]

60. Zwick MB, Labrijn AF, Wang M, et al. Broadly neutralizing antibodies targeted to the membrane-proximal external region of human immunodeficiency virus type 1 glycoprotein gp41. J Virol. 2001;75:10892–10905.

61. Sanders RW, Moore JP. Native-like env trimers as a platform for HIV-1 vaccine design. Immunol Rev. 2017;275:161-82.

62. Barouch DH, Stephenson KE, Borducchi EN, Smith K, Stanley K, McNally AG, et al. Protective efficacy of a global HIV-1 mosaic vaccine against heterologous SHIV challenges in rhesus monkeys. Cell. 2013; 155:531-9.

63. Mothe B, Hu X, Llano A, Rosati M, Olvera A, Kulkarni V, et al. A human immune data-informed vaccine concept elicits strong and broad T-cell specificities associated with HIV-1 control in mice and macaques. J Transl Med. 2015;13:60.

64. Rerks-Ngarm et al. New England Journal of Medicine. 2009; 361 (23): 2209–2220.

65. Arnaud Moris, Mathias Pereira, Lisa Chakrabarti. A role for antibodies in natural HIV control.Curr Opin HIV AIDS. 2019 Jul;14(4):265-272.

66. J. Fuenmayor, F. Gòdia, and L. Cervera. Production of virus-like particles for vaccines. N Biotechnol. 2017 Oct 25; 39: 174–180.

67. A. Manickam, M. Sivanandham, and I. Tourkova, “Immunological role of dendritic cells in cervical cancer,” in Immune-Mediated Diseases, M. Shurin and Y. Smolkin, Eds., pp. 155–162, Springer, New York, NY, USA, 2007.

68. S. L. Giannini, P. Hubert, J. Doyen, J. Boniver, and P. Delvenne, “Influence of the mucosal epithelium microenvironment on Langerhans cells: implications for the development of squamous intraepithelial lesions of the cervix,” International Journal of Cancer, vol. 97, no. 5, pp. 654–659, 2002.

69. S. K. Tay, D. Jenkins, and P. Maddox, “Subpopulations of Langerhans' cells in cervical neoplasia,” British Journal of Obstetrics and Gynaecology, vol. 94, no. 1, pp. 10–15, 1987.

70. S. C. Fausch, D. M. Da Silva, and W. M. Kast, “Differential uptake and cross-presentation of human papillomavirus virus-like particles by dendritic cells and Langerhans cells,” Cancer Research, vol. 63, no. 13, pp. 3478–3482, 2003.

71. S. Akira and K. Takeda, “Toll-like receptor signalling,” Nature Reviews Immunology, vol. 4, no. 7, pp. 499–511, 2004.

72. C. A. DeCarlo, B. Rosa, R. Jackson, S. Niccoli, N. G. Escott, and I. Zehbe, “Toll-like receptor transcriptome in the HPV-positive cervical cancer microenvironment,” Clinical and Developmental Immunology, vol. 2012, Article ID 785825, 9 pages, 2012.

73. U. A. Hasan, E. Bates, F. Takeshita et al., “TLR9 expression and function is abolished by the cervical cancer-associated human papillomavirus type 16,” Journal of Immunology, vol. 178, no. 5, pp. 3186–3197, 2007.

74. C. A. Decarlo, A. Severini, L. Edler et al., “IFN-κ, a novel type i IFN, is undetectable in HPV-positive human cervical keratinocytes,” Laboratory Investigation, vol. 90, no. 10, pp. 1482–1491, 2010.

75. B. Rincon-Orozco, G. Halec, S. Rosenberger et al., “Epigenetic silencing of interferon-κ in human papillomavirus type 16-positive cells,” Cancer Research, vol. 69, no. 22, pp. 8718–8725, 2009.

76. C. Mohan and J. Zhu, “Toll-like receptor signaling pathways—therapeutic opportunities,” Mediators of Inflammation, vol. 2010, Article ID 781235, 7 pages, 2010.

77. E. Y. So and T. Ouchi, “The application of toll like receptors for cancer therapy,” International Journal of Biological Sciences, vol. 6, no. 7, pp. 675–681, 2010.

78. K. Hacke, B. Rincon-Orozco, G. Buchwalter et al., “Regulation of MCP-1 chemokine transcription by p53,” Molecular Cancer, vol. 9, article 82, 2010.

79. J. C. Guess and D. J. McCance, “Decreased migration of Langerhans precursor-like cells in response to human keratinocytes expressing human papillomavirus type 16 E6/E7 is related to reduced macrophage inflammatory protein-3α production,” Journal of Virology, vol. 79, no. 23, pp. 14852–14862, 2005.

80. F. O. Martinez, L. Helming, and S. Gordon, “Alternative activation of macrophages: an immunologic functional perspective,” Annual Review of Immunology, vol. 27, pp. 451–483, 2009.

81. J. G. Quatromoni and E. Eruslanov, “Tumor-associated macrophages: function, phenotype, and link to prognosis in human lung cancer,” American Journal of Translational Research, vol. 4, no. 4, pp. 376–389, 2012.

82. X. Tang, C. Mo, Y. Wang, D. Wei, and H. Xiao, “Anti-tumour strategies aiming to target tumour-associated macrophages,” Immunology, vol. 138, no. 2, pp. 93–104, 2013.

83. L. S. Hammes, R. R. Tekmal, P. Naud et al., “Macrophages, inflammation and risk of cervical intraepithelial neoplasia (CIN) progression-Clinicopathological correlation,” Gynecologic Oncology, vol. 105, no. 1, pp. 157–165, 2007.

84. A. P. Lepique, K. R. P. Daghastanli, I. Cuccovia, and L. L. Villa, “HPV16 tumor associated macrophages suppress antitumor T cell responses,” Clinical Cancer Research, vol. 15, no. 13, pp. 4391–4400, 2009.

85. A. Bolpetti, J. S. Silva, L. L. Villa, and A. P. Lepique, “Interleukin-10 production by tumor infiltrating macrophages plays a role in Human Papillomavirus 16 tumor growth,” BMC Immunology, vol. 11, article 27, 2010.

86. T. Garcia-Iglesias, A. del Toro-Arreola, B. Albarran-Somoza et al., “Low NKp30, NKp46 and NKG2D expression and reduced cytotoxic activity on NK cells in cervical cancer and precursor lesions,” BMC Cancer, vol. 9, article 186, 2009.

87. Toshiyuki Sasagawa, Hiroaki Takagi, Satoru Makinoda. Immune responses against human papillomavirus (HPV) infection and evasion of host defense in cervical cancer, Journal of Infection and Chemotherapy, Volume 18, Issue 6, 2012, Pages 807-815

88. J. J. Carter, L. A. Koutsky, J. P. Hughes et al., “Comparison of human papillomavirus types 16, 18, and 6 capsid antibody responses following incident infection,” Journal of Infectious Diseases, vol. 181, no. 6, pp. 1911–1919, 2000.

89. McNeil C (April 2006). "Who invented the VLP cervical cancer vaccines?". Journal of the National Cancer Institute. 98 (7): 433.

90. U.S. Patent 7,476,389, "Papilloma Virus Vaccines"

91. Bell, N. M., & Lever, A. M. L. (2013). HIV Gag polyprotein: processing and early viral particle assembly. Trends in Microbiology, 21(3), 136–144. doi:10.1016/j.tim.2012.11.006

92. Jacks, T., Power, M., Masiarz, F. *et al.* Characterization of ribosomal frameshifting in HIV-1 *gag-pol* expression. *Nature* **331,** 280–283 (1988). https://doi.org/10.1038/331280a0

93. Arrildt, K.T., Joseph, S.B. & Swanstrom, R. The HIV-1 Env Protein: A Coat of Many Colors. Curr HIV/AIDS Rep 9, 52–63 (2012). https://doi.org/10.1007/s11904-011-0107-3

94. Malim, M. H., & Emerman, M. (2008). HIV-1 Accessory Proteins—Ensuring Viral Survival in a Hostile Environment. Cell Host & Microbe, 3(6), 388–398. doi:10.1016/j.chom.2008.04.008

95. Foley B, Leitner T et al. HIV Sequence Compendium 2013. LA-UR 13-26007.

96. Butler, A.L., Fischinger, S. & Alter, G. The Antibodiome—Mapping the Humoral Immune Response to HIV. Curr HIV/AIDS Rep 16, 169–179 (2019). https://doi.org/10.1007/s11904-019-00432-x

97. NIAID. History of HIV Vaccine Research. Retrieved 15 May 2021.

98. Esparza, J. (2013). What Has 30 Years of HIV Vaccine Research Taught Us? Vaccines, 1(4), 513–526. doi:10.3390/vaccines1040513

99. Tran, AM., Nguyen, TT., Nguyen, CT. et al. Pichia pastoris versus Saccharomyces cerevisiae: a case study on the recombinant production of human granulocyte-macrophage colony-stimulating factor. BMC Res Notes 10, 148 (2017). https://doi.org/10.1186/s13104-017-2471-6

100. Merrington, C.L., Bailey, M.J. & Possee, R.D. Manipulation of baculovirus vectors. Mol Biotechnol 8, 283–297 (1997). https://doi.org/10.1007/BF02760782

101. Ma, B., Maraj, B., Tran, N. P., Knoff, J., Chen, A., Alvarez, R. D., … Wu, T.-C. (2012). Emerging human papillomavirus vaccines. Expert Opinion on Emerging Drugs, 17(4), 469–492. doi:10.1517/14728214.2012.744393

102. NIH U.S. National Library of Medicine ClinicalTrials.gov. Available at https://clinicaltrials.gov/ retrieved 15 May 2021.

103. Adams SE, Dawson KM, Gull K, Kingsman SM, Kingsman AJ. The expression of hybrid HIV: ty virus-like particles in yeast. Nature. 1987; 329:68-70.

104. Sakuragi S, Goto T, Sano K, Morikawa Y. HIV Type 1 gag virus-like particle budding from spheroplasts of Saccharomyces cerevisiae. Proc Natl Acad Sci U S A. 2002;99:7956-61.

105. Yamshchikov GV, Ritter GD, Vey M, Compans RW. Assembly of SIV virus-like particles containing envelope proteins using a baculovirus expression system. Virology. 1995;214:50-8.

106. Quan FS, Sailaja G, Skountzou I, Huang C, Vzorov A, Compans RW, et al. Immunogenicity of virus-like particles containing modified human immunodeficiency virus envelope proteins. Vaccine. 2007;25:3841-50.

107. Cervera L, Gutiérrez-Granados S, Martínez M, Blanco J, Gòdia F, Segura MM, et al. Generation of HIV-1 gag VLPs by transient transfection of HEK 293 suspension cell cultures using an optimized animal-derived component free medium. J Biotechnol. 2013;166:152-65.

108. Tsunetsugu-Yokota Y, Morikawa Y, Isogai M, Kawana-Tachikawa A, Odawara T, Nakamura T, et al. Yeast-derived human immunodeficiency virus Type 1 p55(gag) virus-like particles activate dendritic cells (DCs) and induce perforin expression in gag-specific CD8(+) T cells by cross-presentation of DCs. J Virol. 2003;77:10250-9.

109. Tagliamonte M, Visciano ML, Tornesello ML, De Stradis A, Buonaguro FM, Buonaguro L, et al. Constitutive expression of HIV-VLPs in stably transfected insect cell line for efficient delivery system. Vaccine. 2010;28:6417-24.

110. Crooks ET, Moore PL, Franti M, Cayanan CS, Zhu P, Jiang P, et al. A comparative immunogenicity study of HIV-1 virus-like particles bearing various forms of envelope proteins, particles bearing no envelope and soluble monomeric gp120. Virology. 2007;366:245-62.

111. Tagliamonte M, Visciano ML, Tornesello ML, De Stradis A, Buonaguro FM, Buonaguro L, et al. HIV-gag VLPs presenting trimeric HIV-1 gp140 spikes constitutively expressed in stable double transfected insect cell line. Vaccine. 2011;29:4913-22.

112. Benen TD, Tonks P, Kliche A, Kapzan R, Heeney JL, Wagner R, et al. Development and immunological assessment of VLP-based immuno- gens exposing the membrane-proximal region of the HIV-1 gp41 protein. J Biomed Sci. 2014;21:79.

113. Poteet E, Lewis P, Li F, Zhang S, Gu J, Chen C, et al. A novel prime and boost regimen of HIV virus-like particles with TLR4 adjuvant MPLA in- duces th1 oriented immune responses against HIV. PLoS One. 2015; 10:e0136862.

114. Vzorov AN, Wang L, Chen J, Wang BZ, Compans RW. Effects of modi- fication of the HIV-1 env cytoplasmic tail on immunogenicity of VLP vaccines. Virology. 2016;489:141-50.

115. Beltran-Pavez C, Ferreira CB, Merino-Mansilla A, Fabra-Garcia A, Casa- della M, Noguera-Julian M, et al. Guiding the humoral response against HIV-1 toward a MPER adjacent region by immunization with a VLP-for- mulated antibody-selected envelope variant. PLoS One. 2018; 13:e0208345.

116. Peng S, Frazer IH, Fernando GJ, Zhou J. Papillomavirus virus-like par- ticles can deliver defined CTL epitopes to the MHC class I pathway. Virology. 1998;240:147-57.

117. Chackerian B, Lowy DR, Schiller JT. Induction of autoantibodies to mouse CCR5 with recombinant papillomavirus particles. Proc Natl Acad Sci U S A. 1999;96:2373-8.

118. Dale CJ, Liu XS, De Rose R, Purcell DF, Anderson J, Xu Y, et al. Chimeric human papilloma virus-simian/human immunodeficiency virus virus-like-particle vaccines: immunogenicity and protective efficacy in macaques. Virology. 2002;301:176-87.

119. Zhai Y, Zhong Z, Zariffard M, Spear GT, Qiao L. Bovine papillomavirus- like particles presenting conserved epitopes from membrane-proximal external region of HIV-1 gp41 induced mucosal and systemic antibodies. Vaccine. 2013;31:5422-9.

120. Di Bonito P, Grasso F, Mochi S, Petrone L, Fanales-Belasio E, Mei A, et al. Anti-tumor CD8+ T cell immunity elicited by HIV-1-based virus-like particles incorporating HPV-16 E7 protein. Virology. 2009;395:45-55.

121. Chackerian B, Briglio L, Albert PS, Lowy DR, Schiller JT. Induction of autoantibodies to CCR5 in macaques and subsequent effects upon challenge with an R5-tropic simian/human immunodeficiency virus. J Vi- rol. 2004;78:4037-47.

122. Sadeyen JR, Tourne S, Shkreli M, Sizaret PY, Coursaget P. Insertion of a foreign sequence on capsid surface loops of human papillomavirus Type 16 virus-like particles reduces their capacity to induce neutralizing antibodies and delineates a conformational neutralizing epitope. Virol- ogy. 2003;309:32-40.

123. NIH U.S. National Library of Medicine ClinicalTrials.gov. Available at https://clinicaltrials.gov/ Retrieved on July 1, 2021.

124. Peters BS, Cheingsong-Popov R, Callow D, Foxall R, Patou G, Hodgkin K, et al. A pilot phase II study of the safety and immunogenicity of HIV p17/ p24: vlp (p24-VLP) in asymptomatic HIV seropositive subjects. J Infect. 1997;35:231-5.

125. Kelleher AD, Roggensack M, Jaramillo AB, Smith DE, Walker A, Gow I, et al. Safety and immunogenicity of a candidate therapeutic vaccine, p24 virus-like particle, combined with zidovudine, in asymptomatic sub- jects. Community HIV research network investigators. AIDS. 1998; 12:175-82.

126. Goepfert PA, Elizaga ML, Sato A, Qin L, Cardinali M, Hay CM, et al. Phase 1 safety and immunogenicity testing of DNA and recombinant modified Vaccinia Ankara vaccines expressing HIV-1 virus-like particles. J Infect Dis. 2011;203:610-9.

127. Roldão A, Mellado MC, Castilho LR, Carrondo MJ, Alves PM. Virus-like particles in vaccine development. Expert Rev Vaccines. 2010;9:1149-76.

128. Joseph, J., Fernández-Lloris, R., Pezzat, E., Saubi, N., Cardona, P.-J., Mothe, B., & Gatell, J. M. (2010). Molecular Characterization of Heterologous HIV-1gp120 Gene Expression Disruption inMycobacterium bovisBCG Host Strain: A Critical Issue for Engineering Mycobacterial Based-Vaccine Vectors. Journal of Biomedicine and Biotechnology, 2010, 1–10. doi:10.1155/2010/357370

129. Im EJ, Saubi N, Virgili G, Sander C, Teoh D, et al. (2007) Vaccine platform for prevention of tuberculosis and mother-to-child transmission of human immunodeficiency virus type 1 through breastfeeding. J Virol 81: 9408–9418.

130. Rosario, M., Hopkins, R., Fulkerson, J., Borthwick, N., Quigley, M. F., Joseph, J., … Hanke, T. (2010). Novel Recombinant Mycobacterium bovis BCG, Ovine Atadenovirus, and Modified Vaccinia Virus Ankara Vaccines Combine To Induce Robust Human Immunodeficiency Virus-Specific CD4 and CD8 T-Cell Responses in Rhesus Macaques. Journal of Virology, 84(12), 5898–5908. doi:10.1128/jvi.02607-09

131. Rosario, M., Fulkerson, J., Soneji, S., Parker, J., Im, E.-J., Borthwick, N., … Hanke, T. (2010). Safety and Immunogenicity of Novel Recombinant BCG and Modified Vaccinia Virus Ankara Vaccines in Neonate Rhesus Macaques. Journal of Virology, 84(15), 7815–7821. doi:10.1128/jvi.00726-10

132. Saubi, N., Im, E.-J., Fernández-Lloris, R., Gil, O., Cardona, P.-J., Gatell, J. M., … Joseph, J. (2011). Newborn Mice Vaccination with BCG.HIVA222+ MVA.HIVA Enhances HIV-1-Specific Immune Responses: Influence of Age and Immunization Routes. Clinical and Developmental Immunology, 2011, 1–11. doi:10.1155/2011/516219

133. Saubi, N., Mbewe-Mvula, A., Gea-Mallorqui, E., Rosario, M., Gatell, J. M., Hanke, T., & Joseph, J. (2012). Pre-Clinical Development of BCG.HIVACAT, an Antibiotic-Free Selection Strain, for HIV-TB Pediatric Vaccine Vectored by Lysine Auxotroph of BCG. PLoS ONE, 7(8), e42559. doi:10.1371/journal.pone.0042559

134. Mahant, A., Saubi, N., Eto, Y., Guitart, N., Gatell, J. M., Hanke, T., & Joseph, J. (2017). Preclinical development of BCG.HIVA2auxo.int, harboring an integrative expression vector, for a HIV-TB Pediatric vaccine. Enhancement of stability and specific HIV-1 T-cell immunity. Human Vaccines & Immunotherapeutics, 13(8), 1798–1810. doi:10.1080/21645515.2017.1316911

135. Kilpeläinen, A., Maya-Hoyos, M., Saubí, N., Soto, C. Y., & Joseph Munne, J. (2018). Advances and challenges in recombinant Mycobacterium bovis BCG-based HIV vaccine development: Lessons learned. Expert Review of Vaccines. doi:10.1080/14760584.2018.1534588

136. Broset, E., Saubi, N., Guitart, N., Aguilo, N., Uranga, S., Kilpelainen, A., … Joseph, J. (2019). MTBVAC based TB-HIV vaccine is safe, elicits HIV-T cell responses and protects against Mycobacterium tuberculosis in mice. Molecular Therapy - Methods & Clinical Development. doi:10.1016/j.omtm.2019.01.014

137. Arbues, A., Aguilo, J. I., Gonzalo-Asensio, J., Marinova, D., Uranga, S., Puentes, E., … Martin, C. (2013). Construction, characterization and preclinical evaluation of MTBVAC, the first live-attenuated M. tuberculosis-based vaccine to enter clinical trials. Vaccine, 31(42), 4867–4873. doi:10.1016/j.vaccine.2013.07.051

138. Kilpeläinen, A., Saubi, N., Guitart, N., Moyo, N., Wee, E. G., Ravi, K., … Joseph, J. (2019). Priming With Recombinant BCG Expressing Novel HIV-1 Conserved Mosaic Immunogens and Boosting With Recombinant ChAdOx1 Is Safe, Stable, and Elicits HIV-1-Specific T-Cell Responses in BALB/c Mice. Frontiers in Immunology, 10. doi:10.3389/fimmu.2019.00923

139. Chen, C.-W., Saubi, N., & Joseph-Munné, J. (2020). Design Concepts of Virus-Like Particle-Based HIV-1 Vaccines. Frontiers in Immunology, 11. doi:10.3389/fimmu.2020.573157

140. Joan Lin-Cereghino, William W. Wong, See Xiong, William Giang, Linda T. Luong, Jane Vu, Sabrina D. Johnson, and Geoff P. Lin-Cereghino. Condensed protocol for competent cell preparation and transformation of the methylotrophic yeast *Pichia pastoris.* 38:44-48 (January 2005)

141. Kim HJ, Kim SY, Lim SJ, Kim JY, Lee SJ, Kim HJ. One-step chromatographic purification of human papillomavirus type 16 L1 protein from Saccharomyces cerevisiae. Protein Expression and Purification. 15 Aug 2009, 70(1):68-74 DOI: 10.1016/j.pep.2009.08.005 PMID: 19686852

142. Park, M.-A., Kim, H. J., & Kim, H.-J. (2008). Optimum conditions for production and purification of human papillomavirus type 16 L1 protein from Saccharomyces cerevisiae. Protein Expression and Purification, 59(1), 175–181. doi:10.1016/j.pep.2008.01.021

143. Barrero, J. J., Casler, J. C., Valero, F., Ferrer, P., & Glick, B. S. (2018). An improved secretion signal enhances the secretion of model proteins from Pichia pastoris. Microbial Cell Factories, 17(1). doi:10.1186/s12934-018-1009-5

144. GE Application note 29-0983-01 AB

145. Kuribayashi, H., Wakabayashi, A., Shimizu, M., Kaneko, H., Norose, Y., Nakagawa, Y., … Takahashi, H. (2004). Resistance to viral infection by intraepithelial lymphocytes in HIV-1 P18-I10-specific T-cell receptor transgenic mice. Biochemical and Biophysical Research Communications, 316(2), 356–363. doi:10.1016/j.bbrc.2004.02.058